Novel Size Separation Techniques for Aggregates of Embryonic Stem Cells Using the Stokes Equation

William McAlister, BSc

Thesis Submitted to the University of Nottingham for the degree of Doctor of Philosophy

July 2017

Abstract

Embryoid body formation is a commonly used procedure in embryonic stem cell differentiation as it recapitulates the early stages of embryogenesis and in doing so induces the formation of the three germ layers. Despite being a commonly used step in the differentiation of embryonic stem cells there is still a raft of inconsistencies in this process. As a result, heterogeneity exists in the cells produced in terms of their number and differentiation status; an issue which must be overcome in order to realise the full potential of embryonic stem cells for regenerative medicine. The work produced here is focussed on the issue of size heterogeneity during embryoid body formation. First of all, a closer look at the inherent size-dependent characteristics of embryoid bodies was explored over a 120-hour formation period. This showed that the mean diameter and span of embryoid bodies continued to increase throughout the duration of the 120 hours and provided insight into the population dynamics over this formation period. A non-scalable mesh separation technique was produced to further explore the inherent characteristics of embryoid bodies. This was shown to be successful at collecting size fractions of <100µm, 100-200µm and >200µm. Immunohistochemistry was used to show size-dependent differences in embryoid body differentiation by showing differential surface expression of Gata-4, Brachyury and Nestin in different sized populations. Meanwhile cell counts and a growth rate assay were performed which showed further size-dependent differences in the ability of each fraction to produce large numbers of cells. This showed that EBs within the 100-200µm fraction contained the largest numbers of cells and were the most proliferative fraction. However, they were also the only fraction to not express proteins from all three germ layers to any level.

Due to the clear size-dependent differences in these size fractions perfusion technique was developed to separate embryoid bodies according to their size in a glass column. This depended on the relationship between particle diameter and terminal falling velocity. Key experimental factors that impacted on the efficacy of this technique were shown to be settled bed height, flow rate, sampling height and flow rate. As a result, two artificial neural networks were developed using a model system of Spehadex beads to show how varying these factors impacted the mean

diameter and span of collected particles at a constant settled bed height. These experiments showed that this technique was limited to collecting particles from the lower reaches of the stock for both Sephadex beads and embryoid bodies. This was because the most successful factor for increasing mean diameter, flow rate, also induced the greatest increase in span. Therefore, collecting larger sized fractions reduced their discrete nature to such an extent that they were no longer distinct from one another. This suggested that this technique had potential, but was limited by the flow characteristics caused by increasing flow rate.

As a result, the separation technique was adapted to overcome this by inverting the column and removing the impact of flow rate; instead allowing gravity alone to separate the particles using a top-loading method. This method was shown to be substantially more successful at collecting larger particles in discrete fractions, however, there were issues with collecting the smaller fractions during a 15-minute separation. Adaptation of this technique allowed all three size fractions to be collected effectively. Finally, a growth rate assay was performed to determine if the embryoid bodies could survive the conditions encountered in this technique and continue to grow post-separation. The cells collected from the column were able to continue growing when dissociated and grown in two-dimensional culture. However, their growth rate was lower than that in the unseparated control and it is not known whether this was because the technique is destructive. This research has therefore identified a cheap, effective, tuneable, novel size-separation technique for embryoid bodies that can collect multiple fractions in a single run with high throughput.

Acknowledgments

I would like to give special thanks to my supervisors Colin Scotchford and Lee Buttery for their guidance and support throughout the critical stages of my PhD. I would like to thank Pete Licence and Ed Lester for their helpful feedback as my internal assessors. I would also like to give thanks to Rachel Gomes for her support during some of the more difficult periods of my PhD, especially during my change of supervisor. Thank you also to Yuen Ng for the opportunity.

In addition to all this I must offer huge thanks to everyone within the Tissue Engineering group. First, Glen Kirkham; for his training, support, rational views and endless patience. Without all your experience, unceasing ability to answer all my idiotic questions and conviction that success was just around the corner I'm not entirely sure I would have collected the results that have comprised this thesis. In addition, thank you to all the staff who keep the Tissue Engineering group running, the unsung heroes without whom none of these works would ever be able to reach fruition. I would also like to thank Emily, Jamie, Adam, Lei, Laura, Tom and Jamie for their support and sense of community throughout our studies.

Further I would like to say a big thank you to Youlia Jenidi and Josh Pilkington for their friendship, help and support during the highs and lows of a research degree; not to mention the tea-parties! In addition to this, thank you to Sam Miller, for the many pub-based conversations that never failed to stray to research and also eventually led to some of the key ideas that underpinned this work.

I would like to thank my parents Patrick McAlister and Elizabeth Wadsworth along with their partners Lisa McNaney and Paul Wadsworth for their support, financial and emotional, throughout my PhD and for believing in my ability through thick and thin. I would like to extend this further to my brother, Tom McAlister, who was always available to talk, and occasionally visit, to provide some escapism from the rigours of research.

Above all I would like to thank Alice Beaumont, for always being there during my most difficult moments and sharing with me each of my triumphs as if they were her

own. I can’t thank you enough for supporting me through this, especially during the final few months, as without you none of this would have been possible.

A final thanks to all those not mentioned by name that have supported me and enriched my experience throughout my PhD.

Declaration

I declare that this thesis is a result of my own work which has been undertaken in the main during my period of registration at the University of Nottingham while studying for the degree of Doctor of Philosophy.

Table of Contents

List of Figures

List of Tables

List of Equations

List of Abbreviations

2D	Two-Dimensional
3D	Three-Dimensional
µg	Microgram
µl	Microlitre
µm	Micrometre
AAD	Absolute Average Deviation
AFP	Alpha feto-protein
ANN	Artificial Neural Network
ASC	Adult Stem Cell
B_o	Bodenstein Number
BRANN	Bayesian Regularisation Artificial Neural Network
cm	Centimetre
CO_2	Carbon Dioxide
cP	Centipoise
CPM	Cryopreservation medium
D10	10^{th} percentile of diameter
D90	90^{th} percentile of diameter
d_c	Column diameter
DMEM	Dulbecco's modified Eagle medium
DMSO	Dimethyl sulfoxide
d_p	Particle diameter
EB	Embryoid body
EBR	Expanded bed reactor
ECM	Extracellular matrix
EDTA	Ethylenediaminetetracetic acid
ESC	Embryonic stem cell
FCS	Foetal calf serum
g	Grams
GMP	Good manufacturing practice
HEPA	High efficiency particulate air
HEPES	N-2-hydroxyethylpiperazone-N-2-ethanesulfonic acid
Hsb	Settled bed height
iPSC	Induced pluripotent stem cell
LIF	Leukaemia inhibitory factor
L-Glu	L-Glutamine
m	Metres
mESC	Mouse embryonic stem cell
min	Minutes
ml	Millilitres
mm	Millimetres
MSE	Mean squared error
MTS	(3-(4,5-dimethylthiazol-2-yl)-5-(3-carboxymethoxyphenyl)-2-(4-sulfophenyl)-2H-tetrazolium)
PBS	Phosphate buffered saline
PSC	Pluripotent stem cell

PSD	Particle size distribution
Re_p	Particle Reynold's number
RMSE	Root mean squared error
s	Seconds
SEM	Standard error margin
SOP	Standard operating procedure
TE	Trypsin-ethylenediaminetetracetic acid
TFV	Terminal falling velocity

Chapter 1

Introduction

A multitude of different areas of cell research have shown that the size of cell aggregates impacts on the viability, proliferation, differentiation and hormone secretion of the cells within (Mori et al., 2006, Ge et al., 2012, Lehmann et al., 2007, Machado et al., 2013, Choi et al., 2010). As a result, a wealth of research has focussed on size separating or controlling the size of aggregates of cells during formation (Dang et al., 2004, Choi et al., 2010, Miyamoto and Nakazawa, 2016, Xu et al., 2011, Buschke et al., 2013, Hwang et al., 2009, Kinney et al., 2012). Among those cell types impacted by aggregate size are pancreatic cells, neural stem cells and embryonic stem cells, all of which therefore require a quick, effective and adaptable method of size separation. Among these, embryonic stem cells were selected for this study due to their abundance, ease of culture, propensity for forming aggregates and importance across a range of research areas (Bauwens et al., 2008, Dang et al., 2004, Choi et al., 2010, Miyamoto and Nakazawa, 2016, Bratt-Leal et al., 2009, Ng et al., 2005, Cameron et al., 2006, Mohr et al., 2010, Carpenedo et al., 2007, Sidney et al., 2014).

Embryonic stem cells have long been believed to have the potential to solve a number of issues facing modern medicine. Due to their near infinite ability to proliferate and ability to differentiate into almost any adult cell type, a large body of research has been committed to utilising these cells for producing replacement tissues (Vats et al., 2005, Jukes et al., 2010, Toh et al., 2011, Gepstein, 2002). In order to succeed, these processes first require the controlled, accurate and consistent production of large numbers of highly pure and fully differentiated cells. Many of

these protocols begin with the formation of embryoid bodies (EBs) to prime the cells for differentiation (Kurosawa, 2007). Though there are multiple methods for EB formation, mass suspension is commonly used due to its simplicity and ability to produce large numbers of aggregates (Choi et al., 2005, Dang et al., 2002, Nonaka et al., 2008, Kurosawa, 2007).

Unfortunately, embryoid body formation by mass suspension results in the production of a heterogeneously sized population of aggregates (Cameron et al., 2006, Bauwens et al., 2008, Carpenedo et al., 2007, Karp et al., 2007). This is caused by the uncontrolled agglomeration of aggregates as well as the continued proliferation of cells within each aggregate (Dang et al., 2004, Dang et al., 2002, Cameron et al., 2006). This is important because it has been shown on a number of occasions that EB size can profoundly affect the differentiation of the embryonic stem cells (ESCs) within the aggregates (Choi et al., 2010, Bratt-Leal et al., 2009, Hwang et al., 2009, Lillehoj et al., 2010, Buschke et al., 2013, Kinney et al., 2014, Messana et al., 2008, Cha et al., 2015). As a result, different sized aggregates appear to have a predisposed tendency for differentiation into certain lineages and so can meet with varying levels of success in differentiating into specific cell types. Because of this fact, there is a lack of consistency within the population of cells that is utilised for each differentiation protocol, with various subpopulations existing within the stock (Toyooka et al., 2008, Singer et al., 2014, Kumar et al., 2014, Osorno and Chambers, 2011).

It is therefore important to overcome these inconsistencies by separating out aggregates according to their size. This will allow more control over the differentiation of ESCs by negating the uncertain impact of size on differentiation. In addition, following further research it could be possible to determine what sized EBs have the highest probability of differentiating into a desired cell type. This would allow for the improvement of differentiation protocols by selecting for the most beneficial size of EB, depending on the desired differentiation outcome. Therefore, it would be desirable to determine a separation technique that can collect multiple size fractions from across the full range found in the stock and that can be easily

manipulated to alter the size-properties of the collected fraction of EBs, as well as have the potential to be adapted for size separating other aggregates of cells.

To allow ease of use and provide the scalability required to make this technique commercially viable it will ideally have a high throughput and be readily adapted for full automation. This aim is therefore a key driver for this research as it is essential that homogeneity of cell aggregates, including EBs, can be ensured in tandem with mass production to allow for the utilisation of cells derived from aggregates in a regenerative medicine industry.

Current methods for controlling aggregate size do exist and are separated into two categories. First are techniques that control aggregate size during formation; these techniques aim to ensure that all aggregates in the stock are within a certain size range. This can be done using dynamic culture conditions, controlled sized microwells or encapsulation of cells. Each of these techniques will be discussed in further detail later in the literature review (Chapter 2). These methods have the benefit of being quite selective with the size of aggregates that they produce, however, they can lack flexibility in producing alternative sizes. Secondly, are techniques that separate aggregates into size fractions after their initial formation as a heterogeneously sized stock. These methods have been demonstrated to have the capability to collect several size fractions of aggregates and the potential to be adapted to collect aggregates of different sizes outside those tested. However, in most cases these techniques were relatively low throughput, especially in an industrial sense, and so would need extensive alteration to be applicable to a fully scaled process for the production of cells for a tissue engineering industry.

Given the above, an alternative method is required that will allow for the collection of a variety of aggregates with different size ranges, that has the potential to be quickly and easily scaled up and automated for use in an industrialised setting. This technique must therefore ideally be: effective at collecting multiple different size fractions of aggregates, easy to operate and clean, cheap to build and have high throughput.

In order to meet these goals, this research was undertaken to identify a separation technique that meets these criteria. This endeavour will begin by determining the inherent properties of EBs during their formation by mass suspension. This was followed by the conception of a simple separation technique to provide means of comparison for subsequent, more advanced separation processes.

The initial separation technique involved the use of different porosity meshes to separate out EBs according to their size. This is a method that has been utilised for size separation of other types of non-biological particles previously and so should transfer to biological samples (Konert and Vandenberghe, 1997, Mora et al., 1998). In addition, this will allow for a series of experiments to be performed in order to determine the size fractions that can collected from a heterogeneously sized stock, their inherent, size-dependent, physical characteristics and what impact EB size may have on ESCs.

Subsequent separation techniques make use of phenomena described by the Stokes equation; this dictates that the terminal falling velocity (TFV) of a particle is proportional to its diameter. Research in this area has shown that the larger the particle diameter the higher the TFV. This technique has historically been used for the separation of non-biological samples such as beads, but has recently been shown to have the potential to separate aggregates of cells. As a result, it is hoped that this research will transfer to the separation of EBs and hopefully has the potential to be adapted to allow multiple size fractions representative of the whole stock to be separated.

Once complete it is hoped that the techniques identified here can be easily manipulated to size-separate various, different aggregates of cells with little or no adaptation to the technique itself. As a result, this technique must be adaptable enough to meet these changing demands, but effective and reproducible enough to complete its core aim of size separating aggregates of cells.

Chapter 2

Literature Review

2.1. Background

2.1.1. What Is Tissue Engineering?

Tissue engineering is the process of creating new tissues from cells and materials in order to replace damaged or diseased tissues in an organism. This can be performed in humans or animals using cells taken from healthy tissue from the same or other individuals; in some cases from different species (Marolt et al., 2010, Schoen and Levy, 1999, Caplan, 2007, Pokrywczynska et al., 2014, Trounson et al., 2011, Trounson and McDonald, 2015). By ensuring culture occurs in the correct environmental conditions, this means that a relatively small number of cells can be used to replace a whole, or part, of a malfunctioning tissue (Caplan, 2007, Bianco and Robey, 2001, Hwang et al., 2008, Dado et al., 2012, Griffin et al., 2015). However, this requires a very specific set of conditions, the characteristics of which will be dependent on the cells that are used to generate the tissue and whether or not they are cultured in two-dimensional (2D) or three-dimensional (3D) culture (Antoni et al., 2015, Edmondson et al., 2014, Ravi et al., 2015).

Fully differentiated adult cells can be used to generate new tissues, however, relatively large numbers are required to replace the tissue due to their limited proliferative potential compared to undifferentiated cells (Stenderup et al., 2003, Caplan, 2007, Rumman et al., 2015, Zimmermann et al., 2002, Dvir-Ginzberg et al., 2003). In addition, in the case of diseased tissue it is often not possible to take these cells from the patient themselves, thus causing potential issues with immune

rejection (Unger et al., 2008, Robertson et al., 2007, Taylor et al., 2011, Bradley et al., 2002, Boehler et al., 2011). In order to circumvent this, alternative sources of cells have been sought and a great deal of research has therefore focussed on the use of stem cells (Robertson et al., 2007, Taylor et al., 2011, Bradley et al., 2002).

2.1.2. What Are Stem Cells And What Is Their Potential?

Stem cells are undifferentiated cells that differentiate to form every part of the human body. They are defined by their ability to both self-renew and differentiate into various specialized cell types (Kuehnle and Goodell, 2002). ASC's are partially differentiated cells that are found in sites throughout adult organisms. For example, neural stem cells are found throughout the nervous system and hematopoietic stem cells are found within the bone marrow (Caplan, 2007, Vangsness et al., 2015, Pendleton et al., 2013, De Filippis and Binda, 2012). These cells exist in repositories where they can replace cells as required during an animal's life. However, these cells are still limited in their proliferative potential, though less so than fully differentiated cells (Rumman et al., 2015). Furthermore, their proliferative potential decreases with increasing age of their host, meaning that in later life the cells are less adaptable for this purpose (Stenderup et al., 2003). As such, a great deal of research has centred on the use of ESCs, due to their ability for near limitless proliferation and capability to differentiate into almost any adult cell type (Cai et al., 2006, Marolt et al., 2010, Sidney et al., 2014, De Filippis and Binda, 2012, Przyborski, 2005, Buttery et al., 2001, Dasgupta et al., 2005, Smukler et al., 2006, Redenti et al., 2009, Nsiah et al., 2014, Toh and Voldman, 2011, Soncin et al., 2009, Wolfe and Ahsan, 2013, Rungarunlert et al., 2013).

Stem cells can undergo either asymmetric replication, producing one identical undifferentiated cell and one differentiated cell, or symmetric differentiation, whereby one stem cell will produce two differentiated cells and another will produce two undifferentiated cells (Dingli et al., 2007, Morrison and Kimble, 2006). These mechanisms ensure the maintenance of the stem cell population throughout an organism's life while allowing them to continue to play a role in tissue repair following injury (Stappenbeck and Miyoshi, 2009, Deleyrolle et al., 2011).

2.1.3. Embryonic Stem Cells

ESCs, derived from blastocysts, are a type of pluripotent stem cell (PSC) and therefore capable of differentiating into virtually any cell type of the three germ layers (Sharma et al., 2011, Smith, 2001, Yamanaka, 2008, Martin, 1981). An example of this potential is highlighted in Figure 2.1. They have generated a lot of interest amongst the scientific community by offering the prospect of a potentially unlimited source of cells that can differentiate into most cell types in the body and can be cultured *in vitro* (Martin, 1981). To achieve this aim requires recreating and amplifying the *in vivo* environment as accurately as possible; as will be discussed later. When utilised for tissue engineering, PSCs are generally differentiated *in vitro* first, prior to transplantation *in vivo,* to allow enhanced control of differentiation and to reduce the probability of teratoma formation as this is an inherent characteristic of undifferentiated cells when implanted *in vivo* and is in fact used as a test for their pluripotency (Nakamura and Okano, 2013, Rezania et al., 2014, Park et al., 2005, Hwang et al., 2013, Hentze et al., 2009).

Since their initial discovery and subsequent derivation, a wealth of research has been performed to determine the intrinsic properties of ESCs and to exploit these properties to produce a plethora of fully differentiated tissues. The inherent adaptability of stem cells can therefore be manipulated to be advantageous in the treatment of a range of specific illnesses by selectively producing required cell types. In recent years stem cells have been speculated to have the potential to treat a wide variety of diseases including leukaemia, diabetes, Parkinson's, brain damage caused by stroke, osteoporosis and critical sized bone defects as a result of injury and disease (Diamond et al., 2011, Mimeault and Batra, 2008, Rezania et al., 2014, Park et al., 2005, Choi et al., 2014, Antebi et al., 2014, Rosado-de-Castro et al., 2013). Consequently, this is an area of great interest and has led to the formation of a network of pioneering areas of research.

The majority of these treatments are based around the concept that infusion of stem cells, or differentiated cells derived from stem cells, into diseased tissue will enable them to synthesise new, healthy tissue (Rosado-de-Castro et al., 2013, Choi et al., 2014, Park et al., 2005, Hwang et al., 2013, Rezania et al., 2014). Despite this,

there are many obstacles to overcome before stem cells can be effectively utilised to treat such illnesses in a clinical setting. These include; problems with the efficient *in vitro* culture of stem cells, incomplete or undesired differentiation of cells, attaining a large quantity of high quality, pure cells that meet with good manufacturing practice (GMP) standards, overcoming possible problems with immunorejection and uncertainty over the manner in which these treatments will perform in the markedly more complex *in vivo* environment (Stojkovic et al., 2004, Unger et al., 2008, Taylor et al., 2011, Bradley et al., 2002, Boehler et al., 2011, Gutierrez-Aranda et al., 2010, Hentze et al., 2009).

The use of ESCs is further hindered by the ethical implications of deriving embryonic stem cells from blastocysts. This is a topic that splits opinion and will not be easily resolved without finding an alternative source for these cells, or a method of collecting embryonic stem cells without destroying the embryo. Fortunately, researchers believe that they have identified methods of removing a blastomere from the 8-cell stage embryo while still allowing the embryo to continue to develop (Grompe, 2005, Chung et al., 2008). The success of this procedure owes to the fact that only a single blastomere is removed from the 8-cell stage and so allows the remaining cells to develop normally; although this does still require the cells to be cultured with pre-existing ESCs subsequently (Chung et al., 2008).

Another possible method of circumventing this issue is through the use of induced pluripotent stem cells (iPSCs). These iPSCs are ordinary somatic (adult) cells that have undergone nuclear reprogramming through the targeted use of transcription factors to induce an embryonic stem cell-like phenotype (Yamanaka, 2009b, Yamanaka, 2009a, Lister et al., 2011, Basma et al., 2014, Liu et al., 2013). These cells were shown to be similar to ESCs in their expression of ESC marker genes, their morphology and the ability to form teratomas when injected into mice (Yamanaka, 2009b, Lister et al., 2011, Gutierrez-Aranda et al., 2010, Liu et al., 2013). This negates the need to derive pluripotent stem cells from an embryo and allows them instead to be generated autologously in a way deemed ethically acceptable. As a result, iPSCs are a promising resource for tissue engineering and, due to their similarity to ESCs, many protocols exist for the generation and subsequent differentiation of these cells. In

addition, their differentiation often begins with embryoid body formation, much like ESC's. It is important to note that the use of iPSCs has a raft of unique issues that would need to be resolved in order to utilise these cells as a resource in tissue engineering. These issues include; immunological considerations, a low success rate for iPSC formation, heterogeneity in their inherent capacity for differentiation into cells from the three germ lineages, epigenetic differences dependent on the cell-line from which the cells were derived and continued tumourigenicity of the differentiated products (Ramirez et al., 2011, Polo et al., 2010, Eminli et al., 2009, Kim et al., 2010, Yamanaka, 2009a, Kim et al., 2009, Lister et al., 2011, Ebben et al., 2011, Okano et al., 2013, Liu et al., 2013, Taylor et al., 2011).

2.2. Challenges Facing Stem Cell Therapy

A number of challenges must be overcome before stem cells can be regularly and effectively utilised in a clinical setting. These problems range from: attaining a large enough quantity of stem cells to be clinically applicable, uncontrolled differentiation along undesirable lineages, achieving a pure culture of the desired cell type, reproducibility, and immunorejection of the engineered tissue. In order to expedite the solution of these issues, and in part due to restrictions on the use of human cells in some countries, many researchers use mouse ESCs as a model system for human ESCs because of their comparative ease of use and due to them having the same basic needs in terms of culture and differentiation (Schnerch et al., 2010, Gu et al., 2012).

2.2.1. Good Manufacturing Practice

A major setback currently hindering the use of stem cells for clinical applications is reproducibility. In order to be an effective product there must be a method developed that allows for the culturing of stem cells to be standardised. This would ensure that all batches of stem cells and their differentiated products would be near identical in phenotype, genotype and number, to best ensure that they would all behave the same when implanted into the patient. It is also important to ensure that the cell products are completely pure, not just from external contaminants such as bacteria or fungi, but also from cells that have differentiated into the incorrect cell type, or remained undifferentiated.

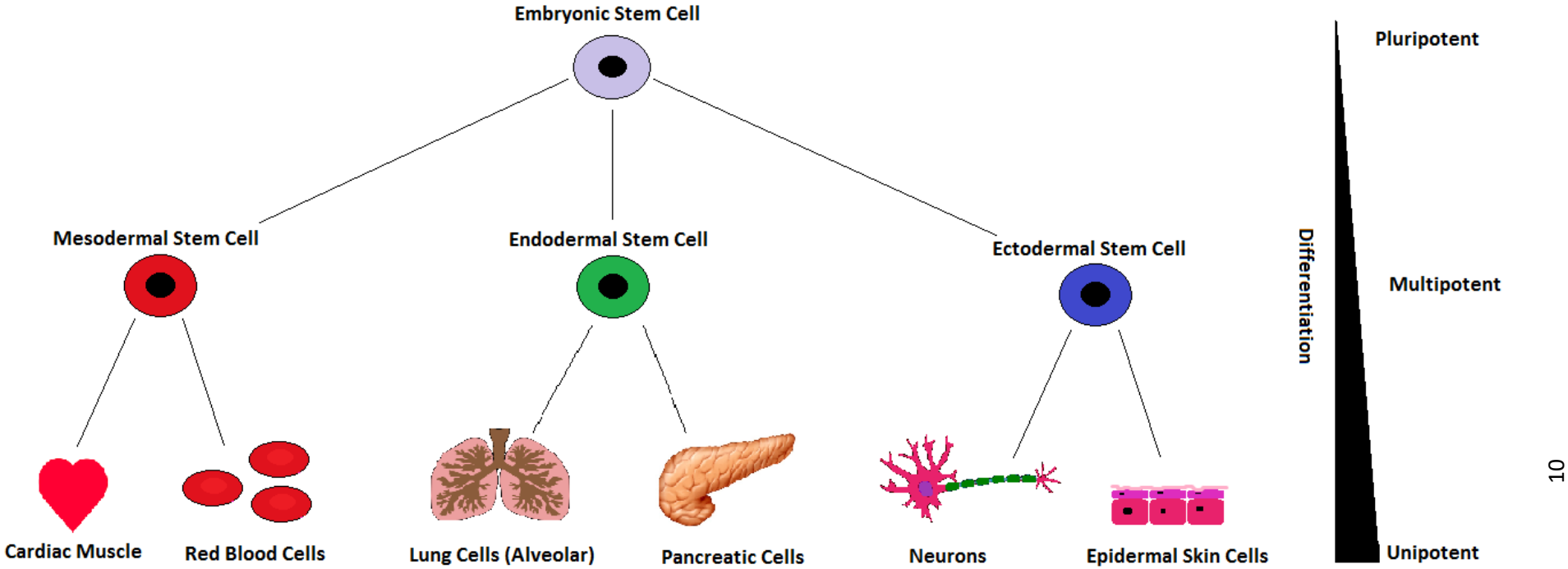

Figure 2.1: This figure shows the potential differentiation routes of an ESC into different example cell types from each of the three major lineages; mesoderm, endoderm and ectoderm. In addition, it is highlighted how the potency of these cells changes throughout their differentiation from the pluripotent ESC to the unipotent, terminally differentiated cell.

GMP is a system that is used in the pharmaceutical industry to ensure that the quality of their products is consistent. It is used to guarantee that the final product meets certain specifications regarding purity, safety, quantity and that their production follows a standard operating procedure (SOP) so as to be reproducible (Unger et al., 2008, Giancola et al., 2012). This SOP must be rigorous in every detail from initial harvesting to the finished product and its storage conditions to ensure that every 'batch' that is produced and certified ready for use in the clinic is identical to all of the others. In the case of cell-based therapies this is an incredibly difficult goal to achieve due to their inherent variability. There are a number of factors that can provide unwanted variability in the generation of differentiated cells from ESCs, starting with cell derivation and culture through to the differentiation protocols and cell harvesting. As a result of this, under EU law the development of any tissues or cells that are used as either starting materials or the finished product are required to comply with Directive 2004/23/EEC and its two subsequent technical directives; Directive 2006/17/EC and Directive 2006/86/EC (Giancola et al., 2012).

2.2.2. Derivation And Continuous Culture Of Embryonic Stem Cells

There are a number of issues and inconsistencies with the derivation and culture of ESCs that need to be overcome in order to ensure GMP compliance of the final desired product (Unger et al., 2008). First of all, the use of a multitude of animal derived products has the potential to create issues with disease transmission and possible immunological considerations. For example, the derivation of cells from the inner cell mass of the embryo typically requires the use of pronase or immunosurgery, both of which require animal or bacteria-derived elements for their processing (Unger et al., 2008, Genbacev et al., 2005, Strom et al., 2007). In addition, foetal calf serum (FCS) is commonly used during continuous culture of ESCs, however, methods are looking at removing this particular animal-derived component by using human serum, or serum-free culture (Genbacev et al., 2005, Amit et al., 2000, Richards et al., 2002, Prathalingam et al., 2012, Koivisto et al., 2004, Wang et al., 2013). A further GMP issue with continuous culture of ESCs revolves around the use of mouse embryonic feeder cells, which are used to support growth and prevent differentiation of ESCs (Richards et al., 2002, Prathalingam et al., 2012). Fortunately,

research has focussed on overcoming this issue through the use of human-derived support cells and the development of feeder-free ESCs (Richards et al., 2002, Prathalingam et al., 2012, Tamm et al., 2013, Xu et al., 2001, Hashemi et al., 2011, Thomson et al., 1998, Ying et al., 2003).

2.3. Control of Stem Cell Fate *in vitro*

Following on from the derivation and subsequent continuous culture of ESCs, there is also a raft of issues and inconsistencies with the differentiation of ESCs into a final desired product *in vitro*. The decision between proliferation and differentiation of ESCs can be controlled by a range of factors; from signalling proteins and transcription factors to small bioactive molecules and oxygen concentration (Griffin et al., 2015, Alberti et al., 2008, Kurosawa et al., 2006). Anything that alters the microenvironment of the cell can have an effect on its outcome. This is why the microenvironment is strictly controlled *in vivo* and therefore needs to be equally stringently controlled when growing tissues *in vitro*. The ability to control the microenvironment on demand could enable the manipulation of stem cells to treat a plethora of diseases; however, to do this first requires an intimate understanding of the various factors that are involved.

2.3.1. 2-Dimensional vs. 3-Dimensional Culture

Stem cells can be differentiated in either 2D on a flat surface, or in 3D as aggregates or on scaffolds (Ravi et al., 2015, Zhang and Ma, 2004, Jungreuthmayer et al., 2009, Annabi et al., 2011, Akkouch et al., 2011, Karageorgiou and Kaplan, 2005, Ahadian et al., 2014, Xu et al., 2010, Langenbach et al., 2013, Antoni et al., 2015, Maltman and Przyborski, 2010). In their favour, 2D cultures are easier to control due to the comparative homogeneity of the culture environment for each cell (Shimokawa and Sato, 2015, Edmondson et al., 2014, Lin and Chang, 2008). In addition, it is easier to provide soluble factors to the cells as they are all in direct contact with the medium in which they are grown (Lin and Chang, 2008, Edmondson et al., 2014). This suggests that 2D cultures may be more homogeneous than 3D cultures as several impactors of their differentiation brought about by 3D culture have been mitigated. However, 2D cultures fail to replicate the *in vivo* environment as accurately as 3D cultures, as tissues *in situ* grow as part of a 3D matrix of cells and

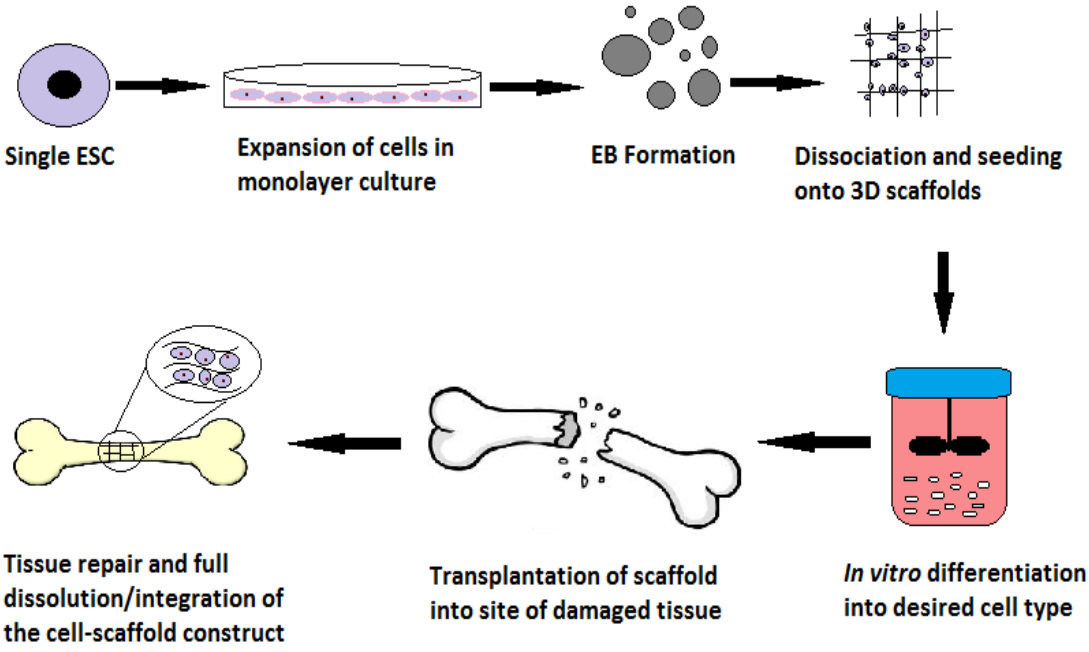

Figure 2.2: This figure shows a process diagram for the production of a cell-loaded scaffold as an example of a tissue engineering product starting from a single ESC. A single cell undergoes initial expansion *in vitro*, differentiation on scaffolds using a bioreactor and finally ends with *in vivo* transplantation and full tissue repair. In this example the chosen differentiated cell type is an osteoblast to repair a critical sized bone-defect.

extracellular matrix (ECM); the composition of which has also been shown to influence differentiation (Ravi et al., 2015, Maltman and Przyborski, 2010, Antoni et al., 2015, Edmondson et al., 2014, Mouw et al., 2014, Watt and Huck, 2013, Bonnans et al., 2014, Chen et al., 2007). This more accurate representation of the natural cell environment makes 3D culture an important area of further research in order to produce tissues for *in vivo* transplantation. To do so will require introducing greater levels of homogeneity into the final differentiated products that are produced in the 3D environment compared to current standards.

2.3.2. Soluble Factors Affecting Stem Cell Fate

A range of factors are responsible for determining the differentiation of ESCs; both soluble and insoluble. Insoluble factors are often utilised as part of scaffolds in 3D culture, though they are also used for continuous culture such as in the case of gelatin and can encourage both proliferation and differentiation (Tamm et al., 2013, Kai et al., 2011, Randle et al., 2007, Hashemi et al., 2011, Lin et al., 2006, Gothard et al.,

2009, Fu et al., 2011, Venugopal et al., 2010, Jayakumar et al., 2011). Meanwhile, soluble factors such as proteins and bioactive molecules are present throughout the culture media and are often altered experimentally as a means of controlling proliferation and differentiation (Chung et al., 1992, Ying et al., 2003, Boeuf et al., 1997, Murray and Edgar, 2001, Abe et al., 2000, Fu et al., 2008).

First of these soluble factors is oxygen concentration, as this is often a limiting factor in the growth of mammalian cells. Oxygen is required to allow the cell to propagate and failure to supply plentiful oxygen to cells can result in their apoptosis. This is seen regularly in larger cell aggregates which often display necrosis at their core (Gothard et al., 2009, Tomov et al., 2015, Koike et al., 2007). In terms of cell survival and metabolism the same applies for a host of other substances that are required for cell metabolism such as glucose, vitamins and essential amino acids etc. as well as the removal of waste products. This inefficient mass transfer results in a vast reduction in the number of cells; making it a key problem with current stem cell research and one that is exacerbated by the use of aggregates of cells or large scaffolds (Van Winkle et al., 2012).

In vivo this is resolved progressively through vascularisation, but *in vitro* this process cannot resolve these issues. Therefore, when culturing cells *in vitro* it is desirable to enhance mass transfer in cell cultures or to discourage the formation of large aggregates in order to enable a suitable concentration of nutrients to be supplied throughout the culture (Anton et al., 2008, Unger et al., 2008, Van Winkle et al., 2012).

Altering the concentration of oxygen within a culture does not simply serve to ensure cell survival and thus continued proliferation; the concentration of oxygen has also been shown to have an effect on the production of transcription factors, surface markers and cytokines in human megakaryocytes (Mostafa et al., 2001). Furthermore, in mouse ESCs oxygen concentrations can have a profound effect on differentiation. Cells cultured in 40% oxygen retained the activity of alkaline phosphatase and expression of Oct4, genes associated with pluripotency, for longer than cells cultured at lower concentrations of oxygen (Kurosawa et al., 2006).

Second are signalling factors; these act as stimulatory signals for either proliferation or differentiation. Cells are in a constant state of turmoil between competing signals, all bombarding the cell with information from both the interior and exterior environments. As well as receiving constant signals from itself and the cells around it to survive and proliferate, a cell will also be receiving signals to induce apoptosis (Lowe et al., 2004). The balance of these signals determines the eventual cellular fate and is one of the mechanisms that provides a safeguard against cancer (Evan and Vousden, 2001).

In much the same way, stem cells are continuously receiving signals directing them towards a differentiated or proliferative outcome. In many cases the signal for one outcome will inhibit signals encouraging the other. It is this interplay that dictates whether or not a stem cell will continue along its proliferative route or begin to undergo differentiation.

2.3.3. Controlling Stem Cell Proliferation *in vitro*

There are numerous signalling factors that encourage proliferation and differentiation of stem cells; first, the proliferative signals. Pluripotency of ESCs in humans and mice is maintained primarily by three transcription factors; Nanog, Oct4 and Sox2 (Chambers and Smith, 2004). Together these transcription factors are crucial for maintaining the pluripotency of stem cells by maintaining their undifferentiated state. Because of the integral role that these transcription factors play in maintaining pluripotency, and the subsequent absence of expression of some of these factors in differentiated cells, these genes are often exploited in research. During experiments, the levels of expression of these factors can be used as an indication of the differentiation state of cells being cultured *in vitro* (Cai et al., 2006, Hyslop et al., 2005). This provides a method of ascertaining the phenotype of the cells that are being produced, which provides important information when trying to produce pure cultures of differentiated or pluripotent cells.

One important proliferative signalling molecule is Leukaemia Inhibitory Factor (LIF), which helps to maintain the pluripotency of mouse ESCs (WILLIAMS et al., 1988). This ability has resulted in its continued use to date as part of the culture medium for culturing mouse ESCs *in vitro*. Removal of LIF is considered to be one of

the primary steps towards encouraging mouse ESCs to differentiate *in vitro*, thus suggesting that as well as encouraging proliferation, it also inhibits differentiation (Smukler et al., 2006). It is important to note that LIF has no effect on the maintenance of human ESCs, which instead maintain self-renewal through the use of Fibroblast Growth Factor (Greber et al., 2010). This factor is added to the culture medium in a similar fashion to LIF and encourages proliferation while maintaining the undifferentiated state of the cells through the mitogen-activate protein kinase pathway (Eiselleova et al., 2009, Dvorak et al., 2005).

2.3.4. Controlling Stem Cell Differentiation *in vitro*

Differentiation requires the precise regulation of specific genes relevant to the induction of the final desired characteristics of the cell (Costa et al., 2008, Liu et al., 2000, Ntambi and Young-Cheul, 2000). The genes that are activated or repressed are controlled by internal and external signals dependent on the local microenvironment within which the cell finds itself (Kumar et al., 2014, Kronenberg, 2003, Wolfe et al., 2012, Calvi et al., 2003, Burdon et al., 2002). This environment is dictated by the cells contained within and the signals that they emit; as well as the culture medium *in vitro*. This combination of signals guides the cell towards its final differentiated state depending on what characteristics it is required to display to fulfil its necessary role as part of the tissue. For example, during osteoblastic differentiation cells increase expression of osteopontin, osteocalcin, bone sialoprotein, Cbfa1 and a multitude of other proteins until a characteristic expression profile for a differentiated osteoblast is displayed (Valenti et al., 2008, Mizuno and Kuboki, 2001, zur Nieden et al., 2003, Sila-Asna et al., 2007).

Cells will respond to both chemical and physical signals as part of the control of their life cycle. While nearby cells can encourage a stem cell to differentiate through signalling molecules, equally important are the tensional, compressive and shear forces experienced by these cells (Wolfe et al., 2012, Calvi et al., 2003, Yeatts and Fisher, 2011, Stolberg and McCloskey, 2009, Glossop and Cartmell, 2009, Nsiah et al., 2014, Toh and Voldman, 2011, Wolfe and Ahsan, 2013, Yourek et al., 2010, Clause et al., 2010). These can be altered through manipulation of the extracellular matrix to which the cells are attached as well as the movement of the medium within which

the cells are cultured (Glossop and Cartmell, 2009, Wolfe et al., 2012, Cormier et al., 2006, Nsiah et al., 2014, Toh and Voldman, 2011, Wolfe and Ahsan, 2013, Yourek et al., 2010, Fok and Zandstra, 2005, Dado et al., 2012).

This expression of cell surface markers indicative of a particular differentiated state has been exploited previously through cell sorting techniques such as magnetic activated cell sorting (MACS) and fluorescence activated cell sorting (FACS) (Schmitz et al., 1994, Malatesta et al., 2000, Herzenberg et al., 1976). Following differentiation of the cells they are selected for based on the display of characteristic cell surface proteins, with only those that display a cell surface protein indicative of a desired cell type being retained (Herzenberg et al., 1976, Malatesta et al., 2000, Schmitz et al., 1994). This has helped to ensure an enriched population of cells with the correct differentiation potential from a heterogeneous stock. However, these methods are limited by their relatively low throughput and high expense which could make them unrealistic for large scale use in industry.

2.3.5. The Effect of Shear Forces on Stem Cell Differentiation

Many research groups have shown that shear forces can impact on both the proliferation and differentiation of ESCs. It has been shown that shear forces encourage the proliferation of stem cells that are seeded onto a surface or grown as aggregates over a time period of several days (King and Miller, 2007, Cormier et al., 2006, Youn et al., 2006, Youn et al., 2005, Fok and Zandstra, 2005, Wang et al., 2013). However, this requires a tight level of control over the shear stresses encountered to ensure that they are high enough to prevent clumping of cells, but low enough so as to not be destructive.

In contrast, it has also been indicated that continuous culture of stem cells subjected to shear forces can also encourage the differentiation of cells (Wolfe and Ahsan, 2013, King and Miller, 2007, Schroeder et al., 2005, Fok and Zandstra, 2005, Yourek et al., 2010, Wolfe et al., 2012, Glossop and Cartmell, 2009, Kreke et al., 2005, McBride et al., 2008, Toh and Voldman, 2011, Nsiah et al., 2014). These effects were generally noted to have an impact after the induction of several days of shear stress, however, some showed an impact on the differentiation of some stem cells after periods of between 30-60 minutes, and even as low as 10 minutes at certain

magnitudes (McBride et al., 2008, Kreke et al., 2005, Glossop and Cartmell, 2009). In summary, these results show that even a relatively low shear stress applied to the cells during their separation could impact on their differentiation, but that the exact outcome is ill-defined and inconsistent across culture conditions.

2.4. Embryoid Bodies

2.4.1. Embryoid Bodies and Their Formation

A common initial step in the differentiation of ESCs is the production of EBs. This is often performed using mass suspension, as this offers a means of generating large numbers of EBs quickly and with a minimum of effort. This is done by seeding ESCs into growth medium devoid of specific differentiation inducing signalling factors at a chosen density of cells and then leaving them to form aggregates over time. In addition to this, multiple other techniques exist for EB formation, some of which are discussed in greater detail in Chapter 2.4.3.

During this formation period ESCs within these aggregates develop into cells from across all three lineages; as occurs during formation in the womb (Kurosawa, 2007, Chen et al., 2014, Robbins et al., 1990, Itskovitz-Eldor et al., 2000). When grown *in vitro* over long periods of time, larger aggregates of cells provide too large a concentration gradient for the nutrients to be able to diffuse across effectively, which therefore leaves the centre of the aggregate bereft of vital nutrients and prone to cavitation (Van Winkle et al., 2012, Tomov et al., 2015). An example image of this is provided in Figure 2.3. This could be circumvented by reducing EB size by limiting aggregation and/or improving mass transfer to the core of the construct. One such method involves the physical mixing of cells to remove concentration gradients and improve consistency of local concentrations of nutrients and waste products; although this encourages the formation of aggregates due to an increased number of cellular collisions, it will also improve mass transfer towards the core of these constructs (Kinney et al., 2012, Carpenedo et al., 2007). This also has a secondary function with respect to encouraging proliferation as discussed previously. Alternatively, EBs can be dissociated following a brief formation period and then seeded down onto a surface to allow their growth as a monolayer or on a scaffold.

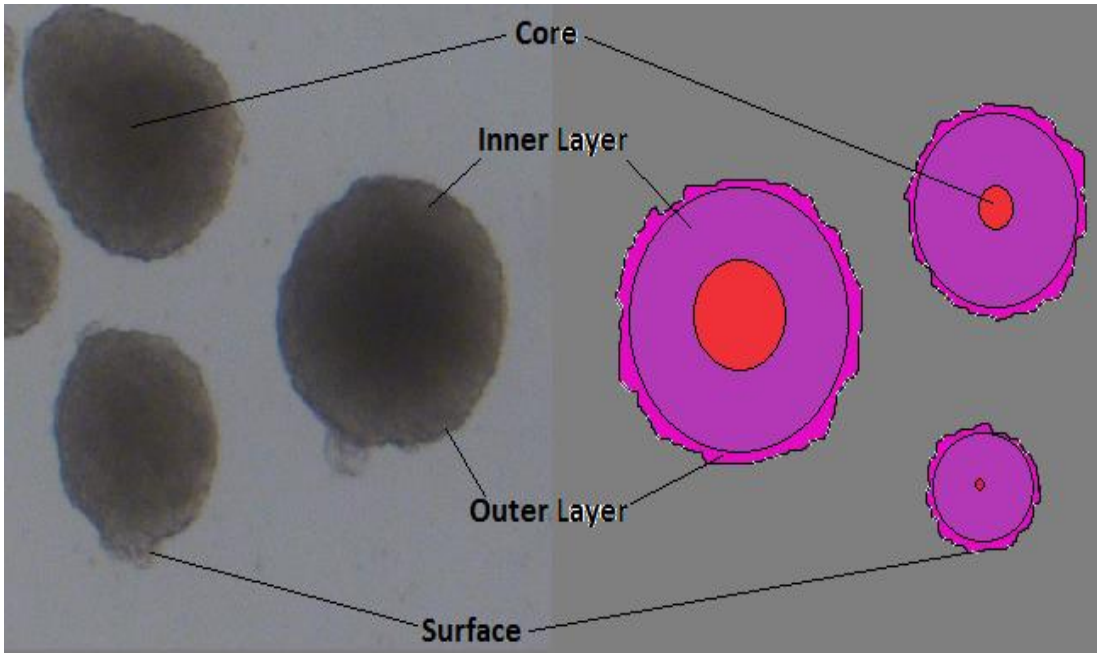

Figure 2.3: This figure shows examples of the internal structure of EBs of different sizes along with an accompanying live image of 72 hour old EBs taken using a phase contrast microscope. On the right is a representative image showing the different layered structures within a fully formed EB, including the cavitation that is characteristic of the core of larger aggregates. The outer layers shown here can also be made out in the image on the left to show the irregular shaped surface of each EB.

However, factors during this initial formation period could still have an impact on the final differentiated product.

Many differentiation protocols involve a dissociation step of EBs following their initial formation (Sidney et al., 2014, Kinney et al., 2012, Gothard et al., 2009, McKinney-Freeman and Daley, 2007, Dang et al., 2002). This negates some of the longer term issues with regards to the mass transfer implications of larger EBs, however, a wealth of research has shown that even over a relatively short period of time during formation there is an enormous degree of size heterogeneity in EBs (Dang et al., 2004, Choi et al., 2010, Xu et al., 2011, Buschke et al., 2013, Hwang et al., 2009, Carpenedo et al., 2007, Kinney et al., 2012). These aggregates vary wildly in size during even a 3-day formation period; this is important because it has been repeatedly shown that EB size can have a profound effect on the subsequent differentiation of dissociated cells.

2.4.2. Impact of Embryoid Body Size on Differentiation

In numerous instances EB size has been shown to impact on the differentiation of the cells within and in some cases the size of the aggregate has been implicated in determining preferential differentiation along certain lineages (Bauwens et al., 2008, Carpenedo et al., 2007, Cha et al., 2015, Choi et al., 2010, Hwang et al., 2009, Moon et al., 2014, Messana et al., 2008, Buschke et al., 2013, Buschke et al., 2012, Valamehr et al., 2008). This has been shown in cases where EBs with a diameter in excess of 200μm have showed increased expression of the endodermal growth factor AFP, EBs with diameter >150μm showed elevated endothelial differentiation and finally, EBs in excess of 330μm diameter showed enhanced cardiogenesis (Choi et al., 2010, Buschke et al., 2013, Hwang et al., 2009). However, due to discrepancies in the techniques used for obtaining different sized EBs a consensus has yet to be reached on exactly what impact size has on the differentiation of EBs (Buschke et al., 2013, Hwang et al., 2009). This is important because it has been shown that the method used for EB formation also impacts on their structure and gene expression (Mogi et al., 2009). Regardless, EB size can have a clear impact on the ability of the cells within an EB to differentiate along a certain lineage or into a specific cell type.

2.4.3. Controlling Embryoid Body Size During Their Formation

Several techniques have been detailed to overcome the issue of variable EB differentiation due to size heterogeneity by controlling the size of EBs during their formation. One such alternative formation technique is the hanging drop, wherein a droplet of medium containing cells no greater than 50μl in volume is placed onto the lid of a petri dish which is then upturned. The force of gravity ensures that the cells all settle to the lowest point of the droplet forcing them to coalesce into a single aggregate (Xu et al., 2011, Ohnuki and Kurosawa, 2013). Unfortunately, each droplet is only capable of forming one EB and so numerous droplets need to be individually seeded in order to make sufficient quantities of EBs to be of clinical use. This greatly restricts the industrial applicability of this technique, although research has focussed on improving this through the use of bioprinting (Xu et al., 2011).

A further alternative is a microwell-mediated technique that follows the same basic principle as the hanging drop. However, instead of using droplets of media

containing cells, the cells are seeded into small cavities generated in part of a material; the cells then coalesce in these areas and form aggregates in each well (Choi et al., 2010, Karp et al., 2007, Sakai et al., 2011, Cha et al., 2015, Pettinato et al., 2014, Hwang et al., 2009). Control of EB size in these instances is impacted by the size of the microwell as the cells cannot grow to be in excess of it and their initial numbers are limited by it. However, this method is quite labour intensive and requires a lot of resources to produce the microwells and collect the subsequently formed EBs and so may have issues with scalability.

In addition to this, a technique has been devised that involves the encapsulation of EBs in agarose beads. The presence of these beads prevents the aggregates from agglomerating with one another by physically obstructing the interactions between cells, including those involving E-cadherin (Dang et al., 2004). As a result, the aggregates are limited in size by the size of the initial bead shell. The resultant aggregates were around 200µm in diameter after 4 days culture for mouse cells and approximately the same size after 8 days culture of human cells, however, while the agarose was shown to be non-toxic the impact of the processing conditions for these experiments was not shown (Dang et al., 2004).

2.4.4. Post-Formation Size-Separation of Embryoid Bodies

In contrast to this, several techniques have instead focussed on separating EBs according to their size after their formation as a heterogeneously sized stock using mass suspension. These techniques generally have the advantage of being easier to manipulate, quicker and having a higher throughput.

One such technique relied on a similar principle to the separation of particles using a mesh; but was developed as a semi-continuous, and therefore more scalable, technique. Three pillars were placed within a channel, with the gap between successive pillars gradually increasing in size; behind each of these gaps was a channel that lead to a separate reservoir. Due to the differing size of the gaps between the pillars the EBs were separated by their size as smaller EBs passed through the initial spaces while larger EBs passed over and progressed to separate reservoirs further along (Lillehoj et al., 2010). The continuous fluid flow provided a throughput of 16µl/min that separated EBs into three size fractions of 0-100µm, 100-

200µm and 200-300µm with a purity of between 80-100% (Lillehoj et al., 2010). This technique represented a great success in adaptability, ease of use and purity of separated product. However, it also had a low throughput of only 16µl/min and showed little potential for scaling as attempts to increase the throughput of this technique meant that it became destructive to the EBs it was separating.

Another alternative also utilised microfluidics to separate EBs via sheathless, asymmetric, curving channels. This was shown to have a throughput of up to 1000µl/min and could separate two fractions of EBs of 247 ± 20µm and 295 ± 12µm size with around 80% purity (Buschke et al., 2012). While this technique has a high throughput it is yet to be refined to separate out multiple distinct size fractions of a discrete nature from across the full range found in the stock.

Finally, a method was devised that used flow cytometry to separate EBs according to their size. This was able to generate three size fractions of EBs of <250µm, 250-330µm and >330µm with a purity of between 80-90% (Buschke et al., 2013). However, due to the reliance on a flow cytometer to perform this separation this would represent an expensive and relatively low throughput separation technique.

While all of the previously mentioned techniques show promise, as yet there has not been identified a cheap, adaptable, easy-to-use and high throughput technique for separating EBs according to their size. As a result, there is still a great deal of work that can be done to address this shortcoming and so provide a high throughput, scalable system to improve the purity of differentiated cells generated from stocks of ESCs.

2.4.5 Further Uses for a Size Separation Technique of Mammalian Cell Aggregates

While the focus of this thesis is on separating out aggregates of ESCs to influence their differentiation, the techniques shown here could also be applied to a raft of other aggregates of mammalian cells due to their similarity in structure. In addition, any difference in physical characteristics could be utilised to assist in the refinement of these techniques to separate these new tissue types. It is hoped that the techniques discussed here could be applied to a variety of different tissue types and therefore help solve a plethora of other commonly encountered cell culture

problems with aggregates of cells including mammospheres, pancreatic islets and neurospheres. In the first instance, the size of mammospheres has been shown to be indicative of the potential of these cells to reconstitute the mammary gland when re-transplanted *in vivo (*Machado *et al., 2013)*. Aggregate size has also been shown to impact on the viability and proliferation of Neurospheres, which has resulted in techniques being designed to separate them by size to help control this (Ge et al., 2012, Mori et al., 2006, Ng and Chase, 2007). In addition, the size of pancreatic islets of Langerhans has been shown to impact on their transplantation outcomes as well as their functionality and so size-separation techniques are being explored to improve transplantation outcomes (Nam et al., 2010, Lehmann et al., 2007). As a result, the techniques presented here could impact on a number of parallel avenues of research and aid in the development of positive outcomes for a host of different fields by allowing size control of aggregates from a range of different tissues.

2.5. Use of Terminal Falling Velocity as Predicted by the Stokes Equation for Size-Separating Particles

The Stokes equation dictates that the TFV of a single particle settling in a fluid is related to its diameter and density. In addition, this TFV is also influenced by the acceleration due to gravity, as well as the density and viscosity of the fluid. In any set of experiments these final three factors will be kept constant, therefore, assuming constant density, the TFV of a particle will be dependent on its diameter. The TFV of a particle is reached when the opposing drag force induced by the movement of the particle through a fluid becomes equal to the acceleration of the particle; when this occurs the particle can no longer accelerate and so has reached a steady speed. This is usually reached quite quickly for small particles, particularly on the micrometre scale.

Fluid density is an important factor in the separation of cells using similar such techniques. For example, density gradient centrifugation has been used in a number of studies to separate out certain populations of cells according to their density by fractioning fluids of different densities on top of one another and forcing the cells to settle into them using a centrifuge until they find a point in the column that is equal to their density and so remain there (Soeth et al., 2005, Zhou et al., Parsons et al.,

2012). As a result, the fluid density was kept consistent for all of the experiments that were performed.

As particles in these experiments will be comprised of only a single material during each experimental run the particle density should remain constant. Consequently, putting the theory of the Stokes equation into practice should allow for the separation of EBs according to their size. In order to do this, certain parameters need to be further explored to ensure that the Stokes equation will apply to EBs and therefore be applicable for this purpose.

The particle Reynold's number (Re_p) of the vast majority of the particles that will be used in these experiments was calculated to be <0.3; as a result, the particles are said to be within the Stokes law region. This means that the predictions made of their settling velocity using the Stokes equation should be accurate to within 3% of the actual collected results for any individual particle (Rhodes, 2008). It should be noted that this is not a single particle system, however, as there are a multitude of particles from across a range of different sizes. Research has shown that individual particles suffer from hindered settling in a multiple particle system because of their interactions with one another (Masliyah, 1979, Krishnamoorthy, 2010, Basson et al., 2009). This is caused by the effects of the displacement of fluid by some particles impacting upon the settling of others during their sedimentation; as a result, in a fluid the upwards liquid flow rate caused by a settling particle will be considered equal to the downwards settling rate of that particle (Lapidus and Elgin, 1957, Krishnamoorthy, 2010). This means that the effective settling velocity of individual particles will be lower compared to the predictions made by the Stokes equation, particularly in the case of the smaller particles. This is because the larger particles will settle faster and in doing so cause an upward liquid flow rate that is in excess of the TFV of the smaller particles.

It was suggested in some of the experiments described above that for a bi-disperse system of particle sizes the column will effectively split into several fractions. The very top fraction should be composed of a clear liquid as all particles will have settled below this; below is a fraction containing only the small particles, then a fraction containing particles from both the large and small fraction and finally the sediment

(Al-Naafa and Selim, 1992, Basson et al., 2009, Krishnamoorthy, 2010). However, while a poly-disperse system of particles is likely to be more complicated, the results discussed here give some insight into what should be expected of the column used in the experiments within this thesis.

In addition, it was shown that the effect that the multiple particle system has is influenced by the number of particles in the system. It has been stated that the predictions made were less accurate as the concentration of particles increased. This was because higher concentrations of particles will suffer from more hindered settling than lower concentrations due to an increased number of inter-particle interactions; accordingly, where concentrations are very low the TFV is approximately the same as for an individual particle (Batchelor, 1982, Krishnamoorthy, 2010, Al-Naafa and Selim, 1992).

2.5.1. Use of Expanded Bed Reactors for Size Separating Particles

Because of the Stokes equations predictions for different sized particles having different TFV's, techniques have been developed to exploit this for the purposes of size separation of a heterogeneously sized stock of particles. This has primarily been performed using expanded bed reactors (EBR's). These reactors pass an upward fluid flow through a packed column of particles for various experimental gains, depending on the desired outcome. During such experiments it has been consistently noted that the particles are separated into size fractions along the length of the column, with the largest particles consistently being found at the bottom of the column and the smallest particles being found at the top at any given flow rate (Lin et al., 2013, Willoughby et al., 2000, Taheri et al., 2012, Yun et al., 2004, Tong and Sun, 2002, Ng and Chase, 2007, Yun et al., 2005). This size separation occurs because when the fluid velocity is in excess of the TFV of an individual particle it will accelerate upwards along the length of the column until either the fluid velocity no longer exceeds the TFV, or the particle elutriates out of the top of the column. As the TFV is greater for particles with a larger diameter, over time these will settle to lower points in the column, while smaller particles will move upwards as a result.

A key factor in the use of EBR's is that the fluid velocity through a pipe, calculated as fluid volumetric flow rate divided by the cross-sectional area, does not account for

the presence of particles (Lin et al., 2013, Willoughby et al., 2000, Yun et al., 2004, Yun et al., 2005). As a result, the presence of a large number of particles in an EBR will drastically affect the fluid velocity, which will in turn affect the movement of the particles within. This is because the presence of the particles in the column reduces its effective cross-sectional area by reducing the volume that can be occupied by the fluid (Lin et al., 2013, Willoughby et al., 2000, Yun et al., 2004, Batchelor, 1982, Yun et al., 2005, Ng and Chase, 2007). Therefore, at the same net flow rate the fluid velocity will be higher in the presence of more particles. The presence of these particles is a quantifiable factor known as voidage; defined as the volume that exists between particles occupied by a liquid, and is represented as a decimal between 0 and 1. At a voidage of 1 there are no particles present in the liquid, while at a voidage of 0.5 half of the volume of the column is occupied by particles and half by the liquid. As a result, by dividing the fluid flow rate by this number a more accurate indication of the fluid velocity is provided by accounting for the presence of these particles.

2.5.2. Use of Expanded Bed Reactors for Size Separating Cell Aggregates

Because of the efficacy of EBRs for separating out particles into size fractions a set of experiments was performed to adapt this technique for separating out cells. This was initially performed on flocs of yeast and then expanded to aggregates of Neural stem cells, a type of adult stem cell that forms aggregates known as neurospheres (Ng and Chase, 2007). This technique met with some success and showed an ability to influence the size distribution of collected fractions from the column (Ng and Chase, 2007). The particle size distribution (PSD) of collected particles was dependent on both the flow rate and column height that was utilised during the collection. However, this research failed to explore what effects the differences in experimental set-up had on the separation process such as the different settled bed heights used between experiments and the impact of time on this process. Furthermore, no comprehensive exploration of this technique was detailed for the separation of multiple size fractions of discrete particles. As a result, this technique shows clear promise for the size-separation of EBs and therefore has the potential to improve the reproducibility of differentiation in ESC's by removing this variable.

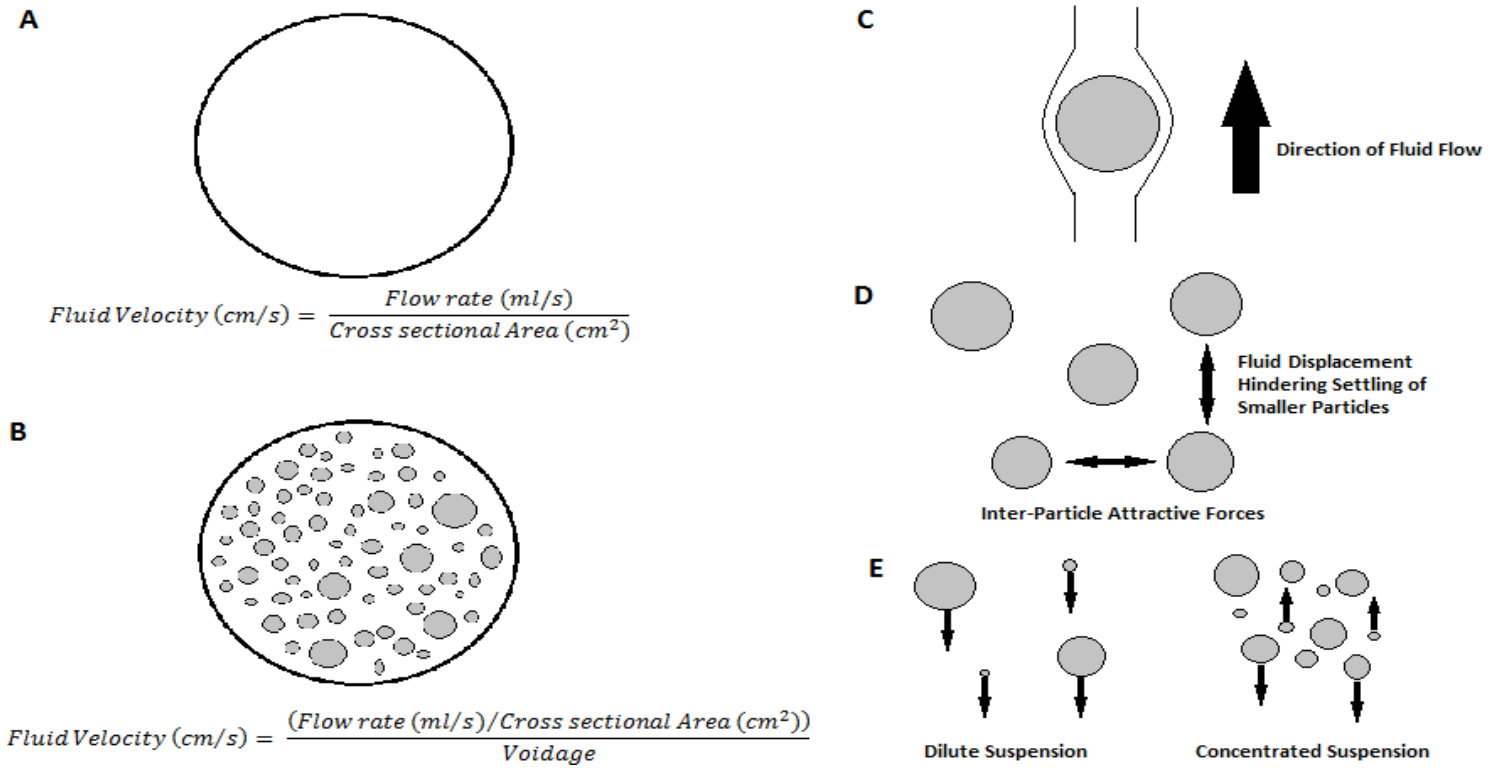

Figure 2.4: Figure 2.4A shows the equation for calculating the fluid velocity in an unoccupied column at a set flow rate; while figure 2.4B shows how this is impacted by the presence of particles within the column. Figure 2.4C shows the motion of fluid around a settling particle whose Re_p is within the Stokes region. Figure 2.4D shows the interactions between settling particles in a column; it shows attractive electrostatic interactions between particles and the hindrance of settling due to the fluid disruption by settling particles shown in Figure 2.4C. Finally, Figure 2.4E shows the how the fluid displacement shown in Figure 2.4C impacts on the settling of particles; this highlights how at low concentrations particles settle individually, but that increased concentrations negatively impact the separation of smaller particles due to fluid displacement.

2.6. Aims and objectives

The principle aim of these experiments is to determine a novel, tuneable, high throughput, reproducible and scalable size separation technique for collecting multiple size fractions EBs. The hypothesis is that, like other particles, EBs will adhere to the predictions made by the Stokes equation and so their terminal falling velocity will be proportional to their diameter, thus allowing for the development of a technique that will size-separate them based on this relationship.

During these experiments the following objectives were intended to be met:

- Develop a non-scalable mesh separation technique
- Ascertain suitable EB size fractions for collection for all techniques
- Identify some of the intrinsic size-dependent characteristics of EBs
- Highlight experimental factors that will impact on EB separation using an expanded bed reactor
- Assess the potential of this technique using an Artificial Neural Network
- Refine this technique to collect multiple size fractions in a reproducible, scalable and high throughput fashion

Chapter 3

Methods and Materials

Methods and materials that were used consistently throughout the experiments presented here are included in this section. Any elements that occurred singularly in a particular set of experiments appear solely in the chapter to which those experimental results belong. This ensured that the size separation techniques that were developed in these experiments were kept with the results that were collected from them, along with any other pertinent information.

Unless specifically stated all reagents were purchased from Sigma Aldrich. All reagents were filtered through 0.22µm filters to ensure sterility (Thermo Fisher Scientific, UK) and pre-warmed to 37^{o}C in a water bath prior to coming into contact with cells.

3.1. Mammalian Cell Culture

3.1.1. Culture Apparatus and Reagents

3.1.1.1. Cell Culture Equipment

T25 tissue culture flasks (Nunc, Thermo Fisher Scientific, UK) were primarily used for cell culture. Prior to the introduction of cells they were coated in a 0.1% w/v solution of bovine gelatin (G1392) overnight at 20^{o}C. The same procedure was performed prior to seeding of cells in tissue culture treated plastic 6-well plates (Falcon, BD Biosciences, UK) for the immunohistochemistry and growth rate assays. The cells were then cultured in a Sanyo incubator with 5% CO_2 at 37^{o}C.

3.1.1.2. Microscopes

Phase contrast microscopy was used to determine confluency of cells during their continuous passage, as well as cell counts using a haemocytometer. A Nikon Eclipse TS100 inverted microscope was used along with an attached imaging screen with a Nikon Digital Sight DS-Fi12 imaging system to record images of EBs for particle size distributions.

Fluorescence microscopy was performed for the immunohistochemistry experiments using a Leica DMRBE inverted microscope and images were captured through Volocity imaging software. Further details of the settings used with this microscope are described in Chapter 4.2.5.

3.1.2. Cell type

3.1.2.1. Feeder Free Embryonic Stem Cells

Feeder free mouse embryonic stem cells (mouse ESCs) of the CGR8 cell-line were used for these experiments due to their similar characteristics to human ESCs as well as their ease of use in comparison to feeder-dependent mouse ESCs. However, these cells may show some differences in cellular activities as a result of alterations to their physical and chemical environment. Feeder-free mouse ESCs are ESCs that have been adapted so that they can be cultured without feeder layers of fibroblasts to support their continuous culture and prevent their differentiation. This was made possible by the addition of the protein leukaemia inhibitory factor (LIF) at a concentration which is sufficient to prevent differentiation in these cells; this concentration is double that which is required for feeder-dependent mouse ESCs. These cells are derived from the inner cell mass of a pre-implantation mouse embryo (3.5 days) and are a germ-line competent cell line. The cells were provided by Dr Glen Kirkham, University of Nottingham, and were between passage 10-30 for all experiments.

3.1.3. Culture Media

3.1.3.1. Feeder Free Mouse Embryonic Stem Cell Medium

Feeder free mouse ESCs were cultured in Dulbecco's Modified Eagle Medium (DMEM) (42430-25, Gibco®, Invitrogen, UK) containing 1% Penicillin/Streptomycin (Pen/Strep) (15070-063, Gibco®, Invitrogen, UK), 500µM β-Mercaptoethanol (31350-

010, Gibco®, Invitrogen, UK), 10% Foetal Calf Serum (FCS) (500-30502, Labtech International Ltd, UK), 2mM L-glutamine (L-Glu) (G7513) and 1000units/ml leukaemia inhibitory factor (LIF) (ESGRO® ESG1106, Millipore, UK). DMEM acts as the base medium for the culture and proliferation of cells *in vitro.* It primarily contains glucose to act as an energy source, N-2-hydroxyethylpiperazone-N-2-ethanesulfonic acid (HEPES) to act as a pH buffer and L-Glu as an essential amino acid. The L-Glu already present in the DMEMwas further supplemented to accommodate the high rate of growth encountered in ESCs. The medium was further supplemented with FCS to supply a multitude of as yet ill-defined factors that are necessary for cellular proliferation. Finally, the LIF was added as a pluripotency factor for ESCs to ensure that they remain undifferentiated and continue to proliferate accordingly.

3.1.3.2. Growth Medium

Growth medium was used to allow for the formation of Embryoid Bodies (EBs) via mass suspension. This was the same as the above detailed medium with the exception of LIF, which is not present in growth medium in order to allow the mouse ESCs to begin the process of differentiation.

3.1.3.3. Cryopreservation Medium

Aliquots of mouse ESCs were frozen at -80^{o}C in cryopreservation medium (CPM) to make stocks that could be thawed when required. The cryopreservation medium consisted of 10% dimethyl-sulfoxide (DMSO (D5879)), 20% FCS made up with DMEM. DMSO is a commonly used solvent for cryoprotection as it reduces the likelihood of ice crystals forming both within and around cells that could prove damaging. It is a polar aprotic solvent that acts as a cryoprotectant by displacing water molecules and therefore reducing their ability to form ice crystals. As DMSO itself is toxic it was important to remove cells from it as quickly as possible when thawing.

3.1.4. Continuous Culture of Embryonic Stem Cells

Mouse ESCs were cultured in T25 flasks in 5ml of mouse ESC medium in the incubator described above. The medium was replaced every 24 hours with fresh medium that had been pre-warmed to 37^{o}C in a water bath. Every 48 hours the cells were passaged to ensure that the cells did not grow over-confluent. Cells were washed twice in 5ml of pre-warmed phosphate buffered saline (PBS) and then incubated with

2ml of Trypsin (T4549) / ethylenediaminetetracetic acid (E5134) (TE) for 5 minutes. This was sequestered with 3ml of mouse ESC medium and the mixture transferred to a centrifuge tube to undergo centrifugation at 180g for 5 minutes. Following this the medium was aspirated off and replaced with fresh mouse ESC medium that was used to resuspend the cell pellet into a single cell suspension. This suspension was then seeded into 4ml of mouse ESC medium in a gelatin-coated T25 flask at an appropriate seeding density of around 1:4-1:6 depending on the confluency at the time of passage. This was determined prior to the beginning of the passage procedure by eye using an inverted light microscope.

3.1.5. Cell counts

Cell counts were performed using a 10µl suspension of cells in the relevant medium using a haemocytometer. A single cell suspension was resuspended in 2ml of growth medium and a 10µl sample taken to be mixed with 10µl of Trypan blue. This was done so that a count could be made of the number of viable cells as those cells that do not stain blue are viable and counted. Any stained cells are discounted as Trypan blue can only enter cells that have permeable membranes, such as those that are necrotic or undergoing apoptosis, and so by staining the cells this highlights that they are non-viable. The 10µl suspension of cells was then pipetted underneath the cover slip and a cell count performed using an inverted Nikon microscope. Counts were taken from 4 sections of the haemocytometer and an average taken. This was then multiplied by 10,000 to give the total number of cells per ml. Cells that came into contact with the top or left hand edge were counted, those that came into contact with the bottom or right hand edge were not. This is demonstrated in the Figure 3.1 below.

3.1.6. Cryopreservation and Reanimation

Cells were removed from liquid nitrogen storage for reanimation and thawed rapidly in a water bath set to 37^{o}C. The 1ml aliquot of cells was then aspirated by pipette and deposited in 9ml of pre-warmed mouse ESC medium. This was quickly centrifuged at 180g for 5 minutes. The media was then aspirated off and the resultant pellet resuspended in 5ml of mouse ESC medium before being seeded into a gelatin-coated T-25 flask and continuous culture begun as described above.

Continuous culture was performed for several passages and a large number of flasks cultured to allow for banking of a large number of cell aliquots. A confluent flask of cells underwent passage as described above using growth medium in place of mouse ESC medium until the resuspension step. At this point a viable cell count was performed using Trypan blue as described above. The ESCs were then mixed with CPM and aliquoted into 1ml cryovials containing 1,000,000 cells per aliquot. The cryovials were then stored in a polystyrene box and stored at -80°C for a period of 48 hours to cool at a rate of 1°C per hour. Once cooled to -80°C the cryovials were transferred to long term storage in canisters containing liquid nitrogen to keep them at a temperature of around -200°C.

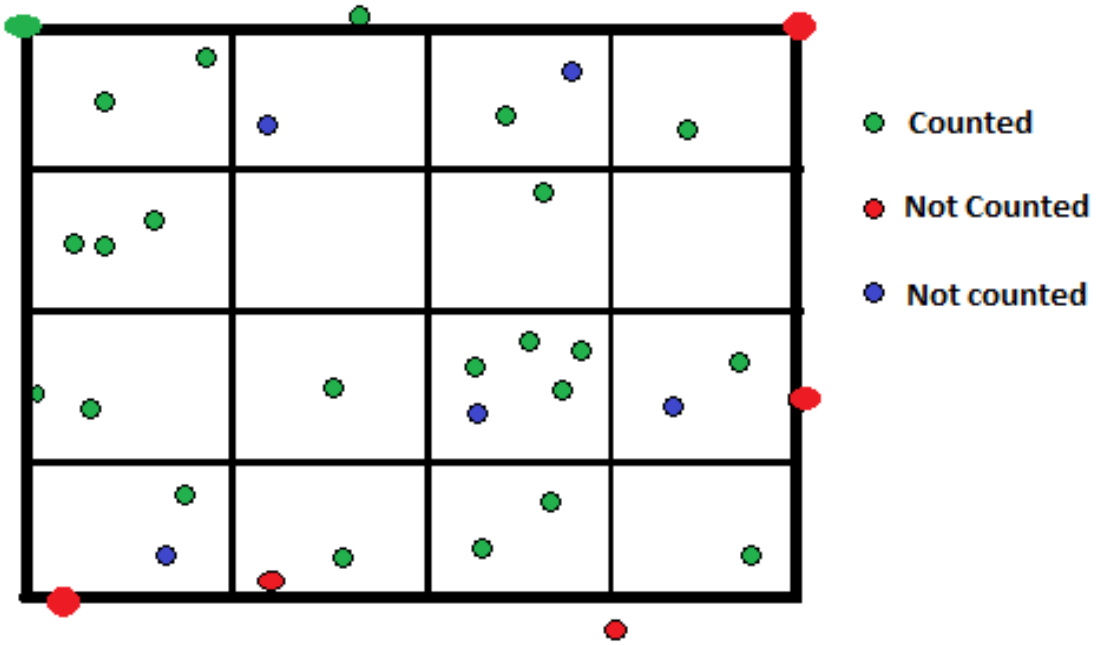

Figure 3.1: A figure to show the use of a haemocytometer for cell counts. Cells within the bounds of the 4x4 grid or touching the top or left hand edge (coloured green) were counted. Cells outside of the grid or touching the bottom or right hand edge (coloured red) were not counted. Cells coloured blue were also not counted as this is indicative of Trypan blue staining showing that these cells were non-viable.

3.1.7. Embryoid Body Formation by Mass Suspension

A confluent flask of cells underwent passage as described above followed by a cell count using growth medium in place of mouse ESC medium until the resuspension step. Cells were then reseeded at a concentration of 2,000,000 cells in 10ml of

growth medium in a petri dish (Thermo Fisher Scientific, UK). EBs were then allowed to aggregate in an incubator undisturbed for 72 hours under normal growth conditions.

3.1.8. Growth Rate Assay

EBs were produced as described above using mass suspension formation for use in the CellTiter 96® aqueous one solution cell proliferation MTS (3-(4,5-dimethylthiazol-2-yl)-5-(3-carboxymethoxyphenyl)-2-(4-sulfophenyl)-2H-tetrazolium) assay. These aggregates were then dissociated with TE as has been described previously and cells seeded in triplicate at 10,600 cells/cm^2 onto gelatin-coated wells of a 6-well plate. They were then cultured in growth medium for 72 hours and a reading was taken every 24 hours. After each elapsed time-period the media was removed from each well and replaced with 100µl per well of MTS (G3580, promega, UK) made up with growth medium to 1ml. This was performed in tandem with a calibration curve, shown individually in each respective chapter, of a known number of cells as determined by a cell count with a haemocytometer under identical conditions. All samples were incubated for 1 hour and then 100µl of each sample was transferred to a 96-well plate in triplicate. Absorbance readings were taken using a plate reader at 490nm while a reference wavelength of 650nm allowed for the removal of background noise. Cell counts were determined by comparison to the calibration curve collected with each data set.

3.1.9. Particle Size Analysis

Particle size analysis was performed using free to download ImageJ software from the NCBI website to calculate the maximum Feret diameter; anything below 10µm^2 was disregarded as background noise. Feret diameter is defined as the greatest distance between two external edges of a particle. This was chosen to try and reduce the impact of the varying size and irregular shape of EBs that would make it difficult to maintain consistency between readings. Further, the orientation of settling particles is related to their longest edge, with this always being perpendicular to the direction of motion, thus allowing for a consistency in the Stokes equation experiments. Finally, larger EB diameter is correlated to increasing core necrosis and it was decided that measurement of the maximum of this would be most

representative across all particles that were being measured (Itskovitz-Eldor et al., 2000, Gothard et al., 2009). To generate images to perform this on, pictures were taken using an inverted Nikon imaging microscope at varying degrees of magnification with a scale bar included. This scale bar provided a standard for the ImageJ software to work from and was collected for each set of experiments at every magnification used.

3.1.10. Statistical Analysis

Where an experiment says that n=3 this means that the results shown here were taken from 3 independent experiments. Determining significance between two populations within a sample was done using Student's t-test. Determining statistical significance between multiple samples in a single experiment was performed using one way-ANOVA. Once determined, this was followed by a Tukey's post hoc test to detail which means were significantly different from one another and to what extent. Significance is determined as *** $P \leq 0.001$, ** $P \leq 0.01$ and * $P \leq 0.05$.

Chapter 4

Impact of Embryoid Body Size on Embryonic Stem Cells

4.1. Introduction

Proliferation and differentiation have been shown to have an inverse relationship during the development of stem cells with more differentiated cells generally being less proliferative and vice versa (Watt et al., 2008, Pino et al., 2012). As a result, the potential of cells to proliferate and the presence of differentiation-specific markers can be used to provide insight into the differentiated state of a population of cells (Tamm et al., 2013, Losino et al., 2011, Ruiz et al., 2011). Germ layer markers for the endodermal, ectodermal and mesodermal lineages are sometimes used to highlight the differentiation potential of a population of ESCs (Tamm et al., 2013, Poh et al., 2014, Choi et al., 2010, Cha et al., 2015). Both of these factors are important for the industrial application of ESCs as the purity of the final differentiated product must be as high as possible for *in vivo* implantation and a large number of cells are required for use in tissue regeneration. This is exemplified by the fact that between $1x10^5$ and $1x10^{10}$ differentiated cells are potentially required for use in the treatment of a range of illnesses such as stroke, ocular degeneration and critical sized bone defects in a single patient (Muschler et al., 2004, Chau et al., 2013, Trounson and McDonald, Trounson et al., 2011, Schwartz et al., Zweigerdt, 2009, Marolt et al., 2010). As such, the techniques tested here will be assessed for their capacity to collect, or potential to collect, up to $1x10^{10}$ cells per run.

This research began by determining the inherent properties of EBs during their formation by mass suspension. This was followed by the conception of a simple separation technique to provide means of comparison for subsequent, more advanced separation processes. The initial separation technique involved the use of different porosity meshes to separate out EBs according to their size; as this is a method that has been utilised for size separation of other types of particles (Konert and Vandenberghe, 1997, Mora et al., 1998, Salama, 2000, Barbanti and Bothner, 1993). In addition, allowed for a series of experiments to be performed in order to determine desirable size fractions that can collected from a heterogeneously sized stock, their inherent size-dependent characteristics and what impact EB size had on ESCs.

4.2. Materials and Methods

Unless specifically stated all reagents were purchased from Sigma Aldrich.

4.2.1. Cell Culture

Basic cell culture was performed as described in the Materials and Methods section (Chapter 3.1.4) to produce a heterogeneously sized population of EBs via mass suspension. Following this cells were washed with PBS, dissociated using TE into a single cell suspension and a cell count performed using Trypan blue to exclude dead cells. Cells were then seeded onto gelatin-coated tissue-culture treated plastic-ware for growth rate experiments and immunohistochemistry at a seeding density of 10,600 cells/cm^2.

4.2.2. Changes in EB size over time

EB formation was performed as detailed in the Materials and Methods section (Chapter 3.1.6) at a seeding density of 200,000 cells/cm^2 (2, 000, 000 cells/petri dish). The point at which the cell-laden petri dish was first stored in the incubator was determined to be time 0. Subsequently images were taken of the EBs every 24 hours using a Nikon inverted phase contrast microscope and particle size distributions (PSD's) were performed by recording the Feret diameter as documented by ImageJ software. A new petri dish was used for every 24-hour period to ensure that the removal of the dish from the incubator and subsequent conditions endured while imaging did not impact on the results. After 72-hours any remaining dishes of EBs were collected using a serological pipette, underwent brief centrifugation to ensure no EBs were lost and re-seeded in 10ml fresh media in a new petri dish; as would be done experimentally for differentiation experiments. All readings were collected in triplicate.

4.2.3. Mesh size-separation technique

EBs were cultured to make a heterogeneously sized stock in petri dishes. After 72-hour formation by mass suspension these EBs then underwent a size separation using two different porosity meshes. The largest mesh had a pore size of 180µm (Merck Millipore - NY8H02500), and the smallest a pore size of 70µm (CLS431751-50EA). EBs were collected from the petri dish using a serological pipette and then washed

through the large mesh, with the flow through being collected in a falcon tube. The mesh was washed with 1ml of PBS in its current orientation to ensure all correctly sized EBs had filtered through. The mesh was then inverted and washed again to collect any entrained EBs off the mesh into a clean falcon tube; this fraction represented the >200µm EBs. The flow through was then collected again using a serological pipette and the process repeated, this time through the smaller mesh. Following this step, the EBs that were retained and collected from the 70µm mesh represented the 100-200µm fraction, while the flow through of this step represented the <100µm EB fraction. Images of each collected fraction were then taken using a Nikon inverted microscope and PSD performed by recording the Feret diameter as determined by ImageJ. These sizes of meshes were selected based on the availability of appropriately sized meshes near the desired minimum size of particle and tested compared to other similarly sized meshes to select the best performing mesh for each size fraction. By using meshes slightly smaller than the lowest desired size it was hoped that there would be limited numbers of mis-oriented particles able to pass through into the elutant.

4.2.4. Cell Growth Assay

EBs were separated into four groups; the three size fractions collected using the mesh and a control group that had not undergone separation and so contained the full range of EB sizes found in the stock. These EBs were then dissociated with TE as has been described in the Materials and Methods section (Chapter 3.1.4). After each elapsed time-period the medium an MTS assay was performed as described in the materials and methods section (Chapter 3.1.8). This was performed in tandem with a calibration curve, shown in Figure 4.1.

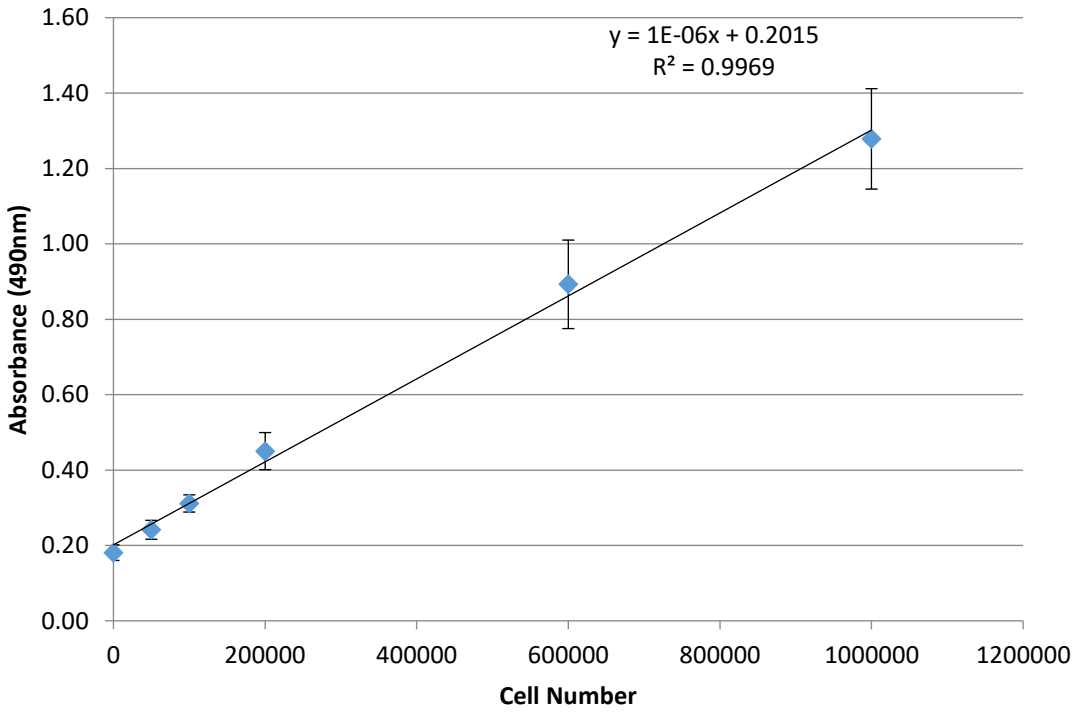

Figure 4.1: Calibration curve for the MTS assay showing the cell number that corresponds to each absorbance reading collected using a plate reader at 490nm. Cell numbers of 50,000, 100,000, 200,000, 600,000 and 1,000,000 were used to produce the data, collected in triplicate for each day of each experimental run. The data shown here is the average of all collected data for these calibration curves, n=3x3, with error bars showing SEM.

4.2.5. Immunohistochemistry

72 hour EBs were cultured and then dissociated with TE to allow seeding onto gelatin-coated tissue culture treated plastic at a seeding density of 10,600 cells/cm^2. The dissociated cells were then cultured in growth medium and fed every 2 days. After 7 days this was followed by a PBS wash (twice) and fixation in 200µl of 3.7% paraformaldehyde per well for 20 minutes. This was then followed by a wash with deionised water and storage at 5-8^{o}C in 2ml deionised water overnight.

Water was removed from each well and permeabilisation performed of cell samples via incubation with 400µl of 0.1% Triton X-100 in PBS per well for 30 minutes. This was followed by a PBS wash; all washes were performed using 2ml per wash and in triplicate. Blocking was then performed using a PBS solution containing 3% goat serum (G9023) and 1% Bovine Serum Albumin (BSA) for Nestin and GATA-4 and a PBS solution containing 3% donkey serum (D9663) and 1% BSA (A2153) for Brachyury; in

each case this was done for 30 minutes. This was followed by a wash in 1% BSA in PBS and then the addition of 400µl of each primary antibody, diluted 1:1000, to the corresponding wells for overnight incubation at 4^{o}C. For mesodermal cells this was anti-Brachyury (R&D- AF2085), for endodermal cells this was anti-GATA-4 (Abcam- Ab81755) and for neural cells this was anti-Nestin (Abcam- Ab63398).

The following day the primary antibodies were removed, followed by a wash in 1% BSA in PBS. This was then followed by the incubation of 400µl of a 1:200 dilution of each secondary antibody for 2 hours at room temperature. The antibody used for anti-Brachyury was a red Donkey Anti-goat AlexaFluor® IgG fluorophore (Invitrogen- A11056), for anti-Nestin this was a red goat anti-chicken AlexaFluor® IgG fluorophore (Invitrogen- A11040), for anti-GATA-4 this was a green goat anti-rabbit AlexaFluor® IgG fluorophore (Invitrogen- A11008).

This was then followed by a further 1% BSA in PBS wash with all wells of the experiment then being incubated with 1:1000 Hoechst 33258 solution for 15 minutes at room temperature and away from direct sunlight. The Hoechst was removed and another wash performed before 500µl of PBS was added to every well in preparation for immediate imaging. For every antibody, controls were used that consisted of only the primary or secondary antibody to ensure that there was no auto-fluorescence or non-specific binding. These underwent the process described as above for the full experimental runs, except with the removal of one of the antibodies, which was replaced with 1% BSA in PBS during the incubation step.

Subsequently, imaging was performed using a fluorescence microscope. The red fluorophores were imaged at 556nm absorption and 573nm emission and the green fluorophore was imaged at 488nm absorption and 519nm emission while the nuclear staining Hoechst was imaged at 350nm absorption and 500nm emission. This experiment was performed once due to time constraints with the resultant images shown here.

4.3. Results

4.3.1. EB Population Characteristics

Initial experiments were conducted to determine how EBs grow over a 120-hour formation period. This was performed to highlight the heterogeneity of EB size after formation by suspension culture and to show how the PSD of the whole stock is altered over time. The results are shown in Figure 4.2, with each PSD sitting adjacent to a representative picture of the EBs taken from those used to calculate their size. It is clear that after every formation time the diameter of aggregates follows a skewed distribution due to the extensive number of EBs that are at the larger end of the size spectrum.

After 24-hours the vast majority of EBs were below 200µm in diameter; with 56% of aggregates being below 100µm. This continued until 72-hours after which the number of EBs in excess of 200µm finally exceeded 10%. After 96 hours, this became 29%, while after a 120-hour formation period 56% of EBs exceeded 200µm. Furthermore, after 96 hours only 6% of EBs were in excess of 300µm diameter, increasing to 17% after 120 hours.

Figure 4.3 shows the mean diameter of the aggregates shown in Figure 4.2 over the 120-hour formation period; with Figure 4.3A giving the standard error for each time point and Figure 4.3B giving the D10 and D90 around the mean. As would be expected, the mean diameter increased steadily with increasing time, with a notable exception of between 48-72 hours where it remained consistent. After 24 hours, the mean diameter was 99µm, increasing to 133µm after 48 hours and 140µm after 72 hours. After this the mean diameter rapidly increased to 162µm after 96 hours and 218µm after 120 hours. The error bars in Figure 4.3A make it clear that the results were consistent between runs; specifically after 48 hours, 72 hours and 96 hours.

Figure 4.3B provides more insight into the reasons behind these changes in mean diameter by showing the changes in D10 and D90 over time; these are the 10^{th} percentile and 90^{th} percentile of the diameter. After 24 hours the span was only 86µm, but this then increased to 108µm after 48 hours, 109µm after 72 hours, 178µm after 96 hours and 224µm after 120 hours.

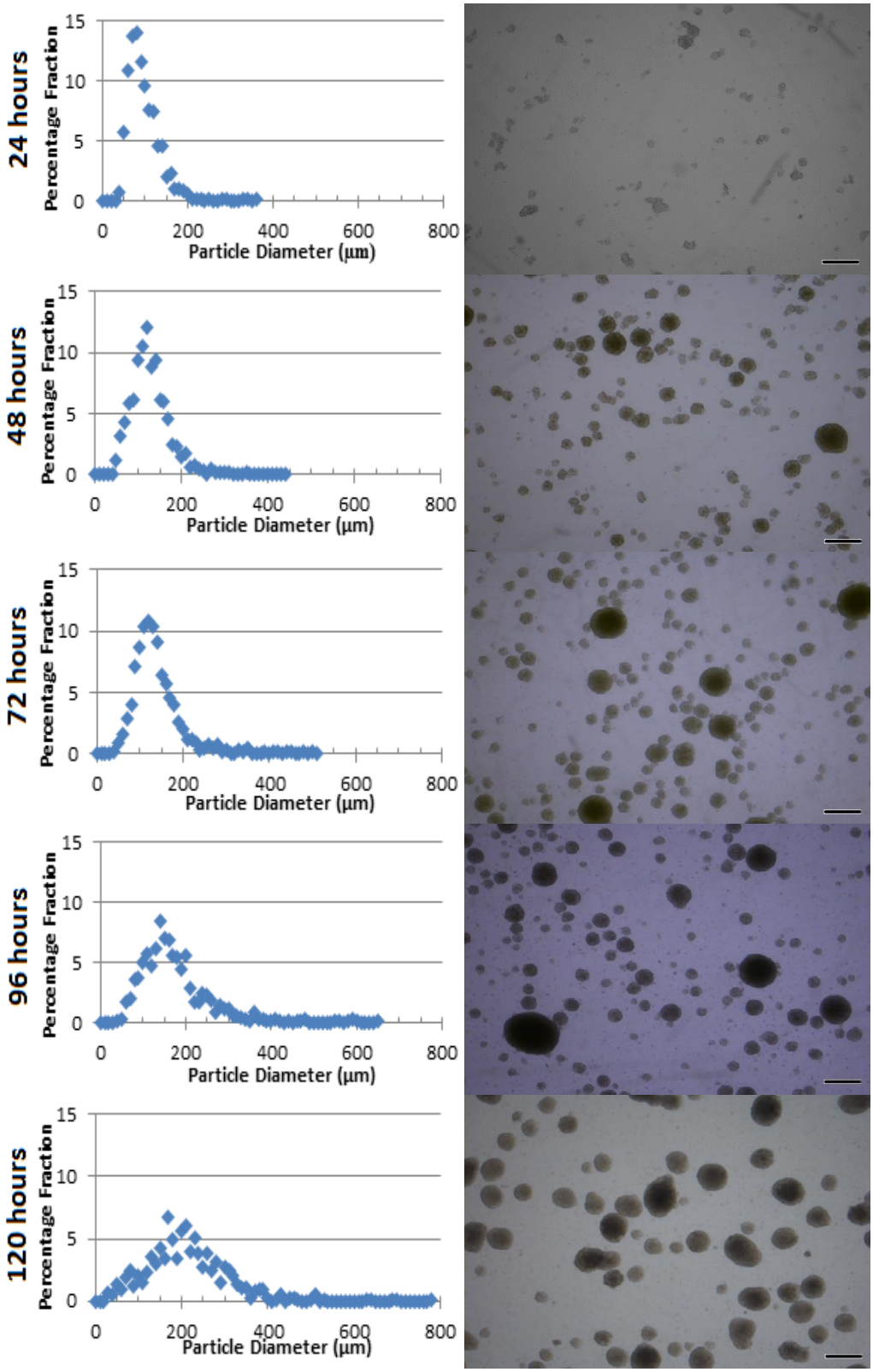

Figure 4.2: Particle size distribution of EBs cultured over 120 hours in a petri dish with growth medium along with accompanying images of their size. All experiments were performed in triplicate (n=3) with representative images and PSD collected using Feret diameter calculated by ImageJ. Scale bars are 300µm.

These results show that the aggregates became more heterogeneously sized with increasing formation times. However, the D10 for each of the collected fractions, with the exception of 62µm after 24 hours, was fairly consistent, increasing from 81µm after 48 hours to 104µm after 120 hours. This shows that there were still a large number of smaller aggregates in the EB stock after every time period. Therefore, the increase in mean diameter with increasing time must have been caused by something other than the complete agglomeration of the smallest EBs. What was clear due to the increasing span is that the increase in mean diameter must therefore be caused by an increasing number of larger particles. However, as the D10 was not increasing to the same extent it is possible that the increase in diameter was caused by an increase in the size of the individual aggregates as opposed to their number. That is to say that there were not necessarily greater numbers of larger aggregates after any specific increase in time, but that some aggregates had grown much larger or that all of the aggregates above a certain size had got slightly larger. This is supported by the fact that the largest particle after any given time period increased from less than 400µm after 24 hours to over 500µm after 72 hours and nearly 800µm after 120 hours. However, the numbers of particles of this massive increase in size were limited and so unlikely to be able to greatly impact the mean diameter to the extent seen here. Instead the PSD given in Figure 4.2 suggests that this was more likely to be caused by a slight increase in the mean diameter of a number of the smaller EBs as shown by the shallowing of the bell curve peak over time with increasing numbers of particles around 200-400µm in diameter and fewer between 50-100µm.

A

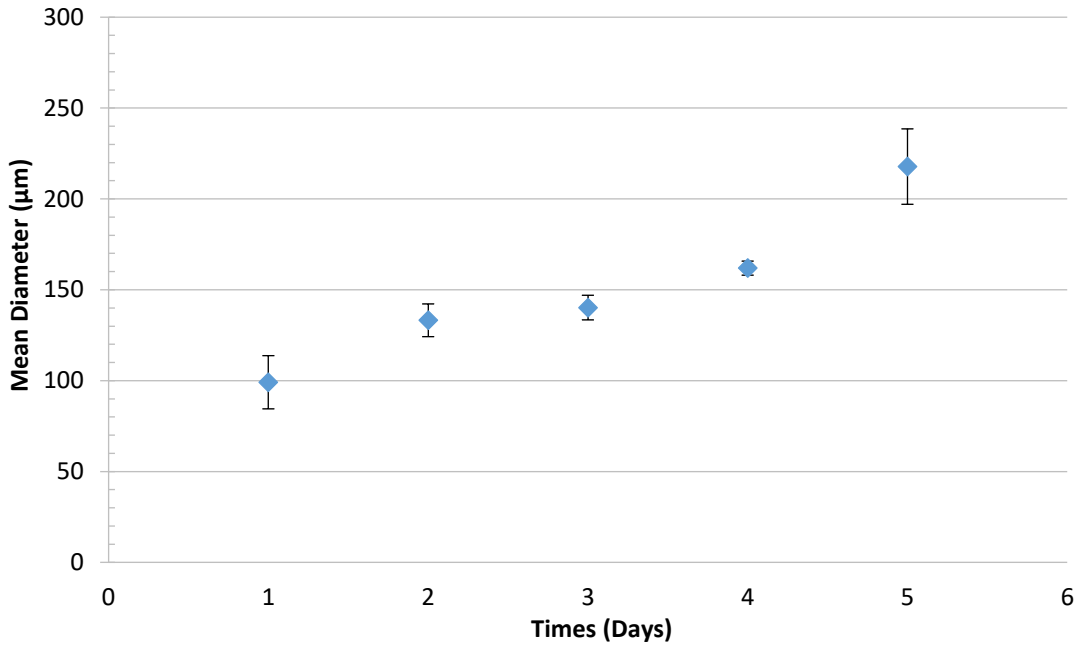

B

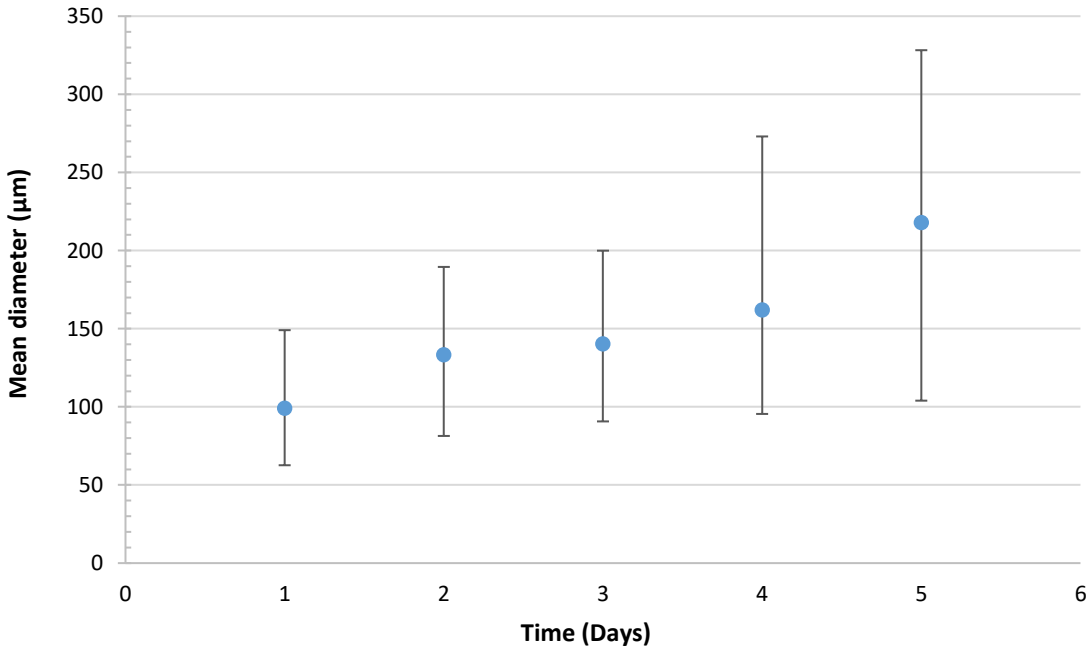

Figure 4.3: The graphs of Figure 4.3 show the growth rate of EBs over a 120-hour (5 day) period. Figure 4.3A shows the mean diameter with error bars showing standard error margin (SEM) from triplicate readings. Figure 4.3B shows the mean diameter with the error bars showing the D10 and D90 diameter. Readings were taken every 24 hours with both sets of experimental data collected from triplicate readings (n=3) using the mean Feret diameter calculated from images using ImageJ software.

4.3.2. Mesh-Based EB Size Separation Technique

A mesh size separation technique was explored for separating out EBs into 3 size fractions. This was done to allow for experiments to be performed that would provide information on the inherent characteristics of EBs of different sizes and to highlight the impact of EB size on ESC proliferation and differentiation. The technique involved sieving a full petri dish of mass suspension EBs through two meshes of different porosities. The resultant size characteristics of these collected fractions are shown in Figure 4.4 in comparison to the relative numbers of the same sized fractions in the stock.

Looking at the stock it was clear that the majority of the EBs comprised the 100-200µm fraction, with over 70% of the EBs being within this size range. The second most populous fraction was <100µm making up 20% of the stock, followed by less than 10% of EBs being larger than 200µm, despite the much larger size range of this fraction. Despite this, the mesh separation managed to produce an improvement in number of EBs that fell within every different size range. As would be expected the increase for the 100-200µm fraction was quite modest due to them making up the majority of the stock anyway. However, the <100µm EBs showed a greater than 3-fold increase in purity from 20% to 66%, with a further 20% being 100-110µm in diameter. Meanwhile, the >200µm fraction increased around 6 fold from 9% to 58% compared to the stock, with a further 14% being 180-200µm in size. This shows that the mesh separation has done a sufficiently good job at isolating three distinct size fractions. As a result, the properties of the aggregates within these size fractions could be further explored.

Figure 4.5 shows the number of cells that were present within each of the collected size fractions isolated using the mesh separation technique. These were then compared to the whole number generated in the stock; each shown as the number of cells per petri dish. The first thing that was clear is that there were more cells in a single unseparated petri dish than were present in the three separated fractions combined. This shows that some cells were lost during the separation process. This was calculated to be 2.3 million cells and represented 27% of the stock being lost during the separation process.

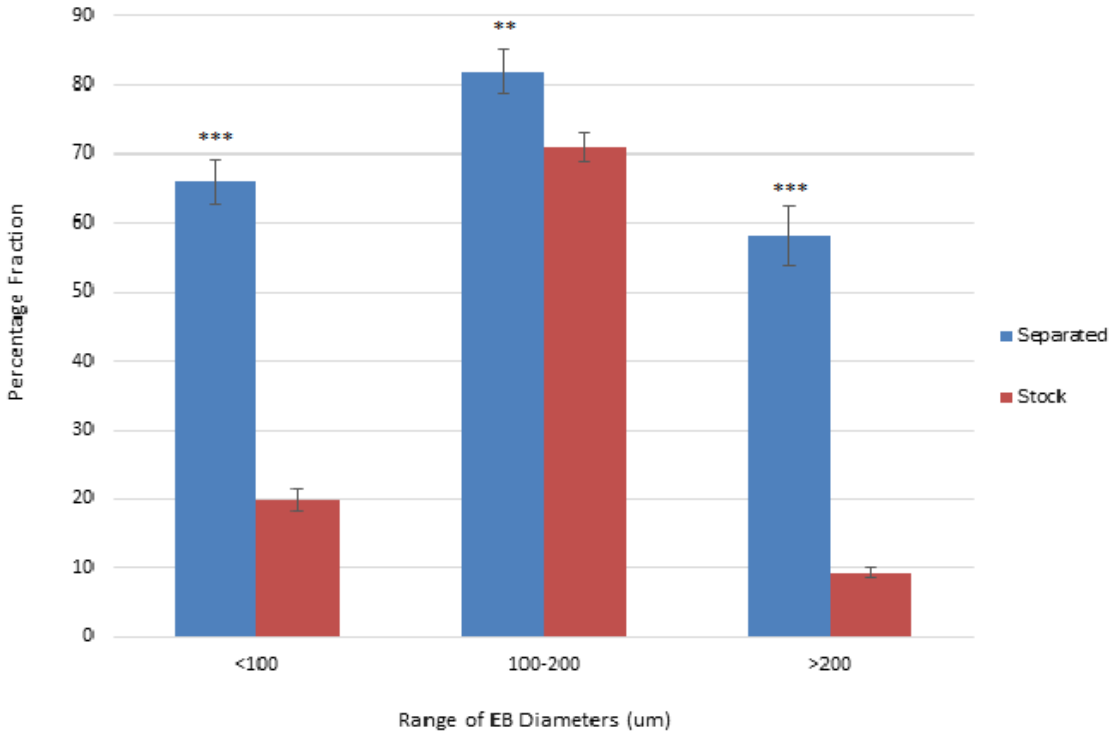

Figure 4.4: This graph shows the number of EBs that fit within each designated size fraction collected using the mesh separation technique compared to the number of EBs within this range in the stock. This is expressed as a percentage of the whole fraction for each collected size range. Readings were taken in triplicate (n=3) and averaged with error bars showing SEM. *** ≤0.001, ** ≤0.01, * ≤0.05.

In Figure 4.5A it is then clear that the 100-200µm fraction made up the largest proportion of the stock in terms of cell number, with 3 million cells per petri dish being collected from within this size range. Meanwhile, the >200µm EBs made up a large proportion of the total cell number, with the 2.4 million cells of this fraction making up 40% of those collected using this technique. This means that EBs between 100-200µm and over 200µm in diameter possessed almost 90% of the cells collected from each petri dish. This was then followed by the <100µm EBs which contained less than 720,000 cells and so made up around 12% of the collected cells. This was despite the >200µm EBs making up only 10% of the stock in terms of number and the <100µm EBs making up 20%, therefore highlighting that there were significantly more cells per EB in the larger set of aggregates.

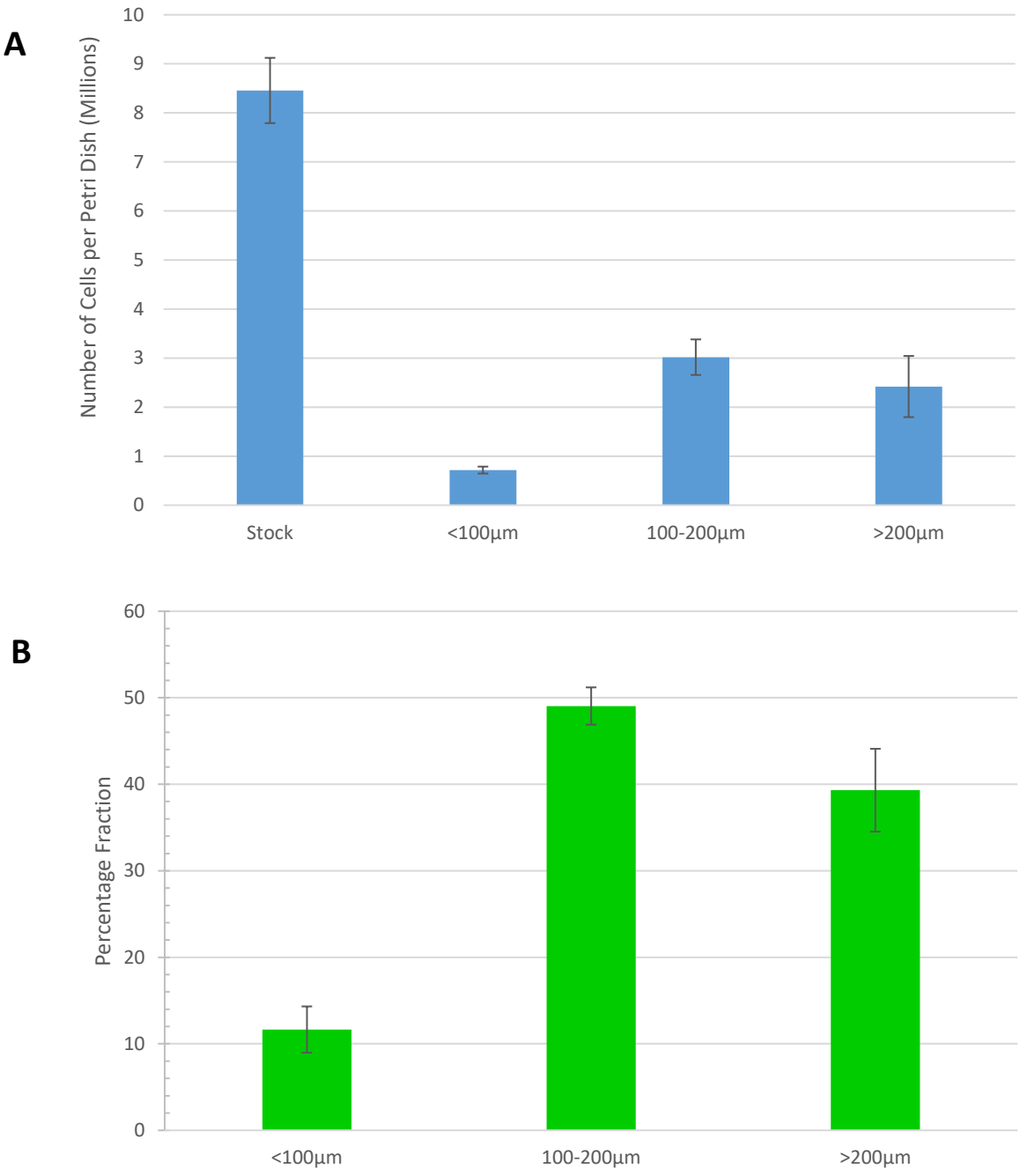

Figure 4.5: The number of cells that are present in each collected size fraction using the mesh separation technique compared to the unseparated stock per petri dish. Graph 4.5A shows the number of collected cells from each fraction using a haemocytometer cell count, with readings taken as triplicate and averaged. Graph 4.5B shows the percentage fraction that each collected size fraction makes up of the total number of collected cells following the mesh separation technique. Error bars shown are SEM (n=3).

Figure 4.5B shows relative ratio of the whole collected fraction of the separation technique, thus showing what fraction of collected EBs were present within each size range, but accounting for the loss of cells during the separation technique; this is expressed as a percentage.

These results show that the mesh separation technique was capable of generating three separate size fractions of EBs, as desired. It was decided that these three size fractions would be sufficient to allow further comparison of the effects that their size had on the subsequently dissociated cells. As a result, this technique was utilised to allow further exploration of the impacts of EB size on ESCs by means of an MTS assay to assess growth rate and immunohistochemistry to allow an insight into their potential differentiation pathways.

4.3.3. Size-Dependent Properties of EBs

The results of Figure 4.6 are important as they allow an understanding of some of the physical properties of the collected aggregates and the numbers of cells that comprise EBs within each size range. However, a large cell number at collection may not translate itself to a large number of cells for subsequent use; this is due to the potential for varying rates of proliferation within each fraction. Therefore, it was important to determine the proliferation rate of these cells after separation to identify the desirability of each size fraction for producing large numbers of differentiated cells. This was to highlight the advantages of cells from each size fraction from a process perspective. A fraction that can produce large numbers of cells with a predilection for differentiating along a certain lineage is preferable to a less proliferative fraction with the same potential for differentiating along that lineage. This is because fewer cells are required from the more proliferative fraction to produce the same number of fully differentiated cells for transplantation *in vivo*. A more proliferative fraction would therefore offer a more effective use of resources by allowing the production of larger amounts of the final product using a reduced quantity of starting materials.

This data was collected by using an MTS assay over 72 hours on each of the collected size fractions with the results compared to the unseparated EB stock; these are shown in Figure 4.6. It is clear that after 24 hours there was little to tell between

the different size fractions and the stock, with the exception of the >200µm EBs which were significantly lower in number by as much as 30,000 cells. In fact this was the only size fraction whose cell number after 24 hours was below the seeding density and therefore suggests that these aggregates were least well-equipped to survive the dissociation and re-seeding process.

After 48 hours the <100µm EBs and stock were near identical, having doubled in number compared to the seeding density. By this point the 100-200µm EBs had more than tripled in number and were by far the most proliferative, while the >200 µm EBs had just increased beyond the seeding density and were still fewer than half the number of any other fraction. Finally, after 72 hours the stock and <100µm EBs had nearly doubled in number again and still failed to differ significantly. The 100-200µm EBs had also doubled in number making them the most numerous by almost 300,000 cells per well after 72 hours. The >200µm EBs also doubled in number between 48-72 hours, however, due to them being in far fewer numbers after 48 hours compared to every other fraction they only just exceeded the cell count collected for the stock after 48 hours, and were still fewer in number after 72 hours than the 100-200µm EBs had been after 48 hours.

The results of Figure 4.7 show the fluorescence imaging results of all three size fractions following immunohistochemistry for markers from all three germ layers. These were the endodermal marker Gata-4 (ABCD), the ectodermal marker Nestin (EFGH), and the mesodermal marker Brachyury (IJKL). As is expected, and has been shown previously, all three germ layer markers were clearly expressed in the unseparated stock of cells. In addition to this the ectodermal and mesodermal markers were both clearly expressed in all three of the separated size fractions. However, the same was not true of the endodermal marker Gata-4. While clearly present in the >200µm fraction, there was minimal, if any, fluorescence in the <100µm fraction and no fluorescence in the 100-200µm fraction.

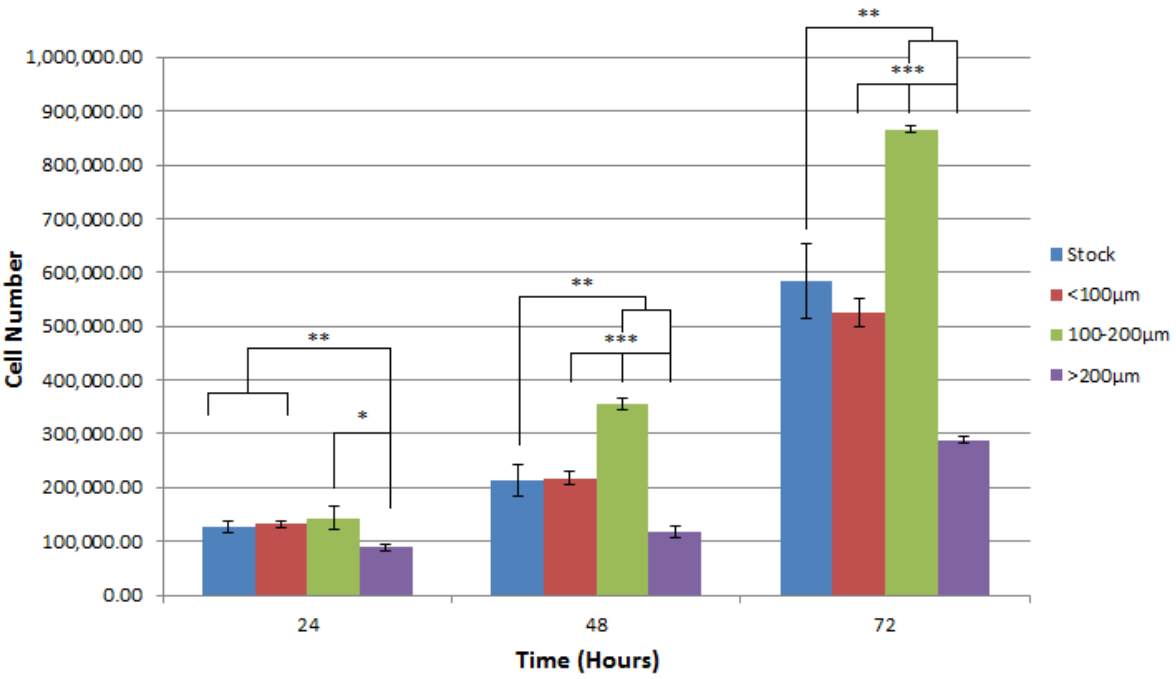

Figure 4.6: Growth rate of different sized fractions of EBs over 72 hours as determined by MTS assay comparative to an unseparated EB stock. Cells were grown over 72 hours in growth medium and absorbance readings taken every 24 hours. Cell number was calculated using a standard curve produced on each day of experiments using known numbers of cells taken from a continuous culture of mESCs grown in parallel. Error bars show SEM and n=3 for each set of conditions. *** ≤0.001, ** ≤0.01, * ≤0.05.

In culmination, these results suggest that EB size does profoundly impact ESC's. It appears to have an impact on both their proliferation and subsequent potential for differentiation. As a result, identifying novel size separation techniques is an important driver for improvement in stem cell research and ultimately the development and refinement of cell-based therapies using ESCs. This is therefore an area that will need extensive further research to determine exactly what effects different size fractions have on a menagerie of full differentiation protocols.

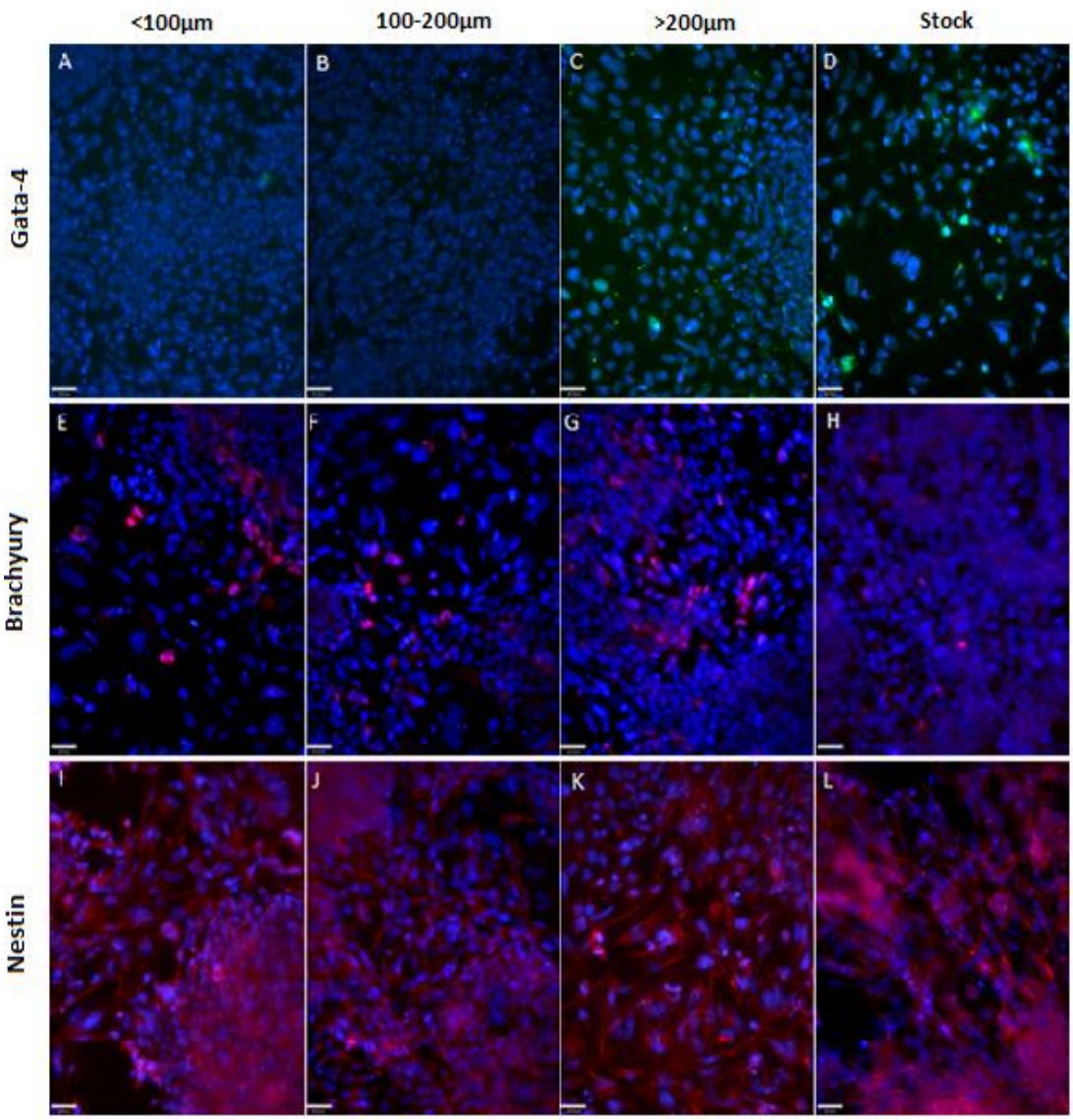

Figure 4.7: Figure 4.7 shows the immunohistochemistry results of dissociated mass suspension EBs after a 72 hour formation period following their size separation using a mesh separation technique. Results are shown from the <100µm size fraction (A,E,I) the 100-200µm size fraction (B,F,J) the >200µm size fraction (C,G,K) and the unseparated stock (D,H,L) for three separate germ layer markers after 7 days spontaneous differentiation. These markers were GATA-4 (A,B,C,D), Brachyury (E,F,G,H) and Nestin (I,J,K,L). Cell nuclei were counterstained with Hoechst 33258 and images were taken at 20x objective magnification. Scale bars are shown and are equal to 25µm.

4.4 Discussion

4.4.1. Embryoid Body Population Dynamics

In multiple previous experiments EB population dynamics have been explored during their formation by mass suspension and have showed that the resultant stock is heterogeneously sized (Bauwens et al., 2008, Carpenedo et al., 2007, Karp et al., 2007, Cameron et al., 2006, Valamehr et al., 2008). Subsequent experiments have then shown that EB size can profoundly impact upon the differentiation of the cells within these aggregates (Bratt-Leal et al., 2009, Buschke et al., 2013, Hwang et al., 2009, Lillehoj et al., 2010, Choi et al., 2010, Valamehr et al., 2008). As a result, a wealth of research has begun to focus on controlling EB size and determining what effects this has on the differentiation of the cells within (Lillehoj et al., 2010, Buschke et al., 2013, Carpenedo et al., 2007, Choi et al., 2010, Magyar et al., 2001, Karp et al., 2007, Dang et al., 2004, Kinney et al., 2012, Valamehr et al., 2008).

Initial experiments performed here looked to build on previously collected results to determine a more accurate representation of the PSD of EBs over a 120-hour formation period. As there is a lack of uniformity in the formation period that is utilised when using EBs it is necessary to discern how formation time affects some of the inherent physical characteristics of EBs, such as their diameter. This is important because this may impact on their ability to be separated and an ideal separation technique must have the flexibility to collect multiple distinct size fractions from a heterogeneously sized stock regardless of the formation time. In addition, it was hoped that detailing the changes in PSD of EBs over time would allow for a greater understanding of the processes that occur during EB formation.

The figures here show that the mean diameter gradually increased over time and that heterogeneity of size was an issue after every tested time period. This is likely to be caused by both the continued proliferation of ESC's within the aggregates as well as the agglomeration of whole EBs to varying degrees (Dang et al., 2004, Cameron et al., 2006, Dang et al., 2002). In addition, the results showed that the D10 of aggregates from 48-120 hours remained consistent; this means that there were still a substantial number of smaller particles after 120 hours. This is interesting because, as the mean diameter and D90 are increasing there are obviously increasing

numbers of larger EBs, however, this doesn't translate to a drastic decrease in the D10; representative of the proportion of smaller EBs. If the continued increase in EB size was caused entirely by agglomeration of smaller aggregates with each other this would drastically diminish their number each time two smaller EBs fused to make one larger EB (Cameron et al., 2006). As this did not occur it would suggest that the increase in mean diameter was caused by continued steady proliferation of EBs throughout the whole stock resulting in a continued increase in size. Contrary to this though, the D90 increased dramatically with time at a far greater rate than the mean. This means that EBs must have been agglomerating to account for the sudden appearance of significant numbers of larger EBs; this is in accordance with previous results which show that agglomeration of EBs continues until around day 6 of formation (Dang et al., 2004). Due to the continued presence of the smaller aggregates in the stock over extended time periods, their representative fraction remained consistent from 3 days onwards, it was therefore likely that they are agglomerating with larger aggregates and not each other. This would have resulted in limited increases in size for larger EBs and an equally limited decrease in the number of smaller EBs. This is supported by the observation that the proliferation of cells within EBs reduced over time during a 5-day formation period. As a result, EBs from the lower end of size range can be found at any of the tested time points, however, aggregates in excess of 200µm did not appear in significant numbers until after 72 hours formation.

4.4.2. Mesh Separation Technique

It was decided that a benchmark technique would need to be produced against which subsequent techniques could be compared. This technique therefore did not require the same scalability, throughput or ease of use as subsequent techniques due to its role as a means of comparison. However, it was desired that this technique would be capable of collecting different sized EBs so that conclusions could be drawn regarding the inherent properties of the cells within each size fraction. This was necessary to determine what size fractions subsequent separation techniques would be assessed for their ability to efficiently collect and would be based on the intrinsic properties of the EBs found throughout the population.

As a result of its simplicity and successful previous uses in various other fields of research it was decided that a mesh separation technique would be used (Mora et al., 1998, Konert and Vandenberghe, 1997). The technique allowed for the collection of multiple discrete fractions by retaining any particles in excess of the pore diameter of the mesh; which were then be collected by washing. This method was successful, as displayed by the results in Figure 4.4. The results showed that after 72 hours, the standard EB formation time for a multitude of differentiation protocols, 70% of EBs in the stock were between 100-200µm, with a further 10% being in excess of 200µm and 20% being below 100µm. With the benefit of the mesh separation technique the percentage of cells falling within all of these fractions was improved, with a minimum percentage fraction of 58% within the desired size range.

An inherent flaw with this separation technique is the lack of sphericity of EBs. As a result, the orientation of an individual particle could affect whether or not it was retained in the mesh (Mora et al., 1998). To ensure consistency between experiments the max Feret diameter was always used to calculate the PSD of every fraction. Consequently, certain particles with a Feret diameter in excess of the pore size of the mesh may have filtered through into the smaller fractions. This is likely to be the main reason for the lack of purity in the smaller collected size fractions. In order to try to counteract this, slightly smaller meshes were used than the maximum desired size of each fraction to try to reduce the numbers of EBs in excess of this maximum filtering through. However, unfortunately in some cases EBs that were noticeably smaller in diameter than the mesh pore size were sometimes retained in the larger fractions. This was likely due to stacking, as the presence of larger EBs in the pore spaces prior to the addition of smaller EBs would likely result in the retention of aggregates below the pore diameter. A washing step was used to try to limit this, however, due to the fragility of the EBs this was necessarily kept to a minimum. The success of this technique to collect the desired fractions is displayed by the fact that the majority of EBs in each fraction that were outside of the desired range were within 10-20µm of it. With the benefit of 20µm leniency in total (10µm either side) for each size fraction this allowed a percentage purity in excess of 67% for the >200µm EBs, 90% for 100-200µm EBs and 80% for <100µm EBs. These results are not dissimilar to other

previously defined EB separation techniques in terms of purity and size range of each fraction. Lillehoj et. al. demonstrated a technique that could separate size fractions of <100µm, 100-200µm and 200-300µm, near identical to those demonstrated here, with an accuracy of near 100%, 80% and 75% respectively (Lillehoj et al., 2010). Another technique demonstrated by Buschke et.al. was shown to collect >330µm EBs with a 94.1 ± 5.6% efficiency and 250-330µm EBs with a 87.9 ± 17.9% efficiency (Buschke et al., 2013). This technique was also said to collect under <250µm EBs as well, but no number was attributed to determine the efficacy of this (Buschke et al., 2013). As a result, the mesh separation technique was judged to be sufficiently successful to be used in further experimentation to determine the impact of EB size and also to act as a benchmark for subsequent separation techniques.

4.4.3. Impact of Embryoid Body Size

4.4.3.1. Total Cell Number

Due to the success in producing a size separation technique, further experimentation was begun to determine the impact that EB size has on the ESCs. First to be determined was the number of cells that were present in each size fraction of the stock; this would give some insight into the availability of large numbers of cells and therefore their applicability for differentiation. A cell count was performed on each of the separated size fractions which was then calibrated to a single petri dish. This was then compared to the number of cells in the unseparated stock.

Immediately it was apparent that a great number of cells were lost from the stock during the separation process, accounting for 27% of the total cell number. This was likely caused by the adherence of EBs to the mesh during the separation and the failure to sufficiently remove them during washing. It was not possible to compare this to other EB separation techniques as this data has not been provided elsewhere, however, this is a further issue with this separation method that undermines its potential application in industry (Buschke et al., 2013, Lillehoj et al., 2010). It should be noted that as only live cells were counted it is possible that this is a reflection of the destructive nature of the separation process. However, while no count was made of the number of non-viable cells, as only viable cells were counted, anecdotally they

did not seem to be present in sufficient numbers to be responsible for a loss of cells on this scale.

Next it became clear that in spite of the >200µm EBs representing less than 10% of the total number of EBs in the stock, they accounted for almost 40% of the cell number. This obviously reduced the fraction of cells from the smaller aggregates comparative to their particle number. This is no great surprise as larger EBs would, by their very nature, be expected to contain greater numbers of cells; as this is what EBs are primarily composed of (Mogi et al., 2009, Zhou et al., 2010). However, it highlights that the cavitation and necrosis that has previously been shown in the core of larger EBs was not having a prohibitively negative effect on the number of cells in these larger aggregates (Hernández-García et al., 2008, Coucouvanis and Martin, 1995). This is despite EBs in excess of 300µm diameter having been shown to have a higher proportion of apoptotic cells, with the least number of apoptotic cells found in the fraction between 100-300µm) (Valamehr et al., 2008). The 100-200µm EBs made up almost 50% of the total number of cells, which was unsurprising as they made up nearly 70% of the EBs. As a result, the <100µm EBs made up around 10% of the cells despite 20% of the EBs being within this size range. What these results make clear, therefore, is that EBs from either fraction in excess of 100µm possess sufficient numbers of cells to be easily viable as a resource for subsequent differentiation. However, the <100µm EBs are limited in cell number, in spite of making up 20% of the number of EBs, and so may struggle to provide sufficient numbers of cells to be a viable resource. As a result, for the separation of this fraction to be worthwhile they must possess a greater proficiency for differentiating into some specific desired lineages comparative to the stock or be sufficiently proliferative to allow their seeding in lower numbers. Fortunately, both of these factors have previously been suggested to be true of EBs around this size and so suggest that this is a valid size range to collect and thus warrants further experimentation (Cha et al., 2015, Valamehr et al., 2008).

It is also clear that no single fraction from within a single petri dish of cells contained enough cells to be sufficient for providing the raw materials required to treat a single patient (Zweigerdt, 2009). Because of this, multiple petri dishes would need to be used to collect each individual fraction in sufficient numbers using this method. This could be up to as many as 14 petri dishes of 72-hour EBs for the >100µm fraction to collect the approximately $1x10^7$ cells required to produce $1cm^3$ of bone for a single patient (Marolt et al., 2010). Therefore, for any technique to be considered sufficiently scalable it must have the potential to facilitate the separation of at least 14 petri dishes (or an equivalent volume of up to 140ml of EB containing medium) simultaneously. As a result, this technique was rendered impractical in an industrial sense as it was not amenable to this level of scaling.

4.4.3.2. Proliferation

To further determine the desirability of each of these fractions for continued experimentation and to give some insight into their inherent characteristics an MTS assay was performed. Readings were taken of the cell numbers every 24 hours for a duration of 72 hours from seeding. This would provide information on the ability of each size fraction to contribute cells to the unseparated stock, as well as their potential for expansion as individual size fractions.

It should be noted that the MTS assay determines cell number by recording the metabolic activity of the cells (Riss et al., 2004). Therefore a higher number of less metabolically active cells could appear to be lower in number than they are due to the need to use a standard curve (Riss et al., 2004). This could skew the results slightly, however, as all cells from every size fraction are subject to this it was decided that this would be a sufficiently accurate means of determining cell number.

It was clear that the most proliferative cells were of the 100-200µm fraction, while the least proliferative cells were from the >200µm fraction. Finally, the <100µm fraction and stock were in between this and very similar to one another. Therefore, as well as representing the greatest number of cells in the stock, 100-200µm EBs were also the most proliferative after seeding. This is similar to previously collected results which showed that 100-300µm EBs are the most proliferative, followed by <100µm EBs and then >300µm EBs (Valamehr et al., 2008). This means that, of the

heterogeneously sized stock, it is cells from the 100-200µm fraction that will likely have the greatest effect on the final differentiation state of the cell population as a whole. As they are present in the largest numbers to begin with and go on to proliferate at a much higher rate, they therefore contribute the greatest number of cells to the heterogeneously-sized stock after dissociation and seeding.

The >200µm cells meanwhile were largely non-proliferative, notably for the fact that it took them 48 hours to exceed the number of cells at which they were seeded. This is likely to be caused both by their reduced viability caused by necrosis at their core and a reduced proliferative potential (Valamehr et al., 2008). Due to the similarity of the <100µm EBs to the stock it is likely, therefore, that it was the presence of larger numbers of cells from less proliferative >200µm EBs that were the cause for the reduced proliferation rate in the unseparated stock fraction comparative to the 100-200µm fraction. Importantly, this shows that cells from the >200µm fraction of EBs can still have an impact on the characteristics of the heterogeneously sized stock population. Finally, the increased proliferative potential of the <100µm EBs comparative to the >200µm EBs means that, following dissociation and seeding of the unseparated stock, the smallest EBs should make up a larger proportion of the cells after a few days culture than at seeding. Therefore, they should still be able to have some influence on the differentiated outcome of the cells from the unseparated stock.

4.4.3.3. Differentiation Potential

Finally, cells separated into these three size fractions were cultured for 7 days in growth medium to encourage their non-specific differentiation. Following this culture period, immunohistochemistry was performed for 3 germ layer markers. This was used to determine the ability of cells from EBs within each of the individual size fractions to differentiate into cells from across the full spectrum of possible desired tissues. Display of markers has been shown to be inconsistent in ESCs over time, so a control of unseparated EBs was run to show that each of the markers was displayed after this time period (Ramirez et al., 2011).

As would be expected the unseparated stock was capable of displaying cell surface markers indicative of all three germ layers. This is in fact one of the defining

characteristics necessary for a population of cells to be termed pluripotent (Przyborski, 2005). In addition, all three size fractions showed similar levels of fluorescence of the ectodermal and mesodermal markers Nestin and Brachyury. However, the display of the endodermal marker GATA-4 was largely limited to the >200µm fraction, with minimal fluorescence observed in the <100µm fraction and none in the 100-200µm fraction. This is in accordance with previous size-dependent experiments performed on a different Endoderm-specific growth factor, AFP. These results showed that among EBs that had been generated using a microwell formation technique, AFP was prominently displayed in larger EBs over 200µm in diameter, but not in smaller EBs of below 200µm diameter (Choi et al., 2010). Further, the results collected in this study corroborate the continued display of mesodermal and ectodermal markers in all large and small EBs shown in those experiments (Choi et al., 2010). This is interesting given that proliferation rates are generally higher in pluripotent ESCs compared to differentiated cells, suggestive of the fact that more naïve cells benefit from enhanced rates of proliferation, and yet here the least proliferative fraction displayed all three early germ layer markers (Burdon et al., 2002, Cooper, 2000). It is possible due to the inconsistent timings of germ layer marker expression that at this tested time point the 100-200µm EBs were simply not displaying GATA-4, whereas the less proliferative, larger EBs were (Ramirez et al., 2011). However, as this marker was clearly present in both the control and the larger EBs it is more likely that endodermal differentiation is downregulated in smaller EBs and so this was the reason for their failure to display GATA-4 to the same extent, suggesting that larger EBs are the most desirable fraction for endodermal differentiation (Choi et al., 2010, Cha et al., 2015). Accordingly, it will be important to ensure that a suitably pure fraction of <200µm EBs can be collected using subsequent separation techniques to allow for the improvement of endodermal differentiation of ESCs.

Due to the clear differences in cell number at seeding, proliferative potential and display of key germ layer markers of the cells from across the three selected size fractions it was decided that these fractions would be suitable for further experimentation. This will involve identifying scalable and potentially automatable

techniques for collecting these same size fractions. Therefore, subsequent tested separation techniques will be judged by their ability to collect discrete fractions of EBs of all three of these size fractions. Future experiments can also focus on further exploring the clear differences in potential of cells from each of these size fractions for proliferation and differentiation. This will hopefully inform on the specific size fractions that are best suited to collect each individual differentiated cell and provide a cheap, effective and easy to use method for collecting these fractions from a heterogeneously size stock of EBs.

4.5 Conclusion

In conclusion, what these results show is that EB size clearly impacts on the inherent characteristics of ESCs. In addition, the direct impact of EB size on the subsequent proliferation and differentiation of dissociated EBs cultured as a monolayer could be illuminated to some extent by the three size fractions that have been collected using this mesh separation technique. While the method demonstrated here was successful at collecting multiple size fractions, it is not inherently scalable, has low throughput and requires a large degree of user input. Therefore, further research will be performed in order to identify a scalable and simple to operate technique that can efficiently collect discrete fractions of viable EBs within these three chosen size ranges with a high throughput. As a result of the experiments performed here it is possible to further explore exactly what impact EB size has on the differentiation of ESCs. These results could then be compared to cells collected from the same size fractions separated using different techniques to determine what direct impact these techniques have on the EBs.

Chapter 5

Particle Size Separation Using an Expanded Bed Reactor

5.1. Introduction

Expanded bed reactors (EBRs) have long been known to separate out particles according to their size and density; with larger and more dense particles residing near the bottom and smaller particles moving towards the upper reaches of the separation column. The method relies on the terminal falling velocity (TFV) of a particle being proportional to its diameter as demonstrated in the Stokes equation (Equation 5.1). In experiments performed previously EBRs were shown to have the potential to be applied to aggregates of cells as well as the inanimate beads for which the literature is dominated (Ng and Chase, 2007). This opened up the possibility of these reactors being applied to the problem of size separation of EBs. However, this study simply showed proof of principle and detailed that this technique could be used to collect two size fractions of Neural Stem Cells and flocs of yeast with distinct mean diameters (Ng and Chase, 2007). It failed to detail the applicability of this method for collecting multiple size fractions, what conditions would be needed to achieve this, the manner in which each of these variables impacted on the separation of the particles and the impact of the separation technique on the cells themselves.

Due to the potential of this technique for separating particles, EBRs have been identified as a possible solution to providing an industrially-viable size separation technique for EBs. Consistency was ensured by utilising a model system of non-reactive, inert beads to minimise the likelihood of inter-particle interactions affecting the separation of the particles. Initially, the use of this model system allowed for

identification of the factors that were likely to influence the mean diameter of collected fractions and then further exploration elucidated what effect each of these variables had on both mean diameter and D10-D90 span of each collected fraction across a variety of conditions. This was then compared to a smaller dataset of representative sets of parameters for EBs to ascertain the strength of the model system and determine the potential of this technique to become a scalable and cost-effective EB size separation technique for use in industry.

5.2. Materials and methods

5.2.1. Cell Culture

For full details on cell culture techniques used for these experiments refer to the Materials and Methods chapter.

5.2.2. The Stokes Equation

The Stokes equation shown in Figure 5.1 was used to predict the terminal falling velocity of particles for both the model bead system and the EBs. The beads were assumed to have a density of 1.1g/cm^3 as has been demonstrated previously and the EBs a density of 1.07g/cm^3 (Ng and Chase, 2007, Kang et al., 2010). The D10-D90 span of the beads was 60µm (98-158µm) and the mean diameter was 127µm. Acceleration due to gravity was assumed constant at 9.81m/s^2. Density of medium was 1g/ml and viscosity of medium was 1.002 cP. All experiments were performed at room temperature of around 20°C.

$$V = \frac{g \times D^2 \times (d_p - d_m)}{18 \times v}$$

V = Terminal Velocity
D = Diameter Of a Particle
g = Acceleration Of Gravity
v = Viscosity Of Medium
d_p = Density Of Particle
d_m = Density Of Medium

Equation 5.1: The Stokes equation shows the relationship between the terminal velocity of a particle and its diameter. This is dependent on, and assumes constant acceleration due to gravity, particle density, viscosity and density of medium.

Calculations performed using this equation allowed for estimations of flow rate to be made in accordance with the ability of those flow rates to mobilise certain size fractions of beads within the column. This relationship is shown in Table 5.1.

Assumptions

The Reynolds number for each of the tested flow rates was 5.30, 6.65 and 9.15, at flow rates 2.5ml/min, 4ml/min and 5.5ml/min respectively. As a result, the flow profile of the fluid throughout the majority of the length of the column was known to be laminar. The only exception would be at the entrance of the column due to the no-slip condition (Day, 1990). The entrance length, after which flow is fully developed

laminar flow, was found to be 0.549cm. This means that flow was fully developed before reaching the lowest port height at 1cm.

Laminar flow states that there is no turbulence in the movement of fluid through a vessel. This means that there is no radial mixing and that the fluid moves only in the axial direction of the flow. This flow profile manifests itself as a series of rings moving outwards from the centre of the column, with the fluid velocity gradually decreasing from its peak (of twice the net flow rate) at the centre of the column to the minimum at the wall of the column (Sibulkin, 1962). This minimum is assumed to be 0 as a result of the no-slip condition (Day, 1990).

Table 5.1 shows how the TFV of an individual particle correlates to its diameter. This was calculated using the Stokes equation which is shown in Equation 5.1; an equation that is based on a multitude of assumptions. First of all, it was assumed that each particle is perfectly spherical, this is more likely to be true of the beads used for the model system than for the EBs, which are decidedly not spherical. However, the total lack of consistency in their sphericity both over time and across size ranges means that they will all be assumed to be such as it is impractical for the calculations to do otherwise.

Based on this assumption the Re_p for almost all of the particles being separated using this technique as part of the model system was found to be below 0.3. This means that the Stokes law calculations for TFV should be accurate to within 3% (Rhodes, 2008). The importance for this is furthered by the fact that in the Stokes law region, defined as Re_p <0.3, non-spherical particles are known to fall with their longest surface almost parallel to the direction of their movement (Rhodes, 2008). This propensity for settling in a uniform manner along with the unlikeliness of the particles to tumble should help improve the efficacy of the technique by ensuring consistency in settling amongst particles across the range of sizes found within the stock in spite of their irregular shape. It is also due to this consistency in settling in relation to the longest surface of the particles that the max Feret diameter was used when calculating the PSD.

Secondly, it was assumed that each individual particle would not interact with any other particle beyond transient interactions. This is clearly not the case for EBs as, in addition to transient non-protein interactions seen in unreactive particles such as the beads, EBs engage in numerous protein interactions over long periods of static culture during their formation and beyond; this process is known as agglomeration (Bratt-Leal et al., 2009, Mohamet et al., 2010). However, this is a relatively long process and there is insufficient time for it to occur fully during the period that they are in contact with each other in the column (Mohamet et al., 2010). Meanwhile, the presence of consistent fluid flow should be sufficient to break any transient surface interactions between the EBs that are mobile as the use of dynamic culture systems has previously been shown to reduce or prevent EB agglomeration (Mogi et al., 2013, Carpenedo et al., 2007).

Thirdly, the Stokes equation assumes a single particle system. However, the presence of multiple particles can be mitigated by accounting for a factor known as voidage as has been discussed previously (Willoughby et al., 2000, Yun et al., 2004).

A fully packed bed comprised of monodisperse particles will have a voidage of 0.4; meaning that the effective flow rate at this point in the column will be 2.5x larger than the net flow rate in an area containing no beads. In separation columns with a large settled bed height this will be the case for most the column, with a small volume nearer the top of the column containing progressively fewer beads. However, in a column with a small settled bed height the volume of the column that contains a large voidage is vastly diminished comparative to the total length of the column. As a result, the voidage will be much lower for the majority of the length of the column and therefore have a limited effect beyond the lowest sampling heights (visualised in Figure 5.2).

Finally, it was assumed that the density of the particles is constant throughout the entire population. Previous studies with these beads showed that the Sephadex beads used in these experiments have a density of 1.1g/ml and so this figure was used in the calculations and assumed constant for particles of every size (Ng and Chase, 2007). The density of the EBs was assumed to be 1.07g/ml (Gorczynski et al., 1970, Kang et al., 2010). In addition, the density and viscosity of the medium was

assumed to be the same as water, being 1g/ml and 1.002cP respectively. In order for these to be calculated room temperature was used and assumed to remain constant at around 20^{o}C. Finally, the acceleration due to gravity was assumed to be 9.81m/s^{2}.

In theory, setting the flow rate through the column to equal the TFV of any individual particle should result in its net velocity to equal 0 and therefore cause it to remain stationary comparative to the column. If the flow rate is any higher the particle will elutriate out of the top of the column; any lower and it will settle to the bottom. It was for this reason that the three tested net flow rates of 2.5ml/min, 4ml/min and 5.5ml/min were chosen to represent particle sizes of around 100µm, 125µm and 150µm respectively.

5.2.3. Size separation of Sephadex beads

Sephadex G-25 medium beads (Sigma) with a swelled density of approximately 1.1g/cm^{3} were used as a model system. These beads were selected due their similarity of physical properties with EBs such as density and shape. The particle size distributions were similar, as the swollen diameter of 70% of beads was between 100-150µm compared to 50% of EBs, as shown in Figure 4.2 and Figure 5.1. It should also be noted that the full size distribution of the EBs was much larger and more varied. In addition, the beads were assumed to have a much higher sphericity than the EBs, which are known for their heterogeneity of shape and thus may have suffered inconsistencies due to the way in which they would settle in the column and also the approach used to calculate PSD.

The dried beads were allowed to swell in an excess of deionised water overnight prior to experimentation. The glass column used for these experiments was 1cm in diameter and 27cm in length from the sintered disc at the bottom to the topmost port (shown in Figure 5.2). The column possessed 14 ports, with the first 1cm above the sintered disc and each of the rest spaced 2cm apart helically around the column. Their presence allowed for samples to be taken from varying heights within the

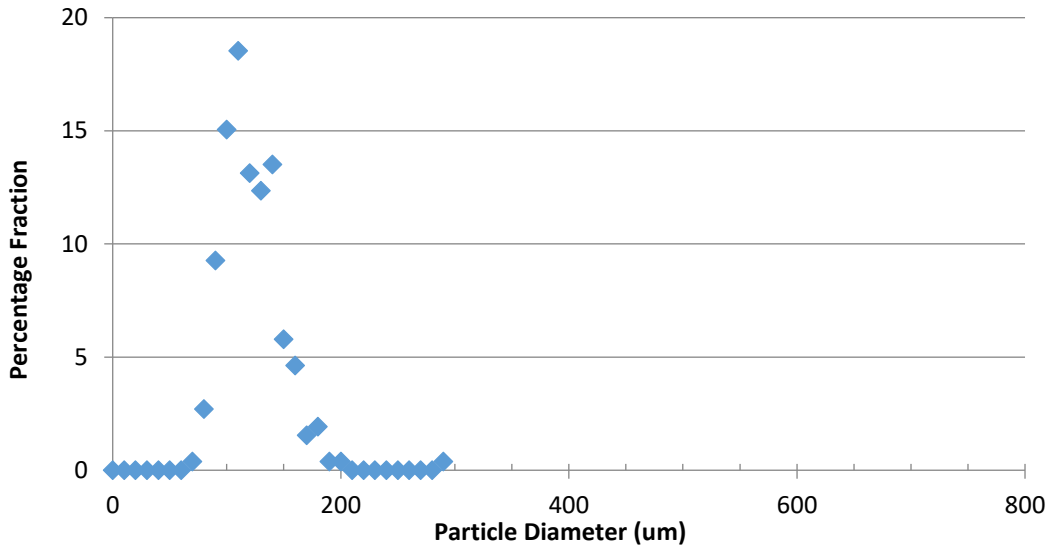

Figure 5.1: Particle size distribution of Sephadex® beads used as a model system. All experiments were performed in triplicate (n=3) with PSD collected using Feret diameter calculated by ImageJ.

column during its operation. A Masterflex L/S 7523-37 peristaltic pump was calibrated and then used to pump Phosphate Buffered Saline (PBS) into the column at defined flow rates. A 1ml syringe connected to a G19 needle was used for sampling during the experiments. Each fraction was 100µl in volume and was deposited into a 12 well plate where a further 900µl of water was added to allow representative images to be collected. Fractions were then imaged to allow for particle size analysis using ImageJ software, which took readings of the max Feret diameter.

Initial bead experiments utilised a large settled bed height (Hsb) of 5.5cm. The Sephadex beads were added to the top of a primed column and allowed to settle for 30 minutes before fluid flow was initiated. The small Hsb experiments were conducted with an Hsb of 0.2cm and allowed 30 minutes for settling before the experiment began. The settled bed was repopulated with new beads for each run to ensure reproducibility.

5.2.4. Size separation of Embryoid bodies

Feeder free mouse embryonic stem cells (mESCs) were cultured on gelatin-coated T25 flasks in mouse ESC medium. A single cell suspension was attained by incubating the cells with 2ml TE for 5 minutes and EB formation performed as described in Chapter 3.1.7.

After this period the aggregates were collected and briefly centrifuged to ensure collection of the entire population. EBs were then resuspended gently in 1ml of PBS and added to the column. Due to the nature of dealing with aggregates of cells and their tendency to agglomerate the particles were left for only 10 minutes before the initiation of flow. After this the separation and collection of the aggregates was performed as with the Sephadex beads above. Again, particle size distribution was performed using the max Feret diameter.

5.2.5. Modelling

A Bayesian Regularisation Artificial Neural Network (BRANN) with 10 hidden neurons was developed in Matlab using the collected data from the experiments. The average of triplicate readings was used as the input data for the training of the model. The BRANN generated data for each of the tested conditions along with all feasible untested conditions that existed within these set limits. New models were continually generated until a BRANN with satisfactory correlation between predicted and collected data was achieved. These were produced using data from across all the tested conditions to make sure that it did not discriminate for any condition set and so was appropriate for all of them. This data was then presented as a 3D graph using Minitab. This was performed for both the mean diameter and span results. Finally, the predictions made by the BRANN for each condition set are plotted against the actual collected results to show the accuracy of the predictions and therefore the strength of the model.

5.2.6. Statistics

Statistical analyses were performed on data sets of collected fractions to determine statistical significance between results as described in Chapter 3.1.10. The BRANN's were assessed using the statistical indices of mean squared error (MSE), root mean squared error (RMSE) and absolute average deviation (AAD). These were used to make up for the inefficiency of using R^2 value as a means of determining the accuracy of non-linear models. A full explanation of these statistical indices is included in the discussion.

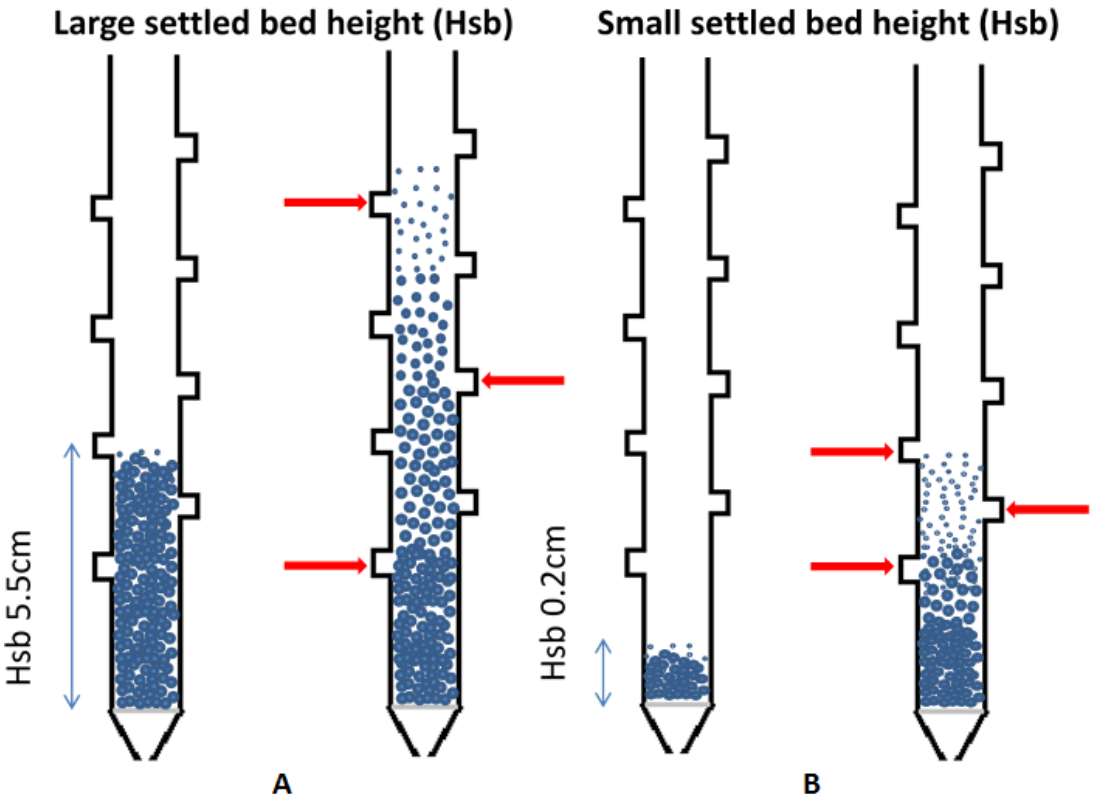

Figure 5.2: Figure 5.2A represents the column before and after the initiation of fluid flow with a large Hsb of 5.5cm, while figure 5.2B represents the column before and after the initiation of fluid flow with a small Hsb of 0.2cm

A

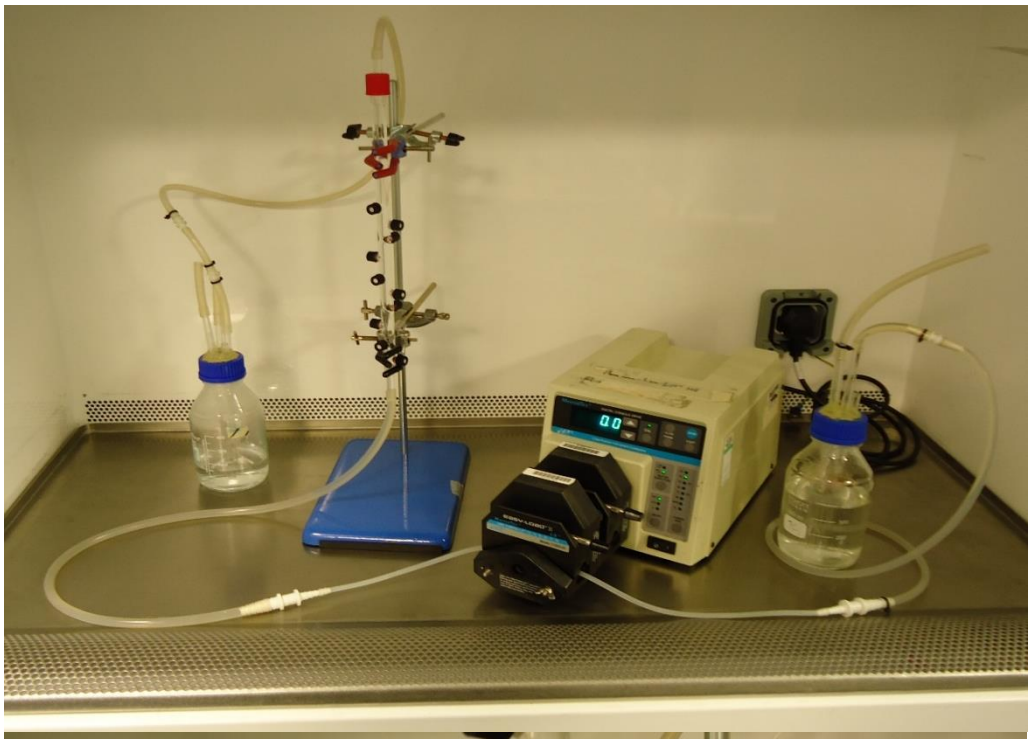

B

Figure 5.3: Figure 5.3A is an image of the perfusion separation column with, from right to left, media reservoir, peristaltic pump, glass column and the media collection vessel. Figure 5.3B is a close-up image of the collection ports near the bottom of the unloaded glass column.

5.3. Results

5.3.1. Identifying important experimental parameters

Table 5.1 shows the calculated TFV of various beads with a constant density of 1.1g/cm^3 and the corresponding net flow rate required to produce an equivalent net columnar fluid velocity. They show that, in theory, TFV increases with diameter and therefore requires a higher columnar flow rate in order to be mobilised. However, the relationship between the two is clearly not linear with each 50µm increase in diameter corresponding to progressively larger increases in TFV and therefore the required flow rate for mobilisation of these particles.

The difference between the net flow rate generated by the peristaltic pump and the actual flow rate in the column is caused by the deviation in the cross-sectional area of the column; which is 0.785cm^2. This means that the fluid velocity in the column will be larger than the net flow rate and so adjustments were made accordingly as net fluid velocity is equal to the net flow rate divided by the cross-sectional area of the column.

The mean diameter of beads collected from the column after 20 minutes of fluid flow using an Hsb of 5.5cm is shown in Figure 5.4. This data was collected at a range of column heights while utilising two different flow rates for comparison. It is quite evident that the mean diameter gradually decreased with increasing port height at both the upper and lower flow rate from around 135µm at port heights 1cm and 7cm for both flow rates to around 110µm and 90µm at port height 15cm for 1.5ml/min and 2.5ml/min flow rates respectively. In addition, it is noted that the mean diameter for both flow rates below a height of 7cm were approximately equal; remaining fairly constant across 1-7cm column height.

Above this point in the column the mean diameter of the particles began to decrease gradually at both flow rates. It is noticeable that it is from this point that the deviation between flow rates becomes apparent, with the lower flow rate showing a marked decrease in mean diameter compared to the higher flow rate at each column height. This shows that after 20-minutes continuous perfusion at this

Bead Diameter (µm)	Bead TFV (cm/min)	Equivalent Net Flow Rate (ml/min)
50	0.82	0.64
100	3.26	2.56
150	7.34	5.76
200	13.05	10.25
250	20.40	16.01
300	29.37	23.06

Table 5.1: A comparison of the terminal falling velocity of individual Sephadex beads to their diameter and the net flow rate required to generate a fluid velocity equal to this in the column. This was calculated using predictions made by the Stokes equation and gives the net flow rate across a cross-section at any point in the column beyond the entrance length.

Hsb both flow rate and column height had an impact on the size of the particles that were collected from the column.

The effects of various other factors that can influence the size of particles that can be collected from the column are shown in Figure 5.5. The impact that settled bed height has on collected particles across the length of the column at a single flow rate of 2.5ml/min after a period of 20-minutes continuous perfusion is demonstrated in Figure 5.5A. It is clear from this graph that at an Hsb of 0.2cm the mean particle diameter was markedly lower at every tested column height. This is particularly pertinent for the 13cm column height, where too few particles were present to be collected in order to make a reliable recording of the mean diameter at this set of conditions.

This shows that settled bed height has a profound impact on the size of particles that can be collected at any given flow rate from across the length of the column. This indicated that assumptions made from previous experiments using a large Hsb could not necessarily be relied on for a smaller Hsb. Therefore, a great deal more

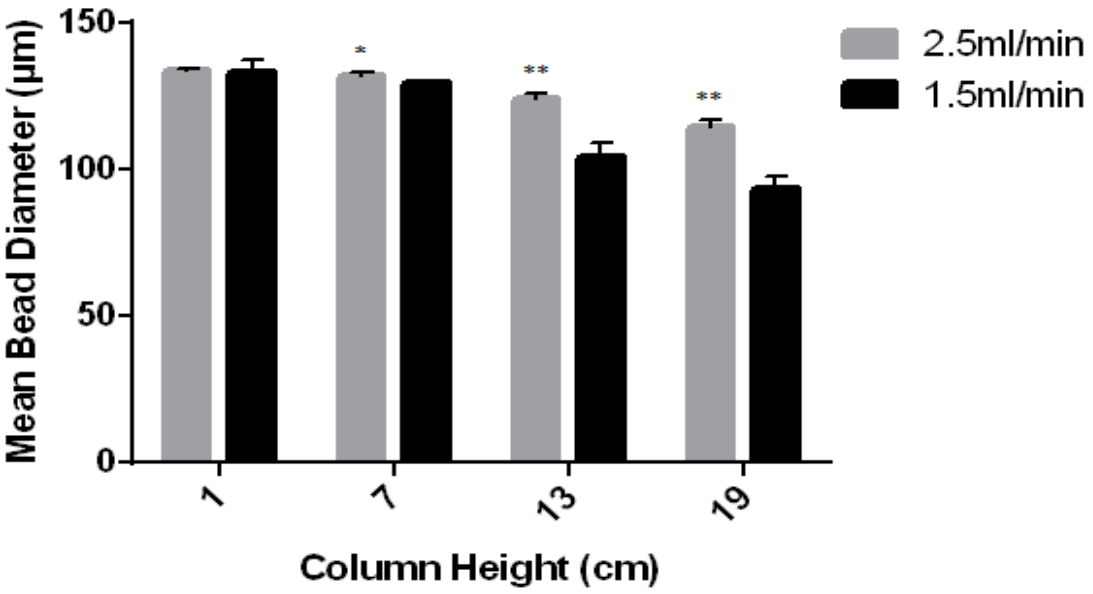

Figure 5.4: A comparison of the mean bead diameter collected at different heights in the column at two distinct flow rates after 20 minutes of perfusion. A settled bed height of 6.7cm was used for each experiment in a fully primed column and 30 minutes was allowed for all particles to settle to the bottom of the column. Readings were generated from images of beads collected from each set of conditions and analysed using ImageJ for their PSD. Significance is determined between different flow rates collected at the same port height and is denoted as follows; *** ≤0.001, ** ≤0.01, * ≤0.05. Each set of conditions had n=3 and was averaged with error bars shown (SEM).

research was needed in order to illuminate the differences that arose in the collected fractions as a result of this new condition.

The importance of time as an impactor on the mean diameter of particles that can be collected across the length of the column at a single flow rate of 2.5ml/min using a 0.2cm Hsb is illustrated in Figure 5.5B. At a column height of 1cm it appears that time made little discernible difference between mean diameters as all of the results fell in or around the standard deviation with no statistically significant difference shown between times.

However, at both 3cm and 7cm column heights time was shown to become an important influencer of mean particle diameter. It can be clearly seen at a column height of 3cm that the mean diameter increases gradually over time before levelling

off after 10 minutes. The difference between the data collected after 10 minutes and 15 minutes was considered negligible due to its lack of significance. At a column height of 7cm an even more striking observation is made; it is evident that until 10 minutes have passed an insufficient number of particles had reached this column height for an indication of their mean diameter to be made as less than 50 particles were collected at this time period when tested.

In addition, the 10 and 15 minute results at this column height follow a similar pattern to those collected at 3cm with both readings being very similar to each other; if a little lower than those collected at 3cm. Again, the difference between these time points was not found to be statistically significant at this port height. In conjunction, these results make clear that time not only has an impact on the mean diameter of particles collected at each column height at any individual flow rate, but was also a determiner of which column heights could actually be used to collect particles over the duration of the experiment.

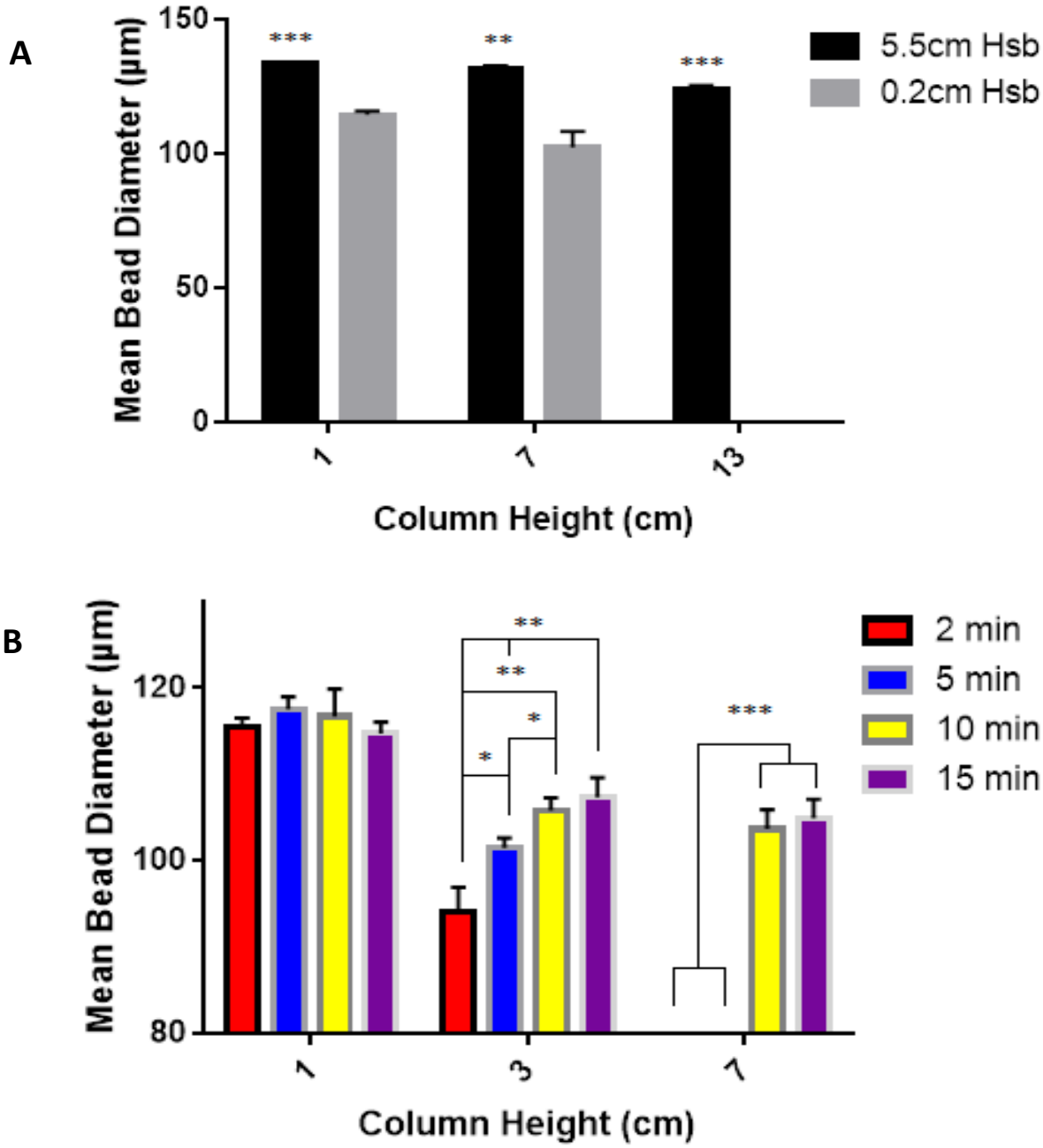

Figure 5.5: A comparison of factors that will have an effect on the size of beads collected from the column. Graph 5.5A shows the mean diameter of beads collected at a single flow rate of 2.5ml/min after 20 minutes over a range of column heights after the column was set up with two different Hsb's. Graph 5.5B shows the mean bead diameter collected across a range of column heights after different periods of time using an Hsb of 0.2cm and a flow rate of 2.5ml/min. Statistical significance is shown in Figure 5.5A between a small and large Hsb and in Figure 5.5B between separation times at a single column height. This is denoted as follows; *** ≤0.001, ** ≤0.01, * ≤0.05. Each set of conditions had n=3 and was averaged with error bars shown (SEM).

5.3.2. BRANN Results

A BRANN was trained using collected results across a range of conditions and then used to make predictions for each condition set as shown in Figure 5.6. At an Hsb of 0.2cm a range of results were collected at different times, port heights and flow rates. This information was then used to create a BRANN which could predict the mean particle diameter that would be collected at each of the possible specified combinations of conditions, including those that were not recorded during experimentation but that exist within the range of those that were. The strength of the model was then assessed by comparing the models predictions to the collected data as seen in graph 5.6D.

Immediately it is evident from the three graphs that flow rate had a profound impact on the mean diameter of each collected fraction; with a clear increase in mean diameter correlating to an increase in flow rate. Another recurring pattern is quickly discernible across each of the 3D graphs with all of them suggesting that the smallest particles were collected from the column at the highest port height and shortest time point. In addition, the largest particles were generally collected at the lowest port height; as would be expected. It is interesting to note that at any given flow rate there was little deviation in the size of particles that is collected at the bottom over the duration of each experiment. In contrast, time clearly had a profound impact on the size of particles that were collected from the column at greater port heights, although the impact of this diminished as the flow rate increased. Finally, it is noticed that as time increased, column height appeared to have less of an impact on particle size with a clear levelling off being evident at each flow rate. It should be noted that the point at which this levelling off occurs was hastened by an increase in flow rate.

All told these results suggest that the largest particles will be found at the bottom of the column at any time point, but that the best way of collecting multiple size fractions at a single flow rate is to use a short time period and the full length of the column. In addition, it seems that time and column height can be manipulated to allow for the collection of a range of smaller particle sizes at a single flow rate.

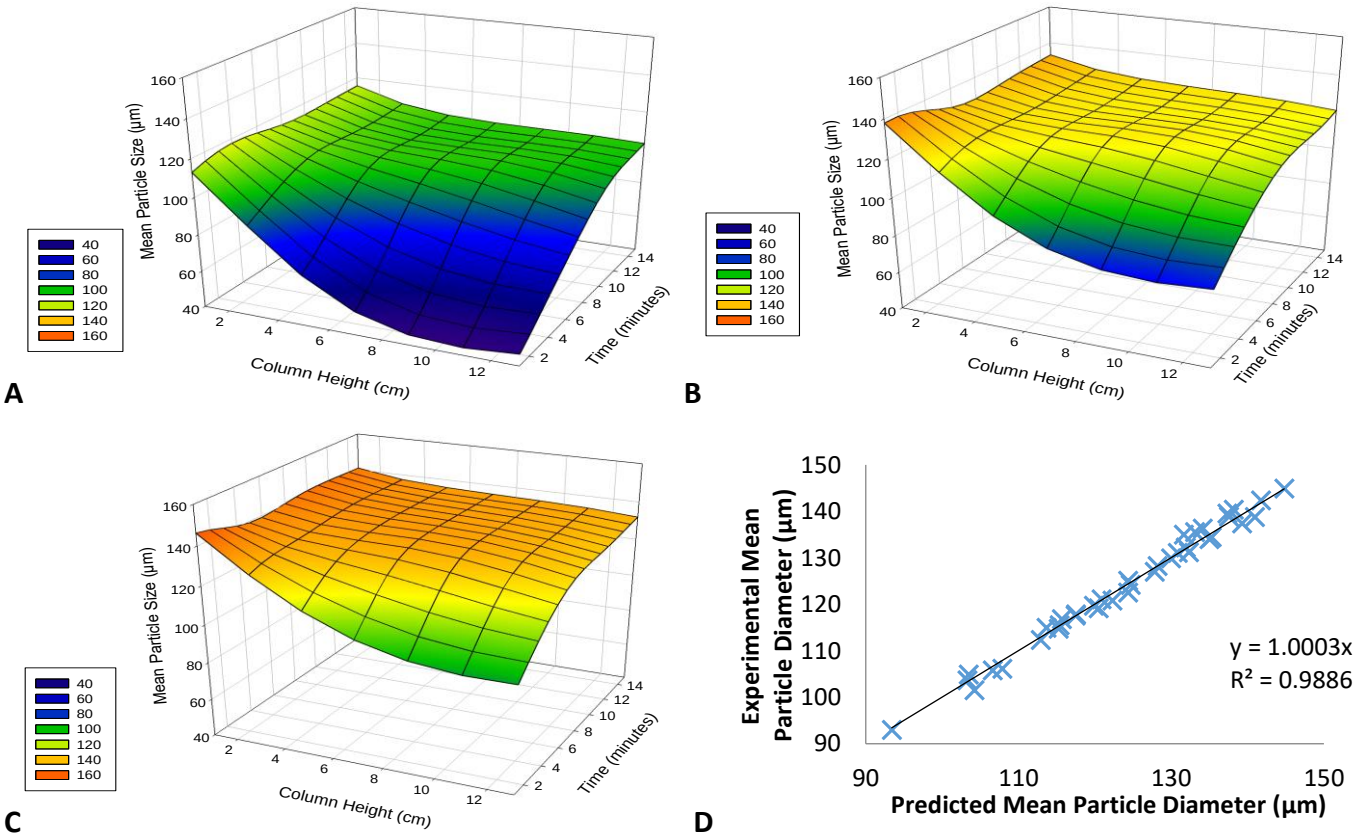

Figure 5.6: 3D graphs of predicted bead diameter (y-axis) based on a statistical model at varying flow rates, column heights (x-axis) and collection times (z-axis). Graph 5.6A represents a net flow rate of 2.5ml/min, 5.6B is 4ml/min and 5.6C is 5.5ml/min. Graph 5.6D shows the relationship between the results predicted by the BRANN model to the actual collected results that were used to generate it; data collections were taken at a range of combinations of flow rate, column height and time. Each set of conditions had n=3 and was averaged.

3D graphs generated from a second BRANN that relate to the particle span collected at each of the conditions tested above are shown in Figure 5.7; with all of the conditions identical to those used to calculate mean diameter. The BRANN was then used to predict the span at every possible combination of conditions within the tested range, even if they were untested. The resultant predictions were compared to the collected results that were used to generate the BRANN and displayed in graph 5.7D. This allows for a comparison of the accuracy of the predictions by providing a direct means of comparison to the actual data.

The general trends observed in these graphs are not dissimilar to those of the mean diameter ANN predictions. It is clear that once again flow rate had the most profound effect on increasing the span of particle sizes collected from each fraction. It was also noticeable that increasing time and decreasing port height resulted in a lesser increase in span.

VALIDATION PARAMETERS	
Absolute Average Deviation (AAD)	0.861
Mean Squared Error (MSE)	1.865
Root-Mean Squared Error (RMSE)	1.365

Table 5.2: Validation of mean diameter ANN by means of AAD, MSE and RMSE to show the how accurate the predictions of the system were compared to the actual collected results.

The span of all fractions collected at the lowest flow rate of 2.5ml/min was quite low, never exceeding 30µm thus suggesting that the fractions collected at this flow rate were quite discrete. At the intermediate flow rate of 4ml/min the span remained quite low for most of the tested conditions; generally below 30µm, except at the lowest port heights of 1 and 3 cm where it exceeded 40µm. This was where the larger mean diameter fractions were collected from at this set of conditions. This trend continued on into the highest tested flow rate of 5.5ml/min. A span of around 20µm was only achieved at the very top tested height of the column after the briefest period of elapsed time. At every other set of conditions it was much higher, peaking

at the lowest column height after a period of around 10 minutes to a span of over 60µm.

Span was seen to increase in relation to decreasing port height and, generally, increasing time. The only exception to this was at the lowest column height for the 5.5ml/min where the increase of span with time peaks at around 10 minutes and then began to decrease again. This trend was also noticeable, albeit to a lesser extent, at the two lower flow rates.

Three statistical indices that give an indication of the accuracy of each BRANN were calculated; these were Absolute Average Deviation (AAD), Mean Squared Error (MSE) and Root-Mean Squared Error (RMSE). For the both the mean diameter and span BRANN's these numbers were quite low. This correlated to the large R^2 value shown in the predicted vs. collected graph to suggest a high degree of accuracy for both BRANN's. It is noticeable that while AAD, MSE and RMSE are still quite small for the span BRANN, all three are significantly larger than for the mean diameter BRANN.

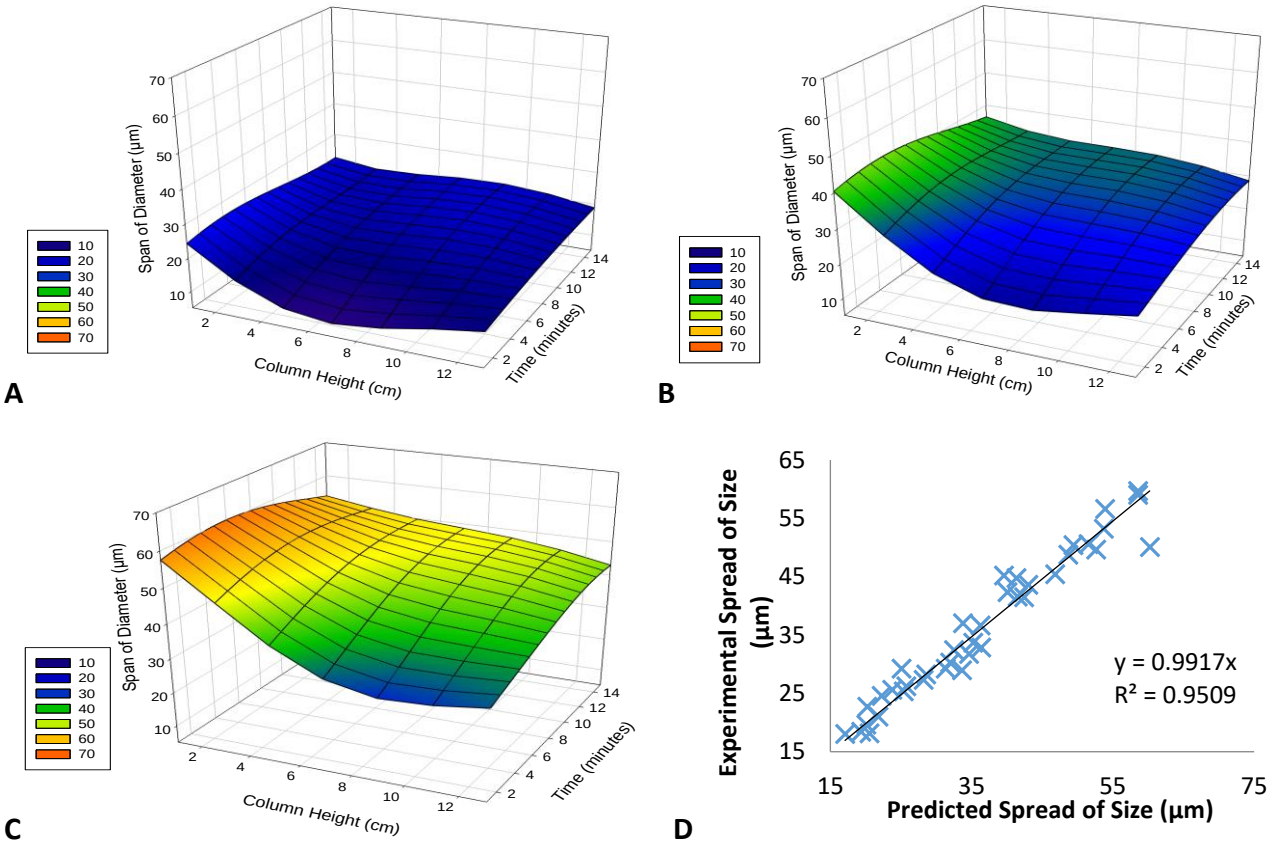

Figure 5.7: 3D graph of predicted bead span (10th to 90th percentile) (y-axis) at varying flow rates, column heights (x-axis) and collection times (z-axis). Graph A represents a net flow rate of 2.5ml/min, B is 4ml/min and C is 5.5ml/min. Graph D shows the relationship between the results predicted by the BRANN model to the actual collected results that were used to generate it with data collections taken at a range of combinations of flow rate, column height and time. Each set of conditions had n=3 and was averaged.

Previously collected model results using beads were built upon by replacing the beads with EBs; these results are shown in Figure 5.8. This was to display that the wealth of modelling results collected with the beads were sufficiently representative of the same conditions with EBs and so prove that they represented a good model system. Two results were collected to be representative of the smallest and largest size fractions that were collected at 2 condition sets; 1 and 2. Condition 1 consisted of a 100µl fraction collected from a port height of 3 cm following 5-minutes perfusion at 2.5ml/min. Condition 2 consisted of a 100µl fraction collected from a port height of 1 cm following 5-minutes perfusion at 5.5ml/min.

VALIDATION PARAMETERS	
Absolute Average Deviation (AAD)	5.568
Mean Squared Error (MSE)	7.351
Root-Mean Squared Error (RMSE)	2.711

Table 5.3: Validation of span ANN by means of AAD, MSE and RMSE to show the how accurate the predictions of the system were compared to the actual collected results.

There is a significant difference between the mean diameters of beads and EBs collected at condition set 1 with the EB fraction being around 15µm larger; this is shown in Figure 5.8A. However, at condition set 2 the difference between the bead and EB results is insignificant and within the standard error margin. The similar trends between data collected with the beads and the EBs shows that the beads provided a reasonable approximation for how the EBs would act in the column, but were more accurate for larger size fractions.

In contrast, figure 5.8B shows a large variation in the span data collected for beads and EBs at both flow rates. The EBs had a significantly larger span at both the 2.5ml/min and 5.5ml/min flow rates. In both instances they were in excess of 100µm. However, the increase in real terms of the span from 2.5ml/min to 5.5ml/min was similar in the beads compared to the EBs with both increasing by around 20µm.

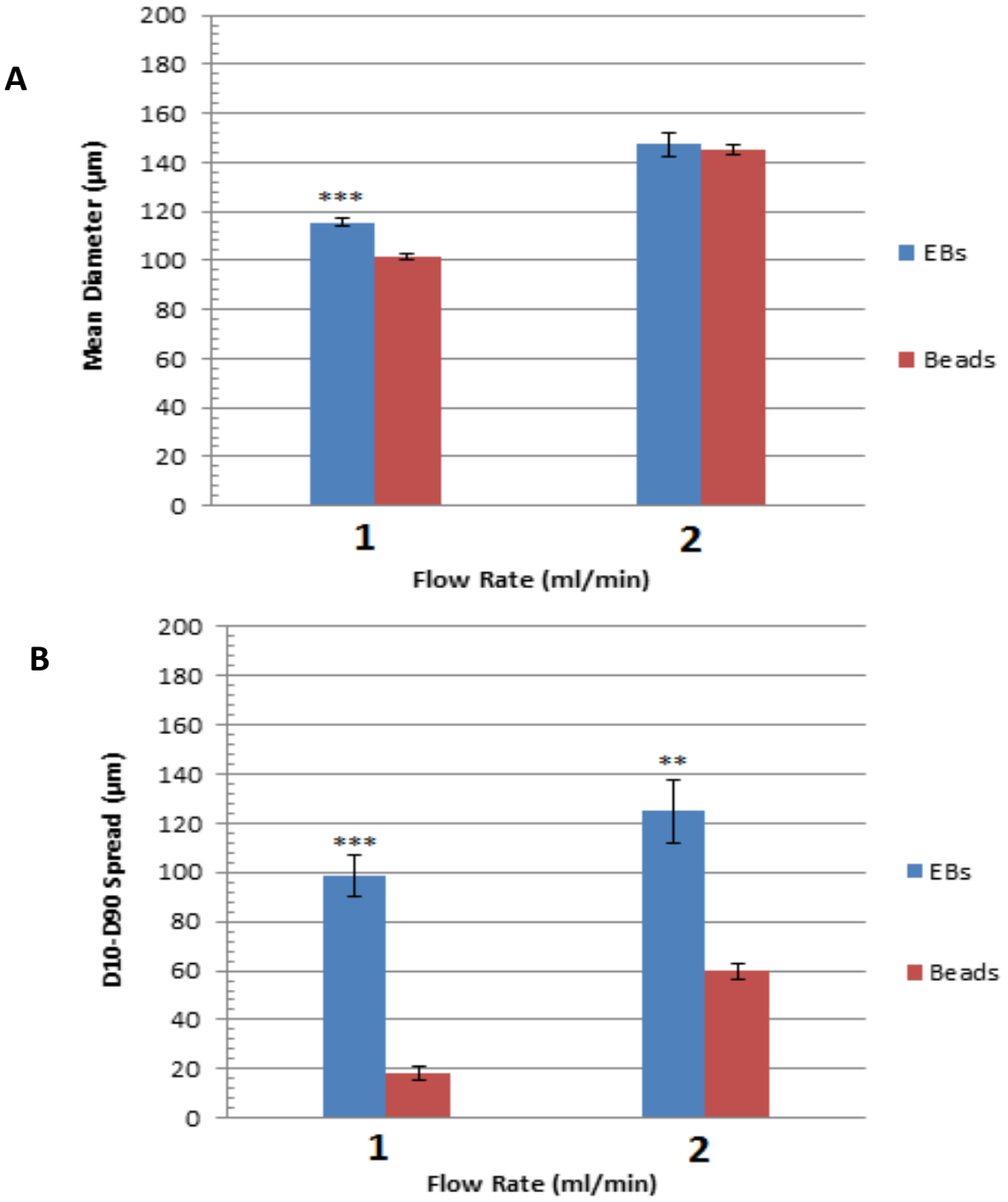

Figure 5.8: The mean diameter and span of collected particles at two distinct sets of conditions designed to collect the largest and smallest fractions of EBs based on the predictions made by the model system. The smallest fraction was predicted to be collected at a flow rate of 2.5ml/min at a column height of 3cm and after 5 minutes, while the largest was predicted to be collected at a flow rate of 5.5ml/min after 5 minutes and at a column height of 1cm. Graph 5.8A shows the mean diameter of EBs collected while Graph 5.8B gives the span (10^{th} to 90^{th} percentile). In both cases they are compared to the bead data collected at identical conditions. *** ≤0.001, ** ≤0.01, * ≤0.05. Each set of conditions had n=3 and was averaged with error bars shown (SEM).

5.4. Discussion

5.4.1. Background

Differentiation of PSCs, including ESCs, remains a process littered with inconsistencies and a distinct lack of standardisation (Serra et al., 2012, Unger et al., 2008). In almost all instances of PSC differentiation a host of undesirable 'contaminant' cells are present that differentiate into an unwanted, unspecified lineage, thus undermining the efficacy of PSCs as a viable source for fully differentiated cells for tissue engineering (Okano et al., 2013, Klimanskaya et al., 2008).

EB size has been previously shown to have a profound effect on the differentiation of cells and has therefore been investigated as a means of improving this issue. EBRs were utilised in this research to attain multiple distinct size fractions of EBs from a heterogeneously sized stock population. In contrast to some previously detailed techniques, this method was designed to be an inexpensive alternative that possesses the potential for scalability to allow for increased throughput.

Prior to the thorough analysis of the column with a model system it was necessary to determine exactly what factors were likely to impact on the separation of particles along the length of the column. Initially this took the form of ensuring that previously documented results could be repeated with this particular experimental set up. This was ascertained by utilising a settled bed height of 5.5cm and two distinct flow rates across the length of the column. Thereafter a series of experiments were performed to determine the impact of Hsb and time.

For the initial large Hsb experiments an upper flow rate of 2.5ml/min and a lower flow rate of 1.5ml/min were selected. Voidage further increased the effective flow rate within the column by an assumed factor of 2.5. Therefore, these flow rates were chosen because when taking voidage into account they equated to the TFV of particles of around 160µm and 120µm in size respectively. In addition, these flow rates have been used previously in the literature thus allow the efficacy of the column to be compared to previous studies (Ng and Chase, 2007).

It should be noted that laminar flow in a column usually exhibits a parabolic flow profile as shown in Figure 5.9, which would impact on the flow rate encountered at particular points across the column. However, a sintered disc was used in these experiments to try and negate this. By forcing the fluid to enter the column through a sintered disc the inlet of fluid was spread across multiple points instead of one single point. As a result, the parabolic flow was levelled out, instead leaving only the impacts of the no-slip condition. This should have reduced the variable flow rates that were encountered across the diameter of the column and encouraged homogeneity of collected particles and consistency in sampling at any given port height.

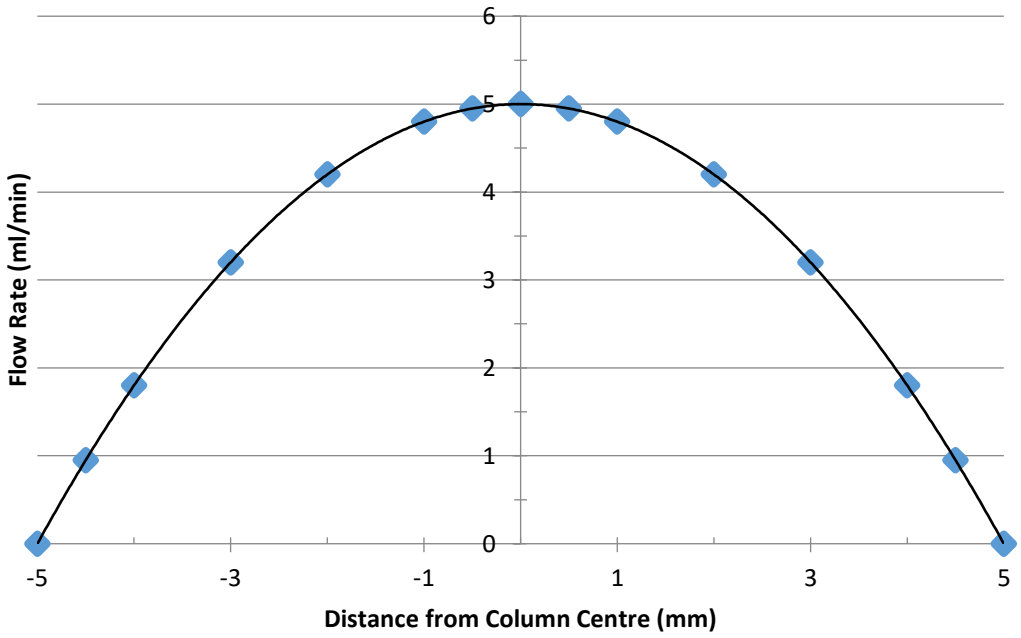

Figure 5.9: The parabolic flow regime of laminar flow encountered in a cylindrical column of 1cm diameter beyond the entrance length at a net flow rate of 2.5ml/min.

5.4.2. Flow Rate

The capability of the column for separating out multiple size fractions of particles at two distinct flow rates was tested and the results shown in Figure 5.4. The results here are in keeping with a multitude of previous experimental results that demonstrated that increasing port height at any individual flow rate resulted in a decrease in mean particle diameter, while increasing flow rate resulted in an increase in particle diameter across all port heights (Ng and Chase, 2007, Willoughby et al.,

2000, Yun et al., 2005, Lin et al., 2013). The lower tested port heights of 1cm and 7cm had a mean particle diameter of around 135µm at both tested flow rates; this was an increase on the mean diameter of the stock that was around 125µm. This was caused by the successful removal of the smallest particles further up the column as has been previously reported in the literature (Willoughby et al., 2000). As a result, the mean diameter was lower at higher port heights as the smaller particles had advanced up the column, above that of the settled bed, where the larger particles were incapable of reaching at these flow rates.

The Tong-Sun equation would predict a slightly larger fraction be collected from the bottom port of around 145µm (Tong and Sun, 2002). However, this requires a relatively large size distribution in the stock, which was not the case for the beads used in this study, as more than 80% of the particles were found to be below 145µm in diameter. It is interesting to note that in an expanded bed the lowest axial dispersion of particles was found for a wide size distribution (Karau et al., 1997). This is contrary to results collected for a packed bed where axial dispersion was shown to be greater when a large distribution of particles sizes was used compared to a more narrow distribution (Han et al., 1985).

Both of these selected flow rates were aimed at mobilising the lower end of the bead stock. However, when taking into account the parabolic flow regime and a maximum assumed voidage of 0.4, the effective flow rate could reach 7.5ml/min for the 1.5ml/min net flow rate and 12.5ml/min for the 2.5ml/min flow rate. These maximum flow rates would, in theory, be found only at the bottom of the column in the fully settled bed and at the very centre of the column. Under these conditions they could move beads up to 150µm in size, around 85% of the stock, for the lower flow rate and around 200µm, or 99% of the stock, for the larger flow rate.

However, once the settled bed height is surpassed the voidage will rapidly increase as you move further up the column thus reducing its impact on flow rate. Accordingly, in the area of fluidised bed the voidage would be significantly lower and so the maximum flow rate at any point here would be likely to be much closer to 3ml/min for the lower flow rate and 5ml/min for the higher flow rate. This explains why the primary difference in diameter of collected fractions between the two flow

rates was found higher up the column as the difference between these maxima correlates to a change in the ability to move around 15% of the beads (<100µm) to around 60% (<150µm) respectively. With the higher flow rate able to generate an increased fluid velocity at higher points along the column length the particle sizes found in these locations continued to be larger than those encountered in the lower flow rate.

It should be noted that as a peristaltic pump was used the particles would have experienced pulsatile flow, which could have caused some minor inconsistencies in the separations due to its oscillating motion (Taber et al., 2006). This could be overcome by using a second reservoir filled with liquid at the outlet of the column to provide a dampening effect and thereby reduce the presence of the pulsatile flow. This would make the movement of the fluid and the particles within more consistent and, while it should not affect the general trends shown in these results, it should improve consistency between runs.

5.4.3. Settled Bed Height

Figure 5.5A shows how settled bed height impacts on the mean diameter of particles collected along the length of the column. The effect of settled bed height has been explored to some degree by various researchers who have documented its effects on fluid hydrodynamics, expanded bed height, the Bodenstein number (B_o) and the axial dispersion of particles (Jahanshahi et al., 2009, Taheri et al., 2012). These results showed that varying Hsb can have a profound effect on the size-separation of particles within the column through its impacts on expanded bed height and therefore, by extension, axial dispersion. Increasing settled bed height allowed more of the column to be utilised as a means of collecting particles, thus improving the potential for the collection of multiple size fractions. However, while a useful indication of how Hsb can impact on the separation of particles within the column, these papers did not address the impacts of reducing Hsb to such a scale as to be commonly encountered in dealings with particles of severely limited number and thus reduced potential for formulating a large Hsb. The lowest Hsb achieved in these experiments was 3cm; still over an order of magnitude larger than that which

can realistically be expected to be achieved on a lab scale with EBs in a column of this size.

Theoretically it would be possible to increase the Hsb using the same number of particles by reducing the diameter of the column. However, this brings with it a number of issues that offset any potential benefit in doing so. A wealth of research has explored the impact that column diameter has on the separation of particles; with an increase in diameter correlating to an increase in axial dispersion and a decrease in B_o (Jahanshahi et al., 2009, Taheri et al., 2012).

In addition, if the column diameter was reduced to such an extent that the ratio of particle diameter to column diameter (d_p/d_c) exceeded 0.01 then wall effects would become more of a consideration (Mehta and Hawley, 1969, Jahanshahi et al., 2009). This dictates that the TFV of a single particle, spherical or not, is reduced as it comes closer to the wall (Chhabra et al., 2003, Brown and Lawler, 2003, Lau et al., 2010). In contrast it has been shown that in a packed bed the TFV of particles close to the wall is increased by up to 100% (Schwartz and Smith, 1953). Although this will likely be caused by the large reduction in flow rate encountered near the column wall as a result of the no-slip condition (Day, 1990). Combined, these effects could reduce the ability of the column to consistently size-separate fractions of particles and therefore negate any benefit of increasing the Hsb.

Consequently, this set of results showed that changing the Hsb did have a profound effect on the capacity of the column to separate out particles by their size. Because of this and due to the unique nature of the Hsb that will be utilised for these experiments there was a need to further explore the effects of separating particles under a range of conditions using this experimental set-up.

5.4.4. Time

The effect of time on the size of particles that can be collected from along the length of the column is shown in Figure 5.5B. The collection height was limited to 7cm because at this flow rate and over the times tested the beads did not reach any further along the column length in sufficient numbers for an accurate measurement of PSD to be calculated. This is reinforced by the fact that it took an elapsed time of

10 minutes before particles reached a height of 7cm in sufficient numbers for a reading to be taken. It should be noted that if more particles within the stock existed at the lower end of the distribution then a shorter time would likely be required for higher port heights to become viable for sampling.

It is evident that the mean diameter of particles collected decreased along the length of the column at each of the tested time points. With voidage unlikely to play much of a role outside of the bottom 1cm of the column this was probably because the larger particles took more time to move up the column, assuming they moved at all. This was a result of the lower differential between the columnar fluid velocity and the TFV of the particles. The closer these numbers are to one another for an individual particle the longer it will take for that particle to elutriate out of the column.

It is also noticeable that the mean diameter of particles at the bottom port height of 1cm remained constant and, despite being the largest fraction at all tested time points, never increased beyond the mean diameter of the stock. The subsequent results made clear that the smaller particles were certainly navigating their way up the column. Accordingly, these results in combination showed that while smaller particles were moving up the column at this flow rate and advancing over time, this was not sufficient to increase the mean diameter at the lowest port height.

This could have been caused by the flow rate that was used for this experiment, which at 2.5ml/min could only really effectively move particles below 150µm; even at the very centre of the column where the flow rate peaked. Across the majority of the width of the column the flow rate was unable to mobilise particles any larger than 100µm, which constituted less than 13% of the stock. This explains in part why the removal of these particles from the bottom of the column had such a minimal impact on the mean diameter found there as they made up such a small fraction of the whole.

It should be noted that this could also be a result of the laminar flow profile preventing all of the smaller particles being removed even from the bottom of the column. This combined with the increased settling velocity of particles caused by wall

effects means that at any flow rate it was not possible to completely remove the smallest particles from the bottom of the column. Instead the aim must be to reduce their number to insignificant proportions.

The culmination of all of the collected results so far indicates that there are a multitude of varied factors that will impact on the ability of the column to mobilise particles of different sizes and therefore separate them out into unique size fractions. It was decided that for the model system the Hsb would be set at 0.2cm, as this is achievable with EBs. A loaded column was therefore tested at this bed height under a multitude of conditions.

5.4.5. Artificial Neural Networks

Due to the variety of conditions required and therefore the difficulty in suitably visualising the dynamic nature of the system, an ANN was produced. This was generated using results collected across a number of different flow rates, times and column heights and allowed for predictions to be made, based on the data, between the tested conditions. The BRANN was produced using 70% of the raw data, which was then compared to the remaining 30% of unseen data. The ability to accurately predict the unseen data was used as selection criteria for the BRANN. Multiple BRANN's were set up and only explored for further testing if they predicted the unseen data with an accuracy of greater than 90%. There was an element of trial and error used to determine some of the conditions, such as best number of hidden layers and nodes within the BRANN. This meant that less time was spent validating inefficient BRANN's as they had already been discounted. In summation, this approach ensured that only the most successful BRANN went forward for further testing.

Subsequently, this data was used to generate 3D graphs to make interpretation of the data simpler. In addition, it meant that the ANN could be used to determine the exact set of conditions required to collect any size fraction that falls within the tested limits, even if it was not directly tested in the initial experiments. Using this approach, any similar separation system can be tested using a multitude of conditions to discern how to collect specific size fractions quickly. By using a BRANN it is not necessary to test every imaginable condition as it can accurately predict what condition will collect

a certain size fraction. Using an appropriate Design of Experiments the fewest condition sets required to collect the most useful data can be discerned. This further reduces the number of experimental variables that will need to be tested in order to get the BRANN to provide the required information accurately.

Two separate ANN's were produced to provide information on both the mean diameter and span of particles collected from the column across all tested conditions. A Bayesian Regularisation Artificial Neural Network (BRANN) was used for this study because the addition of this mathematical process generates a more robust ANN and reduces the need for validation (Burden and Winkler, 2008). This ensured improved accuracy of the predictions generated by the model by weighting the importance of each input therefore reducing the effect that less important factors have on the output.

The BRANN's were generated using 70% of the collected data, which was then tested against the remaining 30% of the unseen data. This ensured that even during its conception the BRANN was self-validated and allowed the most suitable and consistently accurate BRANN of the many generated to be taken forward for further use. An R^2 value of 0.95 for predicted versus collected results was set as the minimum threshold for further consideration of both BRANN's.

The combined BRANN predictions are then shown compared to the actual collected results in figures 5.6D and 5.7D. What these results show is that there is excellent agreement between the results predicted by the model and those actually attained experimentally at each different condition set; as shown by the high R^2 value. This provides a strong level of confidence that these two BRANN's can accurately predict both the mean diameter and span of particles collected from this system between the tested conditions.

This is corroborated by the small AAD, MSE and RMSE for both BRANN's. These three statistical indices are used to validate the ANN because R^2 values have been shown to be insufficient for evaluating nonlinear models (Spiess and Neumeyer, 2010). Low AAD, MSE and RMSE have been repeatedly shown to correlate to a high strength of model and therefore allow data to be interpolated from this model with

a high degree of confidence (Wang et al., 2008, Basri et al., 2007, Mansour Ghaffari et al., 2010). As a result, the trends given by the 3D graphs are sufficiently representative of the actual separations occurring in the column to allow conclusions to be drawn from them.

It should be noted that all three of AAD, MSE and RMSE were larger for the span BRANN compared to the mean diameter BRANN, thus indicating that the accuracy of the model was lower for the span. This would have been caused by a lack of reproducibility in collecting span data. The inherent added complexity of this data set compared to the relative simplicity of the mean could have reduced the efficacy of the BRANN and caused this discrepancy.

5.4.5.1. Mean Diameter

Figures 5.6A, 5.6B and 5.6C show the mean diameter results of the BRANN for 2.5ml/min, 4ml/min and 5.5ml/min respectively across a range of port heights and times. The general trends across the three flow rates were similar, as is to be expected, with the largest particles always being found near the bottom of the column and the smallest near the top. At any time and port height the ultimate limiting factor on maximum mean diameter was flow rate. This was therefore the only factor that could be altered to increase the mean particle diameter of fractions beyond those collected at these tested conditions.

Furthermore, these results agree with those presented in Figure 5.5 and show that the impact of column height diminishes as time increases with a levelling off of the mean diameter at all tested flow rates after around 10 minutes; although it occurs more quickly at higher flow rates. After this period of time the only meaningful impactor of mean diameter was flow rate. This meant that effectively only one size fraction could be collected at each flow rate across the column after a certain period of time; though it was larger at increased flow rates. As a result, in order to collect more than one size fraction at a specific flow rate only the first few minutes of the separation were useful.

In summation, the assorted graphs of Figure 5.6 suggest that in order to collect a range of size fractions across the full distribution found in the stock a high flow rate

was required. By using a combination of relatively short time periods and multiple column heights a number of particle sizes could then be collected during one experiment.

5.4.5.2. Span

In contrast, the results shown in Figure 5.7 highlight an issue with this approach. These graphs show how the span of the particles, i.e. the 10^{th}-90^{th} percentile, was affected by the same conditions as those tested for mean diameter. Here it becomes clear that the same factors that were responsible for increasing mean diameter also elicited a corresponding increase in span. The largest contributor to increasing span was again seen to be increasing flow rate. This means that in order to increase the mean diameter of the collected fractions the discrete nature of the fractions was lost. This is particularly troubling when it is noted that at the bottom port height and briefest elapsed time period the increase in mean diameter from 2.5ml/min to 5.5ml/min was around 25µm, however, this correlated to an even greater increase in span of around 30µm.

What this means is that in order to increase the mean diameter from 120µm to approximately 145µm, the span increased from 25µm to around 60µm. The resultant fractions were therefore not discrete from one another, with a multitude of collected particles existing in both the larger and smaller fractions. It is possible that this issue could be resolved by simply increasing the flow rate to ensure that an even larger fraction of particles could be collected and thus negate the contamination of particles existing in both fractions. However, the results of Figure 5.7 clearly suggest that in doing so a corresponding increase in span would continue to frustrate efforts to isolate a discrete fraction of larger particles. This would then become exponentially more problematic as larger and larger fractions were desired.

The reason for this corresponding increase in span could be a facet of the parabolic flow regime of laminar flow. This dictates that at any given net flow rate a range of fluid velocities will be observed in the column depending on the position across the column diameter. The very centre of the column will have a flow rate twice that of the net and gradually decrease outwardly towards the exterior until at the column wall it is effectively 0 (Day, 1990, Sibulkin, 1962).

It therefore follows that an increase in net flow rate will result in a corresponding range of fluid velocities equal to twice that of the increase in net flow rate. As a result, an assortment of particle sizes can be moved at a single net flow rate due to the different fluid velocities, with this being dependent on the location of the particle across the diameter of the column. Ordinarily this is not considered to be a problem in EBR's as it has been demonstrated that sampling position across the radius of the column had a minimal impact on mean diameter (Willoughby et al., 2000). While this may mean that any sample collected at a particular axial height is the same regardless of the radial position of the needle, it does not mean that there are not different sized particles across the column radius, but that particles across the whole cross-section are all collected during sampling thus maintaining a representative sample regardless of radial sampling position. However, while the use of a sintered disc should have limited the presence and therefore impact of this laminar flow profile it will not negate the fact that a larger flow rate will move particles from across a greater size range along the column length. Due to this fact, and the continued presence of the no-slip condition, a larger span of particles will therefore likely be present at any set of tested conditions, especially in the lower reaches of the column.

This is in accordance with previously collected results that showed that by moving up the column at any individual flow rate the span of collected fractions could be reduced compared to the very bottom of the column (Willoughby et al., 2000). This was due to the removal of the largest particles as they remained at the bottom. However, it was also shown that by moving further up the column this effect was gradually diminished. While the mean diameter and D10 decreased the alteration in D90 was shown to be minimal beyond the bottom of the column, meaning that the smallest particles were encountered throughout the column.

The BRANN could be utilised more efficiently for this and other size separation techniques for various process improvements. This technique could be used for a wide range of data sets across the full potential of a technique to be rapidly tested while collecting a minimum of data. Using this technique, areas of interest on a global scale could be quickly identified for future experimentation at the cost of accuracy and precision on a local scale. Following this, a more intimate exploration using more

data collected within these areas of interest could determine exactly what can be collected within each region.

In summary, these results indicate that this technique can be used to collect a pure fraction of the smallest subset of any individual population of particles. It was also shown that this method could collect multiple fractions of particles with varying mean diameters utilising time, column height and flow rate as independent variables. However, under the conditions tested it was not able to effectively collect fractions with a larger mean diameter without sacrificing the discrete nature of said fractions as determined by their span.

5.4.6. Validation of Model System Using Embryoid Bodies

Finally, Figure 5.8 shows how accurately the ANN model developed with beads matches up to the same conditions using EBs. The conditions that allowed for the largest and smallest mean diameter were chosen as these allowed the full capability of the system to be assessed. It is clear that the predictions for mean diameter of the beads were representative of those of EBs for the collection of the largest size fraction. However, the beads produced a significant overestimation of the mean diameter of the EBs for the smallest size fraction. This difference of 14µm was likely caused by the EB stock having a larger percentage of particles below 100µm, 22% compared to 12% of the beads. This would result in an underestimation for the smallest fractions, but would be overcome as mean particle diameter increased. In all, these results suggest that the beads were sufficiently similar to the EBs in their physical properties to generate similar mean diameter results.

In contrast, the span results generated by the model bead system were shown to underestimate the results generated for EBs at both tested conditions. This may well be because the stock of EBs had a larger range of sizes to begin with thus allowing this characteristic to remain in the separated fractions. This is a particularly concerning issue as it exacerbates the problem already faced by this column as a means of size-separating out EBs into discrete fractions. With the span of the EBs never being below 100µm and reaching up to 150µm the discrete nature of any collected fractions would be entirely lost. A 100µm span for a fraction with a 120µm mean diameter could contain particles from up to almost 80% of the stock of EBs.

Unless it was found that the very largest or very smallest particles were of particular concern in affecting differentiation it is unlikely that this technique would provide sufficient advantage to be of reasonable benefit.

In contrast, one positive is that the actual increase in span from 2.5ml/min to 5.5ml/min with the EBs still remained at around 20µm suggesting that the increased span for both fractions is likely to be caused by an inherent deviation in the population dynamics of the stock with their simply being a much larger number of smaller particles existing in the EB stock compared to the beads which had a more defined range. This offsets fears about the applicability of the model system to predict the outcome of the EB separations.

5.5. Conclusion

These experiments have further explored the nature of size separation of particles in expanded bed reactors. They have successfully highlighted the importance of settled bed height on the separation of particles and in addition shown how port height, time and flow rate can all be used in tandem to control the mean diameter of particles that are collected from the column. Further an ANN was developed that allowed for predictions to be made so that any combination of these factors within tested limits could be exploited to collect a desired size fraction, and showed proof of principle that this modelling technique could be expanded upon to provide further benefit in this field.

On the other hand, these experiments also highlighted some shortcomings with this technique for the size separation of discrete fractions of EBs. Due to the correlation of increasing span with mean diameter the method is limited to collecting discrete fractions of only the smallest fraction of EBs. In addition, it is unlikely that this technique could be sufficiently scaled to collect the numbers of EBs that would be required for a tissue engineering industry due to its necessity for a lot of user input.

These results have made clear two important points that can be of great benefit moving forward. First of all, it seems that the beads do make a good approximation for the separation of EBs with regards to their TFV. Secondly, and most importantly, these results strongly suggest that EB diameter does correlate with TFV and that, while this technique was not sufficient to utilise it, this is a characteristic that can be successfully exploited to size-separate discrete fractions of EBs. As a result, it would be wise to identify a variation on this separation technique that can remove some of the suggested issues herein, such as the laminar flow profile of fluid within the column, to ensure more accurate fractions can be isolated and greater control provided over the mean diameter of said fractions.

Chapter 6

Particle Size Separation Using a Novel Gravity-Based Separation Technique

6.1. Introduction

It has been shown previously that both Sephadex beads and EBs exhibit a clear relationship between their mean diameter and TFV as predicted by the Stokes equation. However, the expanded bed separation technique described previously was unable to exploit this characteristic to its full potential and struggled to collect multiple, discrete size fractions of particles. This was largely attributed to the parabolic fluid velocity profile of laminar flow and the no-slip condition, which prevented consistency being achieved across the column diameter and therefore undermined efforts to collect specific size fractions (Sibulkin, 1962, Day, 1990). The main issue with this arose when attempting to collect size fractions over 150µm in diameter, as increasing the flow rate resulted in a corresponding increase in the range of fluid velocities across the column diameter and therefore the number of particles that could be mobilised at different points across the column diameter.

Due to the limitations of using a perfusion technique an alternative method was devised that relied solely on the settling velocity of the particles and removed the need for perfusion. In doing so, the issues encountered with laminar flow were mitigated and so only the inherent characteristics of the particles themselves should determine the efficacy of their separation. The premise of this technique was to simply allow the particles to settle in a fluid from the top of a glass column and collect them after various time-points when they eluted out of the bottom. This is similar to

previous techniques employed for a variety of different types of particles, but is not one that has been applied to aggregates of cells (Clifton et al., 1999, Vdović et al., 2010, Konert and Vandenberghe, 1997).

It was hoped that the novel application of this separation technique would build on the knowledge gained previously to enable the collection of at least three discrete fractions that represent a plethora of particle sizes from across the full range found in both the bead and EB stocks. Due to its success, this technique was also applied to EBs across a range of formation times to ensure that the technique was flexible in its application and to also help determine any differences in physical properties between EBs of the same size that have been afforded different formation periods. This is important as different differentiation processes have been previously demonstrated to utilise varying EB formation periods.

6.2. Materials and Methods

6.2.1. The Stokes Equation

The Stokes equation, as shown previously in Equation 5.1, was again utilised to make predictions of the TFV of Sephadex beads. The beads were assumed to have a density of 1.1g/cm^3 and the EBs a density of 1.07g/cm^3. The spread of diameters of beads used in these experiments was much larger than that used previously, with a D10 –D90 span of 125µm (109-234µm) and a mean diameter of 158µm. Acceleration due to gravity was assumed constant at 9.81m/s^2. Density of medium was 1g/ml and viscosity of medium was 1.002cP. All experiments were performed at room temperature of around 20^{o}C. Calculations using this equation were used to estimate the elution time of different sized particles to inform on the separation technique and are shown in Figure 6.3A.

6.2.2. Gravity-Settling Separation Technique

A 30cm column was set up perpendicular to the floor and loaded with pre-warmed PBS to a height of 28cm from the collection point at the bottom. The bottom was then blocked off with a cap and particles were loaded to the top of the column in a volume of 1ml PBS. A screw cap was then tightened at the top of the column attached to a syringe to prevent the PBS eluting out of the column and the bottom cap removed. After each time period a 1ml fraction was collected in a well of a 12-well plate from the bottom of the column by forcing filtered air through the apparatus. This was repeated every minute from 2-10 minutes and then once more after 15 minutes in a short burst using the syringe. This technique was performed in identical fashion both for the beads and EBs. The EBs were cultured as has been described previously.

In the second set of experiments performed with this column the remaining contents of the column were purged and collected in a petri dish. This was performed by forcing more filtered air through the column until none of the particle-laden PBS remained in the column. In both cases fractions were then imaged to allow for particle size analysis using ImageJ software, which took readings of the max Feret diameter.

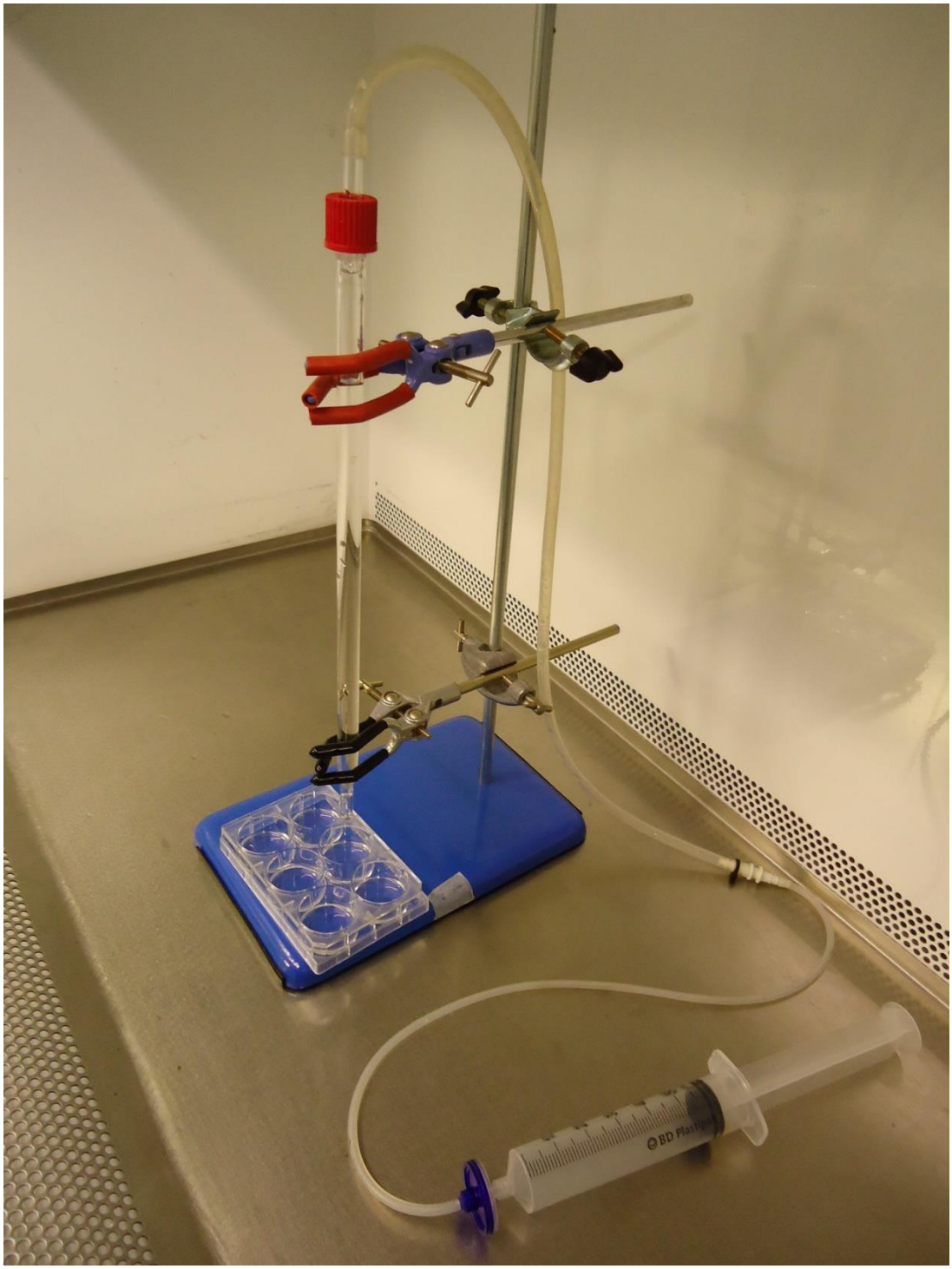

Figure 6.1: Shows the glass gravity settling separation column of 10mm diameter attached by rubber tubing to a 50ml syringe with 0.2µm filter. At the bottom of the column is a 6-well plate used for collection in some experiments.

6.2.3. Pre-separation technique of EBs

A single 10ml petri dish of growth medium containing EBs was collected using a serological pipette and deposited in an upright 15ml falcon tube. A period of 5 minutes was allowed to elapse before the top 8ml of media containing aggregates was collected from the liquid surface, again using a serological pipette. It was ensured that the pellet remained undisturbed during the collection period. The collected EBs were then imaged to allow for a particle size analysis to be performed using ImageJ software, which took readings of the max Feret diameter.

6.2.4. MTS Growth Rate Assay

Aggregates were separated in to two groups; those that had undergone the 15-minute gravity separation technique and those that had not. All aggregates that underwent separation were harvested and coalesced back into a heterogeneously sized mixture to ensure consistency between groups. The MTS assay was then performed as described in the Materials and Methods section (Chapter 4.2.4.). The calibration curve for this set of experiments can be seen below (Figure 6.2).

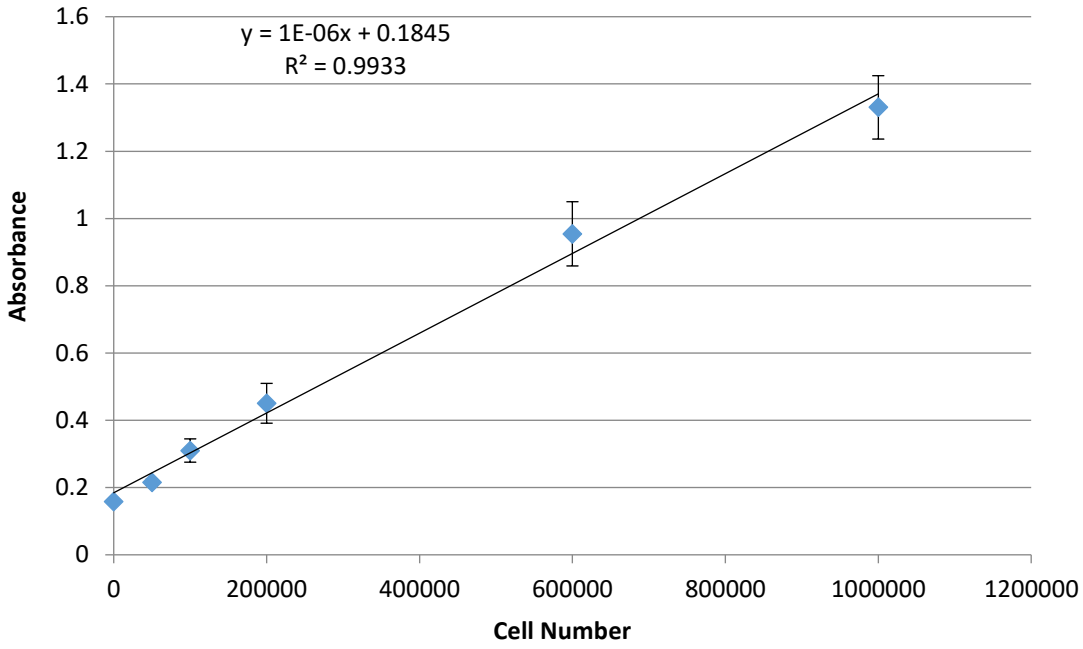

Figure 6.2: Calibration curve for the MTS assay showing the cell number that corresponds to each absorbance reading collected using a plate reader at 490nm. Cell numbers of 50,000, 100,000, 200,000, 600,000 and 1,000,000 were used to produce the data, collected in triplicate for each day of each experimental run. The data shown here is the average of all collected data for these calibration curves, n=3x3, with error bars showing SEM.

6.3. Results

6.3.1. Initial Gravity Separations

The theoretical settling times for Sephadex beads of various sizes to settle 28cm in a column loaded with PBS is shown in Figure 6.3A. These predictions are based on the TFV of these particles calculated using the Stokes equation shown in Equation 5.1. It makes clear that the separation of larger particles happens very quickly during the first few minutes of the separation, while separating out the smaller particles will take progressively longer periods of time. During the second minute there is a 90µm spread in the size of particles that should elute out of the column, while the final 5 minutes corresponds to a change in diameter of less than 20µm for the eluting particles. These predictions suggest that a time period of 15 minutes should be sufficient for collecting fractions of particles greater than 100µm. Particles smaller than this will not have had sufficient time to elutriate and so will remain in the column.

Meanwhile, the actual mean diameter, D10 and D90 of fractions collected from the column at 1 minute intervals is shown in Figure 6.3B. An elapsed time of 2 minutes was chosen for the first collection to ensure that there were no handling errors in the set-up of the data collection. These intervals continued until 10 minutes, after which one final collection was performed at 15 minutes to ensure that there would be no significant difference between collections made after this time.

It is clear that in practice the beads followed a similar trend to that predicted by the theoretical results. The majority of the largest particles eluted within the first two minutes; after which the rest of the particles began to reach the bottom of the column. After the first few minutes the mean diameter of the collected fractions quickly levelled off, with a minimal difference of around 10µm between the mean diameter of beads collected after 5, 10 and 15 minutes. It is also obvious, however, that at least some of the beads were settling faster than predicted by the Stokes equation. This is shown by the fact that 100µm beads were not predicted to elute before 12 minutes, but were present in significant numbers in the collected fractions from 7 minutes onwards.

In addition, it is noticeable that the span was very large for the first collected fraction, but very quickly reduced; becoming very consistent from 5 minutes onward. For the fraction collected after 2 minutes the span was around 200µm, whereas the span for the fraction collected at 3 minutes was less than 100µm. It is clear that after a period of 5 minutes the span remained fairly constant at around 50µm. This, along with the consistency of mean diameter after this point, suggests that the profile of each collected fraction is therefore very similar after 5 minutes and will likely change little over any larger time periods. This is in keeping with the theoretical results and so proposes that the time limit for separation be kept at a maximum of 15 minutes to avoid diminishing returns.

The mean diameter, D10 and D90 of EBs collected from the bottom of the column over a 15-minute settling period are demonstrated in Figure 6.4. The four graphs represent different EB formation times; EBs were cultured over 120 hours with separations being performed after 48 hours formation time and then every subsequent 24 hours. All four graphs follow the same general trend predicted by the Stokes calculation and then shown with the beads in Figure 6.3. The largest EBs eluted from the column during the first few minutes with the mean diameter of collected fractions decreasing as time goes on. This eventually levelled off and produced a size fraction of between 100-200µm consistently once a sufficient period of time had elapsed. It should be noted that this levelling off period was different for each of the different EB formation times, with consistency of mean diameter and span generally being reached quicker for EBs that have undergone a shorter formation time. This ranged from around 7 minutes for the 48-hour EBs to around 10 minutes for the 120-hour EBs. However, by 10 minutes the results were largely the same for 72-120 hour EBs, with the 48 hour EBs being consistently smaller.

It is also evident that the mean diameter of the largest size fraction, collected after 2 minutes, was consistently around 420µm for the 48-96 hour EBs, although there was variation in the span. This variation occurred predominantly in the fraction with a 72-hour formation period, which had both a smaller D90 and larger D10. After a 48-hour and 96-hour formation period the fraction collected after 2-minutes had a span of around 200µm, while after 72 hours' formation the span was reduced to 170µm.

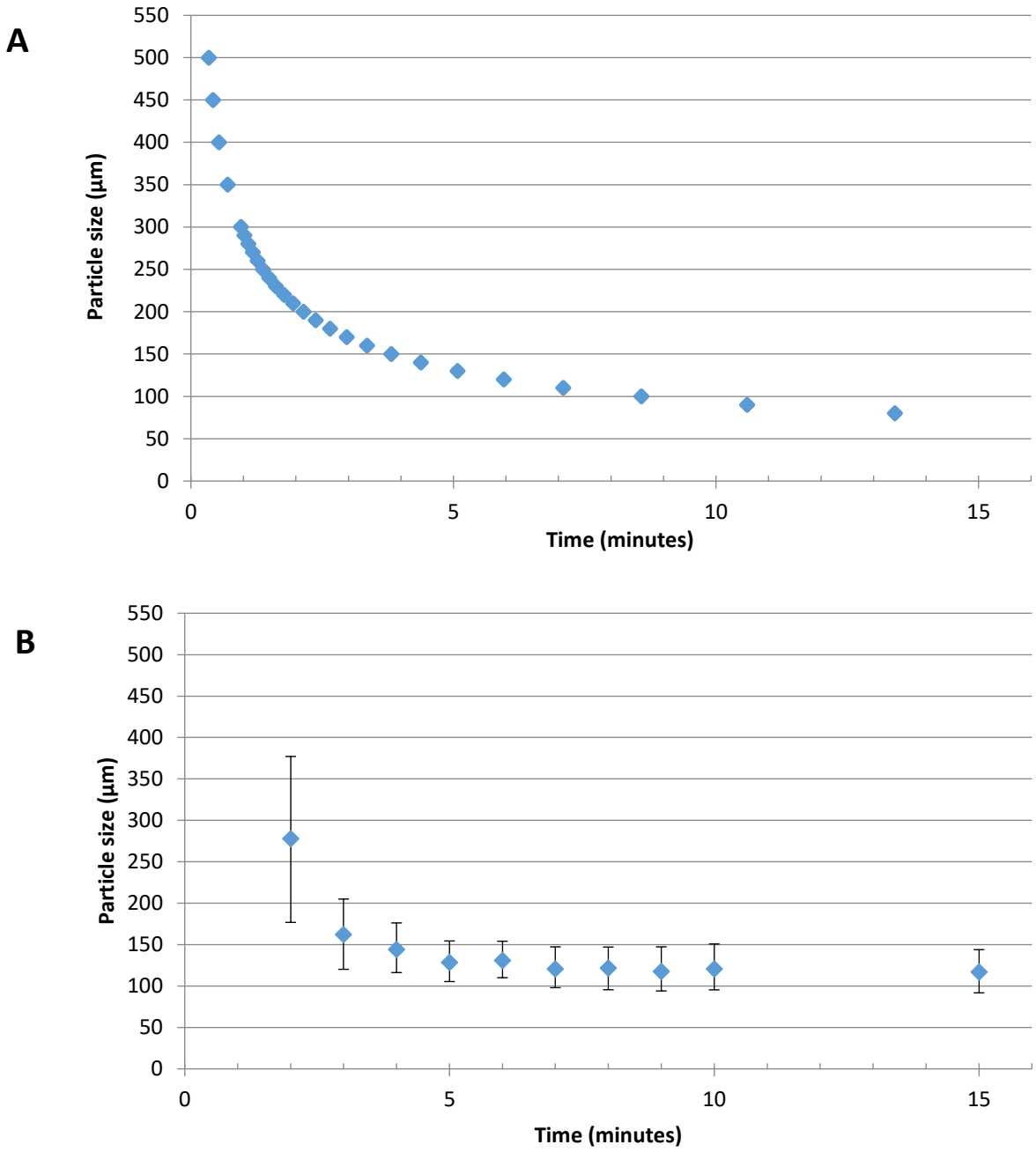

Figure 6.3: Graph 6.3A shows the theoretical settling time it for Sephadex beads of various sizes with a constant density of 1.1g/cm^3 to fall 28cm through PBS. This was calculated using the Stokes equation assuming acceleration due to gravity was 9.81m/s^2. Density of medium was assumed to be 1g/ml and viscosity of medium was 1.002cP at room temperature of around 20^{o}C. Figure 6.3B shows the experimental mean particle diameter of beads collected in a 12-well plate after eluting from the bottom of the column after various time points including the D10 and D90 span for each collected fraction. Particle diameter was calculated using maximum Feret diameter calculated using ImageJ software on images taken from the collected fraction.

In contrast after a 120-hour formation period the mean diameter and D90 of the 2-minute fraction was significantly larger, over 660µm, although the D10 was similar to both the 48 hour and 96 hour fractions at around 320µm. The largest collected fraction therefore contained a minimal number of particles below 300µm in diameter for any formation period.

The 3-minute fraction had a mean diameter of around 325µm and a span of approximately 175µm for all of the 48-120 hour formation period results. At this time point there were minimal EBs below 200µm in size in the collected fraction for any formation period. From 3 minutes onwards the mean diameter between formation periods became generally more consistent, although there were still variations in span across the different formation times. This is shown by the spread of around 35µm in diameter across all tested formation times for 3, 4 and 5 minutes. For the majority of the times tested after this the mean diameter results were quite similar and follow a near identical pattern, with the 48-hour EBs being the smallest and the 120-hour EB fractions being the largest. The main difference between fractions here was the consistent presence of an in increased number of larger particles as displayed by the consistently larger D90 for longer EB formation periods. By 10 minutes there was little discernible difference between 72-120 hour EBs in mean diameter or span, while the 48 hour EBs were similar but slightly smaller in mean diameter, D10 and D90.

What is evident from these results is that multiple large size fractions could be collected regardless of formation time with a strong level of control over the properties of these fractions. However, at none of the time periods tested was it possible to collect a fraction of particles consistently below 100µm. Irrespective of the length of formation period, EBs below 100µm in size only showed up in sufficient numbers to exceed D10 after around 9 minutes; and regardless of this the mean diameter of any fraction never fell below 117µm. This means that this technique was evidently successful for collection larger size fractions, however, in order to collect a fraction of the smallest particles in addition to these larger fractions an alternative must be identified.

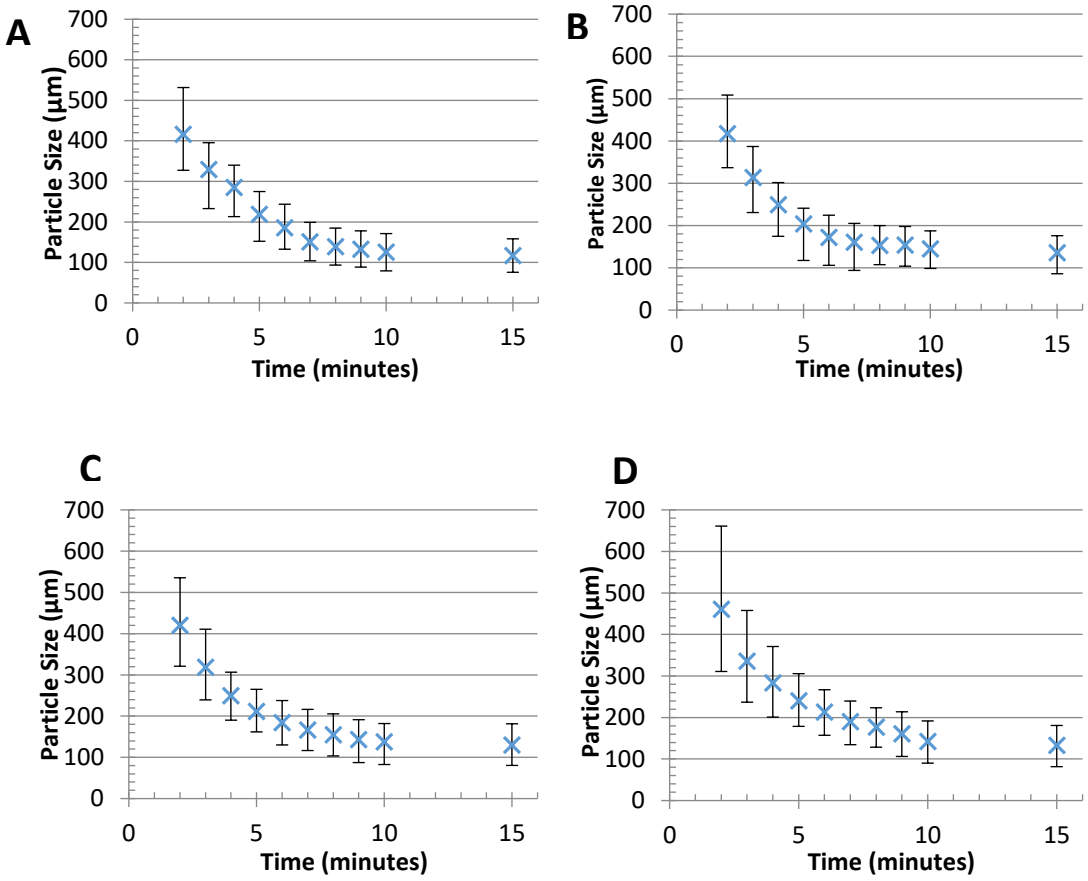

Figure 6.4: Graphs to show the mean particle diameter of EBs collected after eluting from the bottom of the column after various time points including the D10 and D90 span for each collected fraction. ESCs used in this experiment have been cultured for a variety of time points at a density of 200,000 cells/ml to form EBs. Each of the different formation times are as follows; Figure 6.4A corresponds to 48 hour EBs, Figure 6.4B corresponds to 72 hour EBs, Figure 6.4C corresponds to 96 hour EBs and Figure 6.4D corresponds to 120 hour EBs. All results are the average of triplicate collections. Diameter was calculated using maximum Feret diameter calculated using ImageJ software on images taken from the collected fraction.

Figure 6.5A shows the comparison of the three techniques demonstrated so far in this research for their ability to collect the smallest fraction that they can, ideally <100µm, and another, larger fraction aiming to be 100-200µm of 72 hour EBs. It is evident that all three of the separation techniques struggled to effectively collect a discrete fraction of particles below 100µm in diameter. The settling and perfusion techniques particularly struggled, with both possessing a multitude of particles over 150µm resulting in them having a mean diameter of 135µm and 115µm respectively. The mesh technique offered an improvement with its mean diameter being 92µm

and its D90 being 123µm. However, while 65% of collected EBs were below 100µm this still means that this fraction possessed a significant number of particles over the desired upper limit.

The mixed success of the three separation techniques for collecting a 100-200µm fraction of particles is highlighted in Figure 6.5B, with the perfusion technique again struggling in particular. While it succeeded in collecting a mean diameter of 150µm, the D10-D90 span varied from 74-234µm. The mesh technique offered much more accuracy, although struggled to fill the full desired span with its D90 being a little low at only 173µm. As a result, the mean diameter was also lower at 131µm, although this in particular is not necessarily an issue as it could well be an artefact of the overall population dynamics. Finally, the settling technique performed well collecting a discrete 100-200µm fraction of particles. This is clear given that the mean diameter was 154µm and the D10-D90 span is 104-198µm.

These results show that the settling technique could accurately collect a 100-200µm fraction, but struggled to collect a discrete fraction of the <100µm EBs. Meanwhile, the perfusion technique struggled with the discrete nature of its fractions, however, it could be used to collect some separate size fractions of particles towards the lower end of the desired range. Finally, the mesh technique was capable of collecting two size fractions that were near the desired range, but not ideal, with some crossover across the two fractions between 100-120µm.

As a result of this, a further experiment was performed to try to isolate the smallest fraction of particles that exist in the stock. This <100µm fraction represents 10-25% of the stock depending on the formation time, with around 20% of 72-hour EBs being within this range. As a result of the success of the settling technique for collecting other, larger fractions of particles, it was decided to purge the remaining contents of the column following a 15-minute separation using the settling technique and perform a PSD on the particles within to try and collect this fraction of the stock.

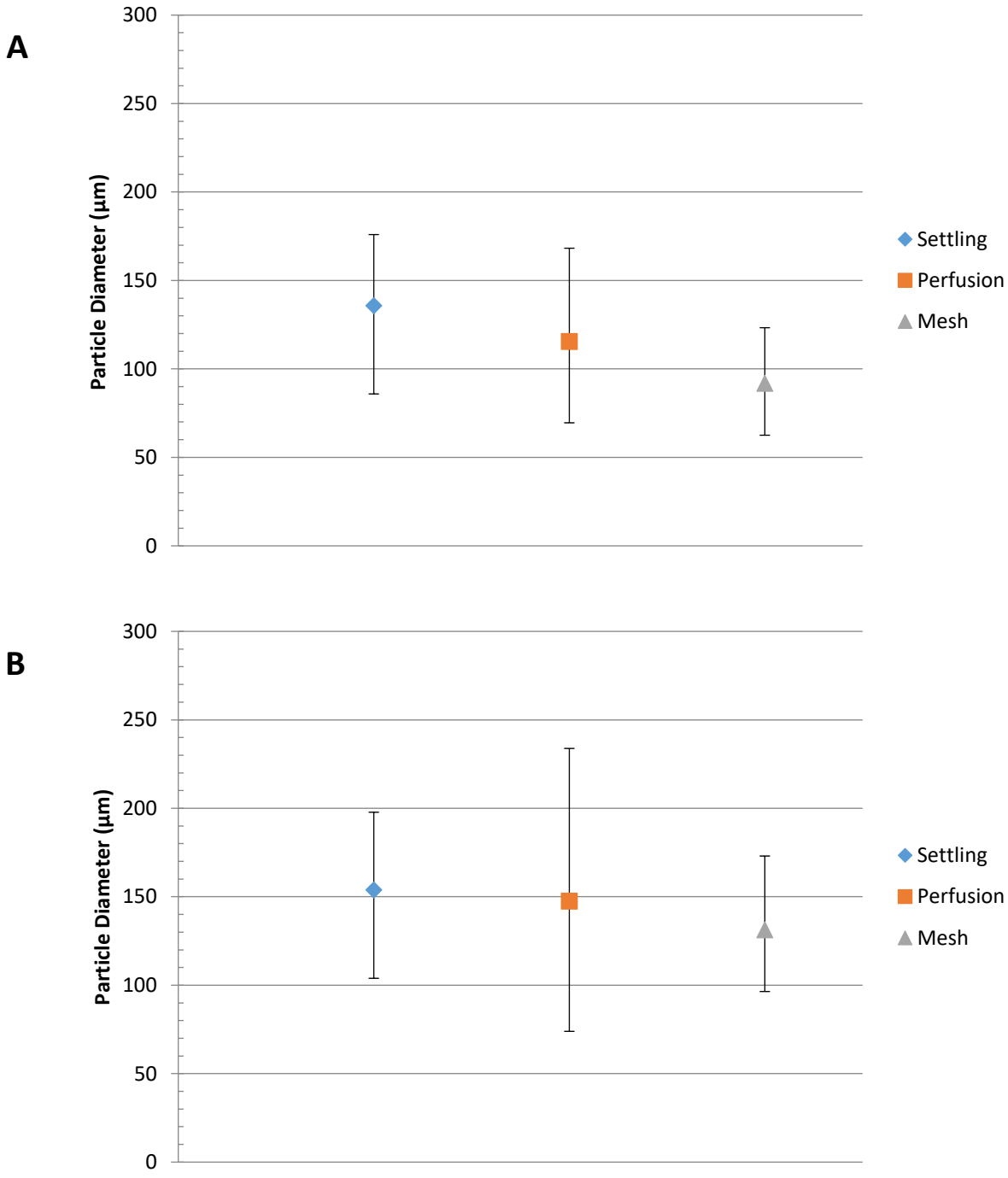

Figure 6.5: Mean diameter of collected EBs for each of the three separation technique showing a comparison for the <100µm and 100-200µm EB size fractions including the D10 and D90 for each. Diameter was calculated using maximum Feret diameter calculated using ImageJ software on images taken from the collected fraction. Figure 6.5A shows the success of collecting a <100µm fraction of particles and Figure 6.5B a 100-200µm fraction of particles.

6.3.2. Refinement of Gravity Settling Separation Technique

The particle size distribution of the EBs that remained in the column following the 15-minute separation experiment of 72-hour EBs is shown in Figure 6.6A. These represented the remaining EBs of the stock that were yet to elute out of the column and so should contain particles predominantly below 100µm according to the predictions made for the beads in Figure 6.3. The results show that a much greater number of particles below 100µm in size made up this collected fraction comparative to those collected previously from the column. This is exemplified by the D10 being reduced to 72µm in this fraction compared to 90µm for the 15-minute fraction. In addition, the mean diameter was reduced to 115µm compared to 135µm collected previously.

In contrast, it is evident that a significant number of the larger particles were still present in the column after this period of time. Of the remaining particles in the column, 65% were over 100µm in diameter with 12% being over 150µm in diameter. As a result, the mean diameter and D90 (152µm) of the collected fraction still remained much larger than would be desired as, while the smaller EBs were now present in sufficient numbers, they were still contaminated by the presence of unwanted, larger EBs. As a result of these issues, an experiment was performed to determine whether or not the gravity settling experiment could settle out a <100µm fraction under a different set of conditions. By allowing settling in a falcon tube of 10cm length it was hoped that it could be determined if altering the column length could sufficiently reduce the settling time required to collect this fraction.

A 72-hour petri dish of EBs containing the full size range was allowed to settle in a 15ml falcon tube for 5 minutes and the resultant particle size distribution of the top 8ml fraction is shown in Figure 6.7. It is clear that the distribution of particles here was significantly smaller than that of the fractions collected from the purged column, with only 0.1% of particles being over 150µm and only 29% over 100µm. Further still, of this 29% nearly half (14%) were between 100-110µm in size meaning that in total around 85% of the collected EBs were below 110µm. This is compared to 35% of the particles below 100µm from the column purge data; representing a 2-fold

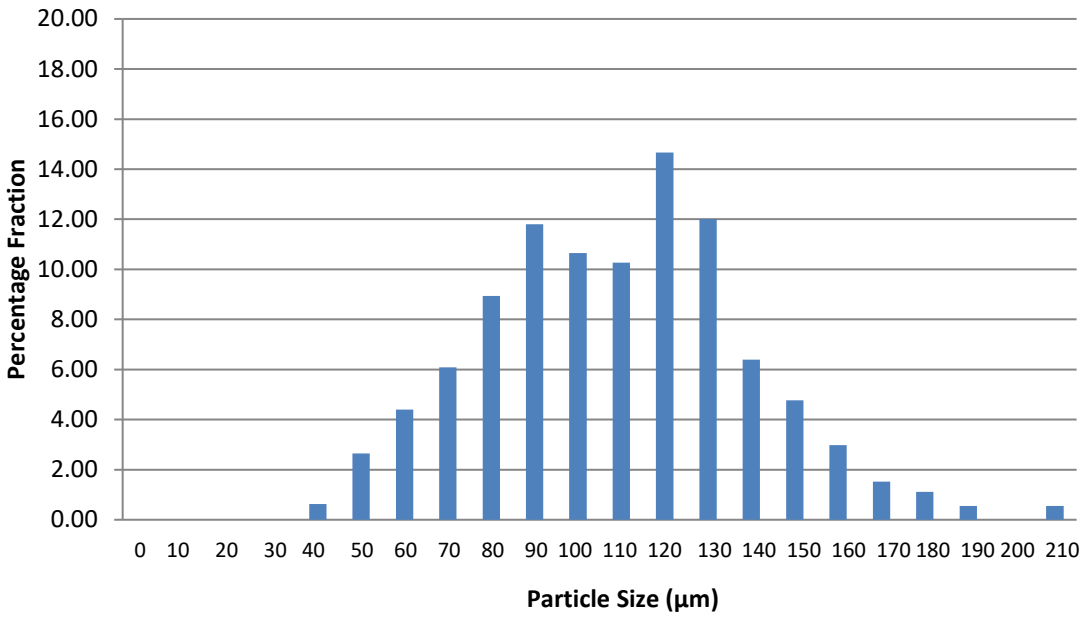

Figure 6.6: Figure 6.6 shows the PSD of EBs collected from the entire column length that remain in the column following a 15-min collection period. EBs were collected as in the above experiments with the remaining liquid content of the column purged to allow the full collection of all residual EBs.

improvement. This is in spite of the fact that only 17% of the stock were below 100µm in diameter, representing an enrichment ratio of greater than 4-fold in total.

Compared to the previous perfusion and mesh separation techniques which managed 40% and 65% of particles below 100µm respectively this represents a marked improvement. As a result, this technique was by some margin the most successful demonstrated here for separating out a fraction of <100µm EBs. It was at this point therefore desirable to try to determine the most applicable separation technique for collecting each different size fraction. The full comparison of these techniques for collecting each of the desired fractions is therefore shown in Figure 6.8.

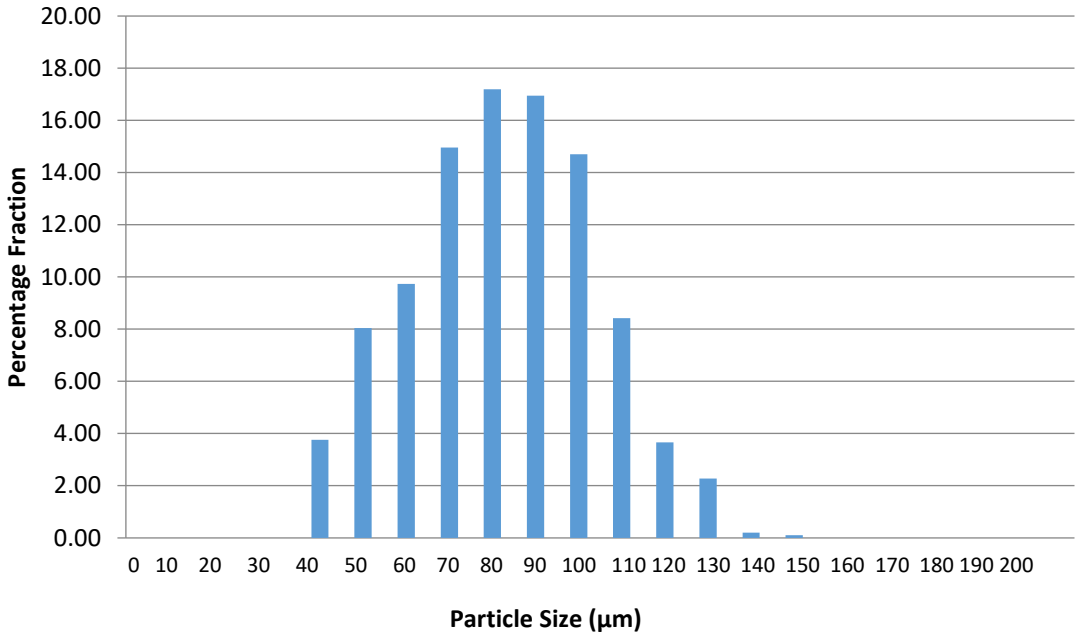

Figure 6.7: Graph 6.7 shows the PSD of EBs collected from the stock present in one petri dish after 5 minutes of settling in a falcon tube. PSD was provided using maximum Feret diameter calculated using ImageJ software on images taken from the collected fraction.

6.3.3. Comparison of Separation Techniques and Their Effect on mESC Growth

It is clear in Figure 6.8 where the strengths and weaknesses of each separation technique lie. The perfusion technique represents an improvement on the discreteness of the <100µm fraction comparative to the stock, yet less than 50% of those collected in this fraction meet this criterion. Meanwhile, due to its inconsistency the settling technique barely represents an improvement on the stock at all for the <100µm fraction. In contrast, the mesh and pre-settling technique were shown to be very successful at separating out the smallest fraction of with both representing around 70% of collected EBs below 100µm; a 4-fold increase on the stock.

The perfusion technique failed to offer an improvement on the percentage fraction of EBs between 100-200µm compared to the stock. Meanwhile, the settling and mesh separation techniques both offer a modest improvement of around 80% of EBs being between 100-200µm compared to around 70% of the stock. However, it should be noted that it was shown previously that the majority of the collected particles in these fractions that are not within this size range are very close to it and have a much smaller overall spread comparative to the stock. The pre-separation technique was omitted as it was not used to collect any fractions beyond 100µm.

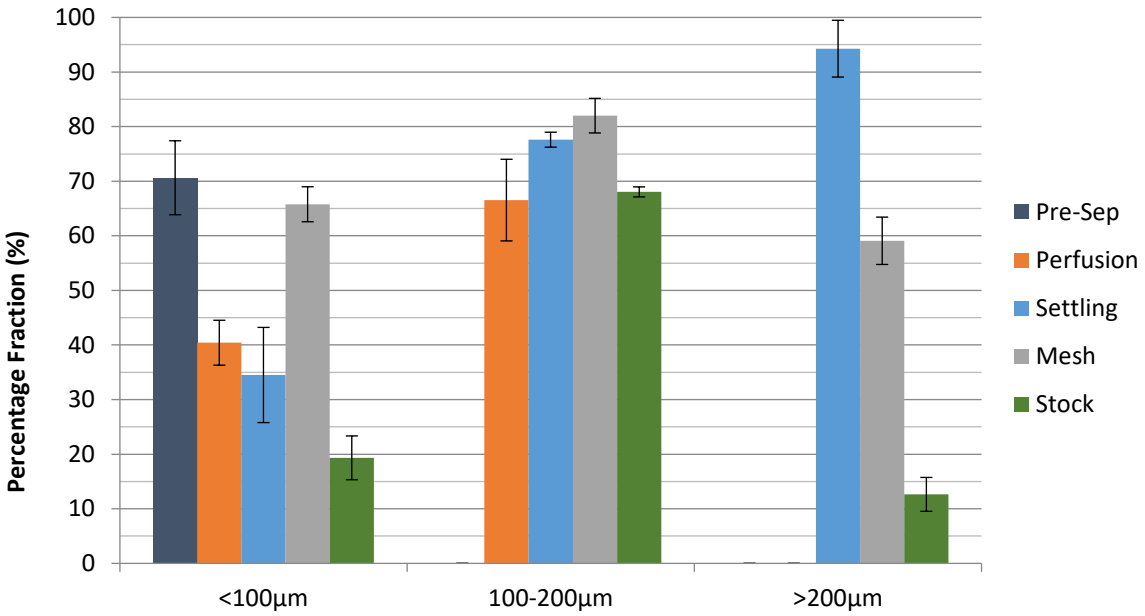

Figure 6.8: Comparison of all demonstrated separation techniques in their separation of EBs including the stock. Shows the percentage of collected EBs that exist within the demonstrated size fractions for each technique. Each set of conditions was repeated 3 times (n=3) with error bars shown (SEM).

Finally, the mesh and settling techniques met with great success in separating out EBs over 200µm in size with around 60-95% of EBs respectively meeting this criterion. This is in comparison to only around 15% of the stock meaning that these techniques represented a 4- and 6-fold increase on the stock for the mesh and settling techniques respectively. It should also be noted that, in addition to this, the settling technique alone was also shown to be able to collect a fraction of <300µm EBs with an efficiency of 98%.

In order to ensure the viability of this technique for use with live cells and thus to allow it to improve the differentiation of EBs it was necessary to show that the column did not negatively affect the viability and proliferative potential of the cells. As such an MTS assay was performed on dissociated cells to determine the survival and growth rate of gravity column-separated EBs compared to unseparated EBs as shown in Figure 6.9.

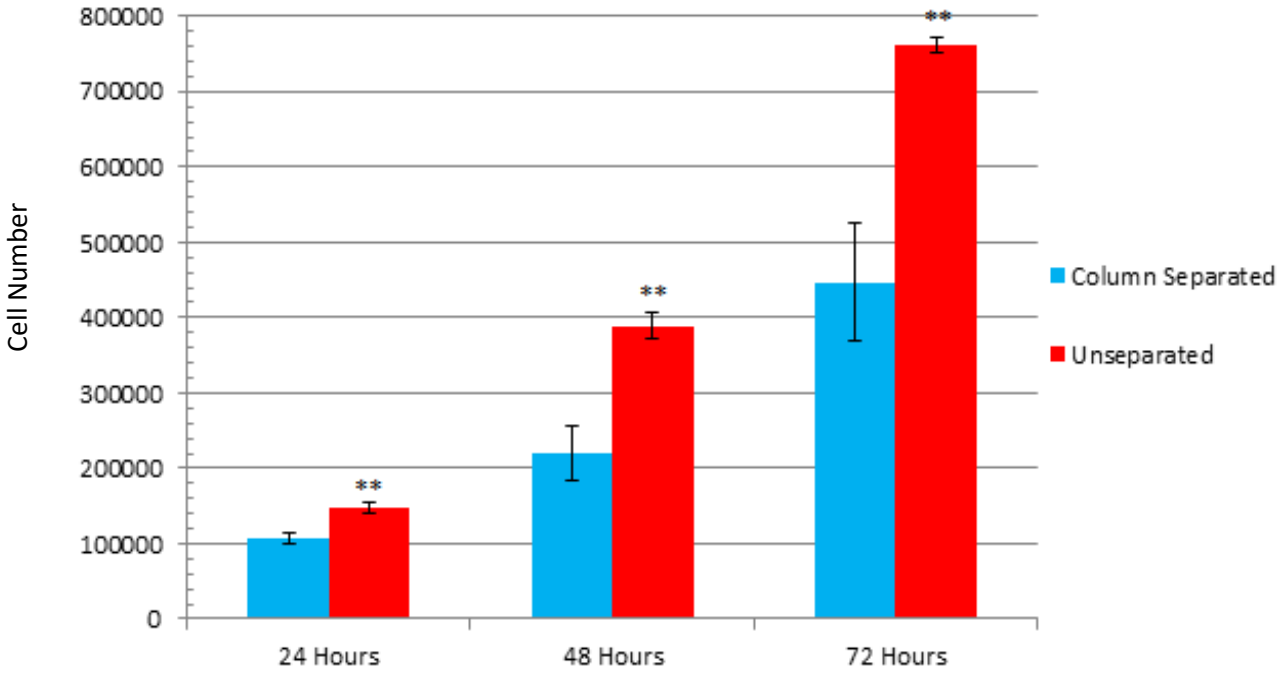

Figure 6.9: Growth rate of mES cells cultured on gelatin-coated six-well plates over 72 hours. Displayed as cell number using an MTS assay for column separated and control EBs with both representing the full range of EB sizes found in the stock. Column separated EBs have undergone the separation technique and then been brought back together for dissociation and seeding at a density of 10,600 cells/cm^2. *** ≤0.001, ** ≤0.01, * ≤0.05. Each set of conditions was repeated 3 times (n=3) with error bars shown (SEM).

Both the separated and unseparated EBs were dissociated and seeded at a density of 10,600 cells/cm^2 in 6-well plates. It can be seen that they both followed the same obvious growth pattern over the course of the 72-hour culture period. However, it is immediately evident that the unseparated cells grew faster than the column separated cells. It is also noticeable that the unseparated cells were in significantly greater numbers than the column separated cells after as little as 24 hours, 148,000 cells compared to 107,000 cells, and that this only increased over the course of the of the experiment. This is highlighted by the fact that the unseparated fraction took 24 hours less than the separated fraction to reach a cell count of 400,000 cells, taking 48 hours instead of 72 hours. All this culminated in a final cell count of around 760,000 cells for the unseparated fraction compared to 450,000 cells for the column separated fraction.

In conclusion, these experiments highlighted that this technique is capable of collecting three distinct size fractions of <100µm, 100-200µm and >200µm; though it requires some modifications to collect the <100µm fraction. This suggests that with some alteration of the technique a single step process could be devised to collect these three size fractions reproducibly and with a high degree of accuracy. It was also shown that by altering the separation time, the mean diameter and span of the collected fractions can be altered to possess the characteristics desired by the user. This system was capable of collecting all desired size fractions from one 10ml petri dish over the course of 10 minutes in the column giving it a throughput of 1ml/min. Finally, it was shown that this technique was non-destructive as the cells survived the separation process and continued to proliferate afterwards, though less so than if the cells did not undergo the separation technique.

6.4. Discussion

6.4.1. Initial Gravity Separations

6.4.1.1. Sephadex Beads

In order to overcome the issues with the parabolic flow profile that is characteristic of laminar flow affecting the separation of EBs by utilising their TFV, the above gravity settling technique was performed. It was hoped that by removing this factor a more consistent method could be determined for collecting multiple discrete fractions of EBs. In addition, it was hoped that the utilisation of this alternative technique may also be able to negate the potential impact of any inter-particle interactions by utilising the full length of the column more effectively and so reducing the effective concentration of particles in particular sections.

Due to the nature of these experiments there should only be a minimal effect caused by the number of particles after the initial moments of the separation. Because there was a large size range in the particle stock for both EBs and beads, they all had vastly different settling velocities. Therefore, the initially high concentration of particles at the top of the column on loading was very quickly reduced as the larger particles advanced much more quickly down the column length. As a result, it did not take long before the concentration of particles in the column was low enough that there was limited hindering of settling due to the presence of a relatively small number of particles per unit area.

The graphs of Figure 6.3 show how the predicted settling time for particles of a range of sizes to settle 28cm through a glass column correlates to the actual collected results for Sephadex beads. It is clear that the predictions made by the Stokes equation were a good estimate and seemingly gave an accurate representation of what occurred in action as the largest particles clearly settled very quickly. However, for some particles at least, the Stokes equation overestimated their settling time. This is made clear by the fact that particles eluted out of the column in significant enough numbers to make the D10-D90 span several minutes before they were predicted to be able to. The results show that after 2 minutes of separation 200µm beads should be just reaching the bottom of the column, however, beads of around 170µm were already making up a significant portion of the fraction (~10%)

by this time point. This trend continued over the next few minutes with some particles eluting sooner than the Stokes equation predicted.

As these calculations were based on assumptions made of an entire population it is possible that some individual particles within this population would possess different characteristics that could affect their settling velocity such as density or sphericity. As a result, if this trend were restricted to the first collected fraction it could be surmised that this was a result of the small number of the largest particles found in the stock. This would result in the limited number of small particles that did elute faster than predicted making up an uncharacteristically large percentage of the total fraction, thus overstating their numbers.

However, this trend was apparent all the way up to 7 minutes, after which point subsequent fractions were relatively homogenous irrespective of time. When all this is considered it becomes apparent that the primary cause of this issue was in fact likely a result of the nature of the particle collection method at each time fraction. After each 1-minute period the particles were collected in approximately 1ml of fluid. This volume of fluid was therefore removed from the column each time a reading was taken. As a result of this, the effective length of the column was reduced after every sample because there was less fluid in the column and therefore a shorter effective length that the particles could settle in. This explains why smaller than expected particles eluted at every time point barring the first collection at 2 minutes.

This is not particularly problematic as this method of collection was employed in identical fashion with the EB separations as well. As an aside, it should be noted that, due to their lower density, the EBs should settle slightly slower and so the particle diameter of the collected fraction should be larger at each time point; a characteristic supported by the results of Figure 6.4.

As time goes on it is apparent that the difference between collected mean diameters was massively reduced for each successive time point; after 7 minutes the difference in mean diameter for collected beads is almost negligible. This shows that increasing the collection time beyond 15 minutes will provide little benefit to collecting smaller size fractions as the required time for 50μm to settle 28cm is nearly

50 minutes according to the Stokes equation predictions. As a result of these experiments working with a living system of cells it is important that the separation time is kept as short as possible. Accordingly, these experiments did not extend beyond 15 minutes to maintain cell viability.

In addition, larger particles remained in the column for longer than was predicted. This could be caused by one of a number of things. First are wall effects, which have been shown previously to reduce the falling velocity of individual particles as they approach it, with an increased inhibition the closer they get to the wall (Chhabra et al., 2003, Brown and Lawler, 2003, Lau et al., 2010). This would result in the retention of particles from across the entire size range found in the stock for longer than would be expected and so could skew results from every fraction by potentially increasing the mean diameter. However, as there is no preference for this effect based on particle size it is likely to be consistent throughout all collected fractions and so should be manageable. Further, the impact of this could be negated by increasing the diameter of the separation vessel and so reduce the number of particles affected by wall effects by reducing the likelihood of particles coming into contact with the column wall.

Secondly, it could also be caused by inter-particle interactions at the beginning of the process hindering the settling of the particles. As was discussed previously the settling velocity of an individual particle will be overestimated by the Stokes equation in a multi-particle system. However, this is limited to relatively concentrated numbers of particles as very dilute concentrations of particles, more similar to those found in these experiments, are suggested to behave similarly to single particles (Batchelor, 1982). Due to the limited number of particles being added to a comparatively large volume of PBS this is likely to be the case for particles in the majority of the column.

Despite this, upon initial loading of the column there will transiently exist a high concentration of particles at the very top of the column. During this time the stock of particles will be thoroughly mixed and so large particles, with their higher TFV, will need to settle through the rest of the smaller particles. This will cause disturbances in the fluid, with an up flow equal to the settling velocity of the largest particles,

which will likely hinder the settling of particles of all sizes for the initial moments. This would likely manifest itself as a slight lengthening of the required settling time, and so further explains the presence of larger particles remaining in the column for longer than was anticipated.

In addition, it was shown that in spite of any issues with hindered settling, the span of the particles was quite consistent with the exception of the first few fractions. This is in keeping with predictions made by the Stokes equation as a much larger range of sizes were predicted to settle over the first few minutes of the separation. As a result, this could likely be overcome by enabling more fine-control over the column length and utilised separation times, allowing for more control over the size of the larger collected fractions.

Importantly, what these results show is that the column can separate a heterogeneous mix of particles into discrete fractions according to their size; including the largest particles. However, they also highlighted a shortcoming in collecting a discrete fraction of particles <100μm within a reasonable time limit.

6.4.1.2. Embryoid Bodies

Figure 6.4 shows the size separation over time of EBs that have undergone various different formation periods from 48-120 hours. This is because it was desired that this technique be as adaptable as possible and so it was decided to determine not only its applicability to the most commonly used 72 hour EBs, but also to determine its applicability for EBs that have undergone less commonly used formation times. This is important as different differentiation protocols often disagree on the length of EB formation that should preclude their dissociation (Hwang et al., 2009, Fehling et al., 2003, Nakagami et al., 2006, Yamashita et al., 2000, Sidney et al., 2014, Gothard et al., 2009). In addition, this would allow certain physical properties of the EBs to be determined such as density and extent of cavitation, which are both likely to be a function of cell number. Special attention would be paid to differences recorded between formation times, as significant cavitation has been noted after extended periods of EB culture due to apoptosis of the cells (Gothard et al., 2009, Rungarunlert et al., 2013).

It was noted that the D10 and mean diameter, with the exception of the 120-hour mean diameter, were all very similar irrespective of formation time. The D90 varied greatly for each different formation time, however, this variation in D90 had largely subsided by 3 minutes, again with the exception of the 120 hour EBs. This suggests that generally the differences between fractions collected at each time point across different formation periods was caused by the presence of larger EBs in the stock, as this would affect primarily the D90 and mean diameter. The presence of larger EBs over time would be brought about by continued proliferation of cells within the aggregates and agglomeration, which would be allowed to occur due to the longer formation period (Khoo et al., 2005, Pettinato et al., 2014, Dang et al., 2002). This suggests that it was the presence of larger EBs in the stock that was impacting on the separation technique by increasing mean diameter due to being present in greater numbers. However, this variation in D90 could also have been caused by a greater degree of cavitation in larger EBs after longer formation periods. At the very least the lack of variation in D10, D90 and mean diameter amongst the smallest collected fraction at 10 minutes onwards, regardless of formation time, suggests that this did not occur to such a great extent in EBs up to and likely in excess of 200µm.

Again a certain degree of consistency is shown between results after 10 minutes, irrespective of EB formation time. This again showed that the smallest fraction of <100µm EBs were yet to elute from the column in significant numbers. With the EBs being a living system they will ideally spend as little time as possible in the column and out of their ideal growth conditions. As the trends throughout Figure 6.4 show that increasing the separation time beyond those tested will have a negligible impact on the mean diameter and span of collected fractions in the short term, an alternative needed to be identified to collect the smallest fraction of particles.

6.4.2. Comparison of Separation Techniques

Figure 6.5 shows how the three separation techniques tested in this body of work; a mesh separation, perfusion and gravity settling separation technique, compare to one another in their efficacy for collecting distinct size fractions of EBs. These size fractions were hoped to be <100µm (Figure 6.5A) and 100-200µm (Figure 6.5B). These results made clear that the mesh was the most effective at separating the

smallest fraction and that the settling technique was most effective at collecting the larger fraction.

Figure 6.5A shows that all three separation techniques struggled to collect a discrete fraction of <100µm EBs. This was caused by the consistent presence of larger than desired particles in all three cases. For the mesh this was likely a result of the non-spherical nature of the EBs allowing larger, oblong EBs to pass through. As the EBs were not spherical and could fall in any orientation through the mesh, many EBs larger than the porosity would be able to pass through the mesh. Reducing the mesh size or multiple separations through the same sized mesh could help counteract this, but would reduce the number of particles that could collected as more would be lost in the process due to mesh retention. Further, the mesh separation technique lacks the adaptability and potential for scaling of the other mechanisms. Due to its physical capturing of the cells this could only be run as a batch process that would require deconstruction of the apparatus in order for each collection to be performed. This in itself is time consuming, but also increases the risk of contamination and would increase the need for subsequent sterilisation between procedures.

For the perfusion separation technique this was a result of the parabolic fluid velocity profile moving a range of particles above the desired size. This could be overcome by further reducing the flow rate, but this too would hinder the collection of large numbers of particles. The settling technique struggled because the time allowed had not yet exceeded the time required for all of the >100µm particles to elute from the column. This shows that further work is needed to collect this size fraction to a sufficient standard and that the settling technique is likely to be the most readily adaptable.

Figure 6.5B shows the largest fraction that could be collected under the tested conditions for the perfusion technique. The mean diameter was very similar to that collected with the settling technique, but the perfusion technique suffered from both an increased D90 and decreased D10 in comparison. As both systems were likely to suffer from the same issues with regards to inter-particle interactions and wall effects this means that this issue can likely be attributed to the parabolic flow profile of laminar flow. This shows that the removal of this factor from the separation of the

particles, leaving them to be separated out only by their own intrinsic properties, has vastly improved the efficacy of this technique for collecting larger size fractions of particles. This is especially pertinent when it is considered that the settling technique also successfully collected even larger fractions of EBs than those collected with the perfusion technique. Attempts were made to determine whether or not the settling column experiment possessed the potential for collecting the <100µm fraction. This began with an analysis of the particle size distribution of EBs that remained in the column after a 15-minute separation performed as previously described as shown in Figure 6.6A. The results show that there are a number of EBs with a diameter in excess of 100µm remaining in the column after 15 minutes. This is despite theoretical predictions based on the beads suggesting that the majority of particles above this size should have been removed some time ago. However, this is in keeping with the data collected after 10 and 15 minutes during the initial separation. What this shows is that irrespective of the number of smaller particles present in the fraction there are still a lot of larger particles remaining in the column after this length of time. This would have been caused by the hindered settling and wall effects that have been detailed previously (Chhabra et al., 2003, Brown and Lawler, 2003, Lau et al., 2010, Masliyah, 1979, Basson et al., 2009, Krishnamoorthy, 2010). This is in addition to a slight discrepancy between the predictions for beads and the EB results as a result of the reduced density of EBs lowering their TFV (Kang et al., 2010, Gorczynski et al., 1970). While this collected fraction represents an improvement in the number and percentage purity of <100µm EBs comparative to the 15-minute fraction, 65% of the particles are still in excess of the desired size. Due to the desire to collect a discrete fraction of <100µm EBs further experimentation was required.

6.4.3. Refinement of the Gravity Separation Technique

It was now important to discern whether this system would be capable of collecting the smallest size fraction under any set of conditions. This therefore required that it be shown that the larger particles could be removed from the supernatant during settling outside of the column. Figure 6.7B shows the PSD of EBs collected after 5 minutes settling in a 15ml falcon tube; this was used as it reduced the settling distance and therefore effectively allowed the separation to occur much

faster. After the addition of the medium containing EBs to the falcon tube the height from the top of the liquid surface to the bottom of the tube was 10cm. As this is significantly shorter than the length of the separation column, it should result in a vast reduction in the required settling time. This was calculated to be less than 3 minutes for any particles with a diameter in excess of 100µm from the very top of the fluid. Therefore, in spite of the continued presence of wall effects and inter-particle interactions hindering particle settling, the supernatant layer should contain predominantly smaller sized particles; hopefully <100µm.

The results show that this was the case, with 71% of EBs collected from the top 8ml of each falcon tube being <100µm in size. Of those in excess of this diameter, a further 14% were between 100-110µm in size. This improvement was likely caused primarily by the vastly reduced settling distance, thus requiring a correspondingly lower settling time per particle. In addition, the increased concentration of particles in the vessel resulted in increased inter-particle reactions. As discussed previously the downward motion of particles settling in a fluid induces an equal and opposite fluid motion (Krishnamoorthy, 2010, Lapidus and Elgin, 1957). As it is the larger particles that will settle fastest, this upwards fluid flow is likely to exceed the TFV of any smaller EBs. As a result, the upper portion of the medium should contain an enriched population of the smaller particles.

This showed that the gravity-settling technique had the potential to collect a discrete fraction of <100µm, but was hindered in its current format by time limits imposed on it by the application of living cells. Therefore, it would seem that the technique could be improved for collection of <100µm EBs by reducing the column length to improve collection of smaller particles more quickly and reducing the separation times for larger fractions accordingly. In addition, the technique could further be improved by increasing the diameter of the separation column to reduce the impact of wall effects and reduce inter-particle interactions due to a reduced concentration of EBs (Cohen and Metzner, 1981, Chhabra et al., 2003). This will allow more particles to settle at their TFV unhindered and so should result in more discrete size fractions.

It was decided to limit the gravity separation technique to 15 minutes to ensure that the cells were not subjected to undesirable conditions for an extended period. However, if it was necessary to improve these conditions to allow for extended separation times, or even to enhance the current separation period, then a number of relatively simple improvements could be made to facilitate this. First of all, the separation could be performed in SNL medium instead of PBS to allow the cells to continue to draw nutrients as necessary during their separation. This could then also be performed under standard growth conditions at 37°C with 5% CO_2 as is routinely found in an incubator.

Another method of refining the separation technique would be to alter the density or viscosity of the fluid that the separation was being performed in, as these are fundamental impactors on TFV as determined by the Stokes equation and has been used previously (Hunter et al., 2014, Doostmohammadi et al., 2014, Zhou et al., Soeth et al., 2005). Increasing the density or viscosity of the separation fluid would reduce the settling speed of all particles and so allow more fine control over the collection of particles, especially at the beginning of the separation. In addition, this could be used to allow for a reduction in the length of the column to achieve the same success of separation as a longer column for easier use and space saving when scaling the process.

6.4.4. Industrial Applicability of Tested Techniques

Figure 6.8 shows how effective each of the different tested separation techniques were at collecting all three desired size fractions from across the full range of the stock. The mesh provides a good baseline for comparison as it does an acceptable job of collecting all three size fractions, however, such a system would be considered sub-optimal for use industrially due to its lack of adaptability, scalability and limited throughput as a result of it being a batch process.

The perfusion technique managed to collect a good fraction of 100-200µm, however, this was no real improvement on the stock in terms of percentage purity within the desired size range. In addition, it performed poorly comparative to the mesh for the <100µm fraction and failed to collect a fraction of EBs >200µm in size at any of the conditions tested. Finally, the settling technique collected by far the

purest fraction of >200µm EBs and a comparable 100-200µm fraction to both the mesh and perfusion techniques. However, in its original guise it struggled to collect a pure fraction of <100µm EBs. Fortunately, the falcon tube pre-separation showed that this method did possess the potential to collect this fraction to a high degree of purity. Therefore, due to its adaptability and potential for scaling, the settling technique should be able to collect all three fractions to a satisfactory standard with further honing of the required conditions.

One of the main considerations when developing an effective size-separation technique for industrial use is that it must have the potential for scalability. This dictates that the technique must have the ability to be run at high throughput, with a minimum of user input and ideally in a continuous or semi-continuous fashion. This technique showed that it possessed this potential as it could be designed to be nearly autonomous with minimum input from a human user and also had high throughput. In the first instance it was shown that the column had the potential to separate out multiple samples of EBs simultaneously; as was performed in these experiments. Each run of the experiment took no more than 20 minutes including the loading, separation and purging steps. As a result, the throughput of this technique was calculated to be 100µl/min. This compared favourably to previous techniques, some of which possessed a throughput as low as 16µl/min (Lillehoj et al., 2010, Buschke et al., 2013). Another technique achieved a throughput of 800µl/min, although this technique did not show the ability to collect multiple different size fractions (Buschke et al., 2012). By increasing the radius of the column far greater numbers of EBs could be collected in one run while, the separation conditions could be kept the same; including the length of time required for each separation. This would also increase the throughput by allowing the column to be loaded with a larger volume of EBs, but retaining the same separation time. In theory this means that the throughput can be continually increased by increasing the diameter of the column to accommodate the loading of a larger number of EBs, although a point will be reached where this becomes impractical due to size and the volume of fluid required to load the column. In this respect this method also benefits from adaptability, as the length of the column can also be altered to reduce the run time required for the experiment or to

allow more fine control over the size of collected fractions. However, these two things would be exclusive of one another as increasing the column length would allow more fine control over size due to the particles separating into more discrete fractions, but this would also take more time. The opposite of this is also true if the column length were reduced; a shorter separation time would result in the collection of less discrete size fractions. In addition to this, the technique could be made to require limited user input. Using pre-sets plugged into a computer, the required size fractions could be collected in an autonomous fashion using two time points as the limiting factor with a computer determining when the column purging should occur based on previous collected results. This could then be followed by a full column purge and a steam in place sterilisation so that after the 15-minute separation the column could be quickly ready for the next run. By having two input ports at the top to allow the addition of sterile PBS from one and the next batch of EBs from the other the separation itself could theoretically run semi-continuously with no further input from the human user beyond determining the initial constraints and programming them into a computer system. This would make for an eminently reproducible technique and therefore improve GMP compliance of industrially applied stem cell differentiation (Unger et al., 2008).

In addition, it should allow the system to easily collect the estimated $1x10^7$ cells required for an individual patient from any of the chosen size fractions thus making this technique commercially viable (Marolt et al., 2010). Furthermore, the success of this technique for size-separating EBs should readily transfer to other aggregates of cells. Provided that the density of these aggregates is consistent as their size increases, then their TFV should remain proportional to their diameter and so should allow them to be separated effectively using this technique. This may require some refinement to ascertain the exact lengths of time required to collect specific size fractions of each different aggregate type, but by following the process delineated here this should be relatively quick and simple and meet with an equivalent level of success.

6.4.5. Viability of Cells Separated Using the Gravity Separation Technique

As a result of this success, EBs separated using this technique were subjected to an MTS assay to determine if the separation conditions resulted in any negative effects on the survival and growth of EBs that underwent separation. It was ensured that the entirety of the stock from every size range was collected for both fractions to ensure that size effects did not alter the outcome, as EB size has previously been shown to profoundly affect proliferation.

Both sets of EBs were counted without the use of a Trypan Blue assay to preclude dead cells from the cell count for seeding. This meant that the seeding of 10,600 cells/cm^2 for both fractions was of total cells, not necessarily all of which were viable. The idea was to show how the effects of the separation technique would manifest themselves in the total cell number over the course of 3 days. This was largely because the technique itself may be destructive, but also research has shown that shear forces, to which the EBs would be subjected during settling, can also have an impact on the proliferation and differentiation of ESC's (Toh and Voldman, 2011, Nsiah et al., 2014, Wolfe et al., 2012, Wolfe and Ahsan, 2013).

It was hoped that taking a reading of cell number after 24 hours would give a good approximation of the number of viable cells as proliferation up to this point is believed to be comparatively low after seeding (Miura et al., 2014). After this, readings were taken after 48 and 72 hours to show how the total possible yield of cells was altered through the use of the separation technique. It was hoped that this would provide some insight into how the separation technique affected the cells as a resource by judging their ability to produce more cells. In addition, under these conditions the cells would not be able to reach confluence and so would not be affected by contact inhibition over this time period.

The results show that right from 24 hours the unseparated cells were in much larger numbers, with 40% more cells compared to the separated cells after this time point despite the same seeding density. While there has obviously been some proliferation for the unseparated fraction, with an increase in cell number of approximately 40,000 compared to the number of cells seeded, the separated cell count was around the number at which they were seeded. This could be considered

surprising as it has previously been shown that mESCs cultured on gelatin undergo population doubling every 16-20 hours; although these cells were taken from continuous culture, not dissociated EBs and the data presented as an average doubling time over 48 hours (Tamm et al., 2013). In contrast, other data has shown a far more consistent proliferation profile to that shown above when utilising ESCs taken from dissociated EBs (Carpenedo et al., 2007). This is likely caused by the cessation of proliferation being a common step in the differentiation process of ESCs; thereby resulting in reduced proliferation of cells taken from dissociated EBs (Ruiz et al., 2011).

However, it quickly became apparent that the separated cells were still proliferating due to the profound increase in cell number after 48 and 72 hours. This suggests that the lower cell number in the separated fraction was not caused by a cessation of proliferation, but more likely due to a reduced number of viable cells being seeded. In spite of the clear trend of increasing cell numbers caused by proliferation in the separated fraction, the cell count never managed to equal that of the unseparated fraction. This is more than likely to have been caused by the reduced number of viable cells that were seeded initially and so could be indicative of the separation technique being destructive and causing cell death. This trend is understandable as it has previously been shown that cell proliferation is reduced at lower initial seeding densities of mESCs (Willerth et al., 2006).

These results show that the separation technique does appear to be slightly destructive for the cells. In spite of this, cells collected from the separated fraction were still able to proliferate and therefore the technique should be perfectly viable for industrial use. However, it still needs to be determined exactly what effect the separation conditions have on the cells to determine whether or not it will impact on their differentiation outcome. In addition, due to the range of particle settling velocities being dependent on their size the EBs will be subjected to variable shear forces. Therefore, the effect that these shear forces have on the cells may well need to be elucidated as well. This could be performed by subjecting a full stock of EBs to different shear forces from across the range experienced during separation and then

performing proliferation and differentiation assays to determine the impact compared to a control sample.

6.5. Conclusion

In conclusion, these results show that the gravity settling separation technique suggested here has the potential to be a scalable and adaptable separation technique to collect numerous discrete size fractions of EBs from a heterogeneously sized stock, regardless of formation time up to 120 hours. In addition, the results shown here suggest that of the techniques demonstrated in this body of work that this technique is the most adaptable for collecting a multitude of size fractions and possesses the most potential for scaling due to its inherent simplicity. However, further work will need to be performed to detail exactly how this method will be able to collect the smallest <100µm fraction. Finally, it was shown that, while there were some negative effects as a result of using this column on cell survival, that cells subjected to the conditions generated by this technique were still viable and capable of proliferating. As a result, further experimentation can be performed to determine what effect, if any, this technique has on differentiation of the cells and to apply this technique to aggregates of different types of cells.

Chapter 7

Summary and Conclusion

To summarize, the results here have again highlighted the heterogeneous nature of EBs produced via mass suspension and explored the use of three different size separation techniques that could be utilised to overcome this issue. First of all, it is clear that mass suspension produces EBs of a wide range of shapes and sizes during their formation over a 5-day period. Over this time the size of these aggregates continues to increase and produces a more and more diverse population of aggregates (Dang et al., 2002, Carpenedo et al., 2007).

The initial mesh separation technique was successful in collecting three different size ranges of EBs of <100µm, 100-200µm and >200µm and allowed for further characterization of the EBs culture for 72 hours to be performed. These subsequent experiments showed the relative frequency with which the aggregates appeared in each of these size fractions in the stock. Further, these experiments then showed the number of cells that were present in each size fraction. Again, as would be expected due to them making up over two thirds of the total number of aggregates, the majority of cells were in the 100-200µm fraction, followed by the >200µm fraction and then the <100 µm fraction. However, the proliferative potential of cells taken from EBs within each of these fractions showed that cells from the <100µm fraction were twice as proliferative as the >200µm fraction, while the most proliferative fraction was again the 100-200µm EBs. This shows that the largest and smallest sets of EBs both have the potential to produce similar numbers of cells when dissociated and cultured following EB formation. However, the most valuable fraction of cells in

terms of raw numbers was the 100-200µm fraction as they started off with the most number of cells and were the most proliferative. This means that cells taken from this size fraction can be relied on to produce the greatest number of cells from a heterogeneously sized mass suspension formation when cultured subsequently; enjoying the greatest output for the same initial use of resources comparative to the other two size fractions. Finally, all three size fractions were shown to be able to express markers from two of the three germ layers to varying degrees after 7-days spontaneous differentiation, with the 100-200µm fraction being the only one unable to express all three germ layer markers due to its failure to present GATA-4. This shows that the size fractions collected here have differing potentials for differentiation, and so in accordance with previously shown results will show a preference for differentiating into certain cell types (Bauwens et al., 2008, Dang et al., 2004, Choi et al., 2010, Xu et al., 2011, Buschke et al., 2013, Carpenedo et al., 2007, Kinney et al., 2012).

These experiments were followed by two attempts to manipulate the characteristics of the Stokes equation to identify a scalable, cheap, easy to use, adaptable and effective separation technique to attain the three size fractions of EBs collected previously across a 120-hour formation period. An adapted expanded bed reactor was utilised using a model system of inanimate beads, as it has previously been shown to have the potential to size separate particles, and an ANN was produced to minimise the number of results that would need to be collected. These results showed that, while the reactor was capable of collecting some different size fractions, specifically the <100µm EBs, it struggled to collect discrete fractions of larger particles. This was shown to be the case in both the model system and in the EB experiments. It was apparent that this was a result of the parabolic flow profile of laminar flow, which causes differential flow rates across the diameter of a column (Sibulkin, 1962, Day, 1990). As a result, the higher the flow rate the greater the spread of flow rates found across the column and so the more particles were moved, resulting in an increase in the D10-D90 span of particle sizes collected with increasing particle diameter. While this is not sufficient for an effective size separation technique for multiple size fractions, the experiments performed here highlighted

the potential of the Stokes equation to be utilised for the separation of EBs, as the >100µm were collected very effectively at low flow rates, with none of the larger particles being disturbed from the bottom of the column.

As a result of this the settling velocity of the aggregates was utilised to separate out particles without relying on fluid flow, but instead utilising gravity to separate the particles; effectively turning the EBR on its head. By top-loading the column with a heterogeneously sized stock of particles and allowing them to settle over time, different sized particles could be collected at different time points reproducibly and with a high degree of accuracy. This was particularly effective for the larger particles, although due to time constraints imposed on the experiment as a result of using living cells, this was less successful for the collection of the <100µm fraction. However, this method was still highlighted to have the potential to collect this size fraction with some adaptation. As a result, a cheap and easy to use method of collecting multiple different size fractions of EBs was identified. This method is easily tuneable to collect different sized fractions of EBs by simply altering the collection conditions, specifically time, and can be used to collect myriad different size fractions of EBs from across the full size range found in the stock. In addition, this method has a high throughput of 100µl, comparable to other techniques, and can easily be scaled to separate larger numbers of EBs allowing it to be utilised industrially. As was discussed in Chapter 6, this separation technique can be easily altered to increase the number of EBs that can be separated in a single experiment, reduce separation time or increase fine control over the range of each collected fraction by altering the dimensions of the column. As a result, this technique is easy to amend to enhance its industrial applicability. In addition, it is simple to operate in a sterile fashion as most of the separation has the potential to be automated and so reduce the potential for contamination, thus improving its GMP compliance (Unger et al., 2008).

In conclusion, these results show that EBs do comply with the predictions of the Stokes equation for settling across their full size range and so can be collected based on this characteristic (Rhodes, 2008). A method was described that allowed for this separation to take place, overcoming the issues of parabolic flow by using gravity as a separating factor instead. As a result, the clear heterogeneity of cells taken from

different sized EBs can be explored further and work can be undertaken to determine what size fractions are most suited to produce specific differentiated cell types from EBs. Upon completion of that research, this technique has the potential to collect multiple different sized fractions of EBs selected specifically for their differentiation potential and therefore improve the successful differentiation of ESCs into their final desired lineage. This will move one step closer to realising the potential of ESCs for tissue engineering in a controlled and reproducible fashion.

Chapter 8

Future Work

Following on from the success of these experiments in producing an adaptable and accurate size separation technique for multiple size fractions of EBs a number of possibilities have opened up for new avenues of research. First among these would be to further explore the impact, if any, that the separation technique has on the cells. While there was some suggestion that the technique reduced the possible cell number, it is not certain whether this was caused by reduced viability or decreased proliferation. An investigation will therefore need to take place to discern whether or not this technique is destructive, to quantify this impact as best as possible and to try to negate or mitigate this impact to ensure that the maximum number of cells can be collected from each experimental run. This will require looking at the survival rate of non-proliferating cells that are subjected to the conditions encountered in the column and compare this to the viability of cells pre-separation to determine percentage viability of the collected cells that have been subjected to the separation conditions against this baseline.

This will then need to be further expanded to determine what effect, if any, the technique has on the differentiation potential of EBs that are collected using the column across the 5-day formation period. This will involve looking at terminal differentiation of cells from a single heterogeneously sized fraction collected from this column for cell types from across the three main lineages, and compared to the same cells that have not undergone the separation process. This will inform on whether or not the conditions encountered here during this early stage of the process will have any impact on the final differentiated outcome of the cells. If it was decided that the results of longer term separations were desired, then this could also

be performed. This would be done with beads first to identify if the predictions made by the Stokes equation still ring true before performing these experiments over a longer period with EBs. As said previously, if these longer duration experiments were to be performed with EBs then amendments would need to be made to improve the conditions by using SNL media and standard culture conditions to allow further longevity of the cells during separation.

These experiments can be performed in conjunction with attempts to automate the process described here so as to make it as useful as possible for industrial practices. Creating scale models of a fully automated separation technique would further endorse the potential of this technique to improve the reliable differentiation of ESCs on an industrial scale, as this is an important step in realising the full potential of ESCs (Soares et al., 2014, Kami et al., 2013, Ker et al., 2011). This will involve an automated column loading sequence followed by timed collections using a pre-programmed pump to collect desired size fractions. Further repeated experiments could then determine what combination of collection times should be utilised to collect fractions with different size properties.

In parallel to the experiments focused on improving the separation technique and preparing it for industry will be experiments that focus more on the biological aspects of this process. First of all, the ability of this technique to collect multiple different size fractions from a stock of heterogeneously sized aggregates means that experiments can be performed to provide greater insight into the inherent differences in EBs of different sizes formed using mass suspension (Bauwens et al., 2008, Dang et al., 2004, Choi et al., 2010, Xu et al., 2011, Bratt-Leal et al., 2009, Buschke et al., 2013, Hwang et al., 2009, Carpenedo et al., 2007, Kinney et al., 2012). From the impact of size on viability and core necrosis to their potential for directed differentiation into specific lineages a great deal can be learned from further experimentation. In order for the separation technique to maximise its potential it is important that the size fractions with the greatest potential for differentiating into each desired, fully differentiated cell type are explored. While much research has been performed on this previously, and is ongoing across several research groups, this is an area that still has a lot of disagreement and inconsistencies, and so the

impact of EB size on the terminal differentiation of ESCs separated using this technique will need to be further elucidated (Bauwens et al., 2008, Dang et al., 2004, Choi et al., 2010, Xu et al., 2011, Bratt-Leal et al., 2009, Ng et al., 2005, Cameron et al., 2006, Buschke et al., 2013, Hwang et al., 2009, Carpenedo et al., 2007, Kinney et al., 2012). In addition, in some cases the particular size separation techniques that have been used in these experiments may have impacted on the differentiation of the cells themselves and so it will be important to corroborate these findings with results collected from EBs separated using this column to make sure that the already identified desirable size fractions are applicable to this process (Yeatts and Fisher, 2011, Stolberg and McCloskey, 2009, Jacobs et al., 1998, Wolfe et al., 2012, Toh and Voldman, 2011, Wolfe and Ahsan, 2013, Kinney et al., 2012).

Finally, on the back of these results the conditions that were tested here on EBs can now be applied to alternative aggregates of cells including mammospheres and pancreatic islets. This would involve simply following the process described here to determine the inherent characteristics of the aggregates that were to be separated and then to trial their separation in the column over different time periods. Provided that their density can be calculated, these cell types should fit into the model as described here. This could very quickly discern the efficacy of this technique for separating these different cell types and then what time periods allowed for the collection of the desired size of each of these different cell types. However, due to the ease of use of this technique, even without this information a relatively brief set of trial and error experiments could easily ascertain the conditions that were required to collect different sized fractions of these cells.

Chapter 9

References

Abe, E., Yamamoto, M., Taguchi, Y., Lecka-Czernik, B., O'Brien, C., Economides, A., Stahl, N., Jilka, R. and Manolagas, S. (2000) 'Essential requirement of BMPs-2/4 for both osteoblast and osteoclast formation in murine bone marrow cultures from adult mice: Antagonism by noggin', *Journal of Bone and Mineral Research,* 15(4), pp. 663-673.

Ahadian, S., Yamada, S., Ramón-Azcón, J., Ino, K., Shiku, H., Khademhosseini, A. and Matsue, T. (2014) 'Rapid and high-throughput formation of 3D embryoid bodies in hydrogels using the dielectrophoresis technique', *Lab on a Chip,* 14(19), pp. 3690-3694.

Akkouch, A., Zhang, Z. and Rouabhia, M. (2011) 'A novel collagen/hydroxyapatite/poly(lactide-co-epsilon-caprolactone) biodegradable and bioactive 3D porous scaffold for bone regeneration', *Journal of Biomedical Materials Research Part a,* 96A(4), pp. 693-704.

Al-Naafa, M. A. and Selim, M. S. (1992) 'Sedimentation of monodisperse and bidisperse hard-sphere colloidal suspensions', *AIChE Journal,* 38(10), pp. 1618-1630.

Alberti, K., Davey, R., Onishi, K., George, S., Salchert, K., Seib, F., Bornhauser, M., Pompe, T., Nagy, A., Werner, C. and Zandstra, P. (2008) 'Functional immobilization of signaling proteins enables control of stem cell fate', *Nature Methods,* 5(7), pp. 645-650.

Amit, M., Carpenter, M., Inokuma, M., Chiu, C., Harris, C., Waknitz, M., Itskovitz-Eldor, J. and Thomson, J. (2000) 'Clonally derived human embryonic stem cell lines maintain pluripotency and proliferative potential for prolonged periods of culture', *Developmental Biology,* 227(2), pp. 271-278.

Annabi, N., Fathi, A., Mithieux, S., Weiss, A. and Dehghani, F. (2011) 'Fabrication of porous PCL/elastin composite scaffolds for tissue engineering applications', *Journal of Supercritical Fluids,* 59, pp. 157-167.

Antebi, B., Pelled, G. and Gazit, D. (2014) 'Stem cell therapy for osteoporosis', *Curr Osteoporos Rep,* 12(1), pp. 41-7.

Anton, F., Suck, K., Diederichs, S., Behr, L., Hitzmann, B., van Griensven, M., Scheper, T. and Kasper, C. (2008) 'Design and characterization of a rotating bed system bioreactor for tissue engineering applications', *Biotechnology Progress,* 24(1), pp. 140-147.

Antoni, D., Burckel, H., Josset, E. and Noel, G. (2015) 'Three-dimensional cell culture: a breakthrough in vivo', *Int J Mol Sci,* 16(3), pp. 5517-27.

Barbanti, A. and Bothner, M. H. (1993) 'A procedure for partitioning bulk sediments into distinct grain-size fractions for geochemical analysis', *Environmental Geology,* 21(1-2), pp. 3-13.

Basma, H., Gunji, Y., Iwasawa, S., Nelson, A., Farid, M., Ikari, J., Liu, X., Wang, X., Michalski, J., Smith, L., Iqbal, J., Behery, R. E., West, W., Yelamanchili, S., Rennard, D., Holz, O.,

Mueller, K.-C., Magnussen, H., Rabe, K., Castaldi, P. J. and Rennard, S. I. (2014) 'Reprogramming of COPD lung fibroblasts through formation of induced pluripotent stem cells', *American Journal of Physiology - Lung Cellular and Molecular Physiology,* 306(6), pp. L552-L565.

Basri, M., Rahman, R. N., Ebrahimpour, A., Salleh, A. B., Gunawan, E. R. and Rahman, M. B. (2007) 'Comparison of estimation capabilities of response surface methodology (RSM) with artificial neural network (ANN) in lipase-catalyzed synthesis of palm-based wax ester', *BMC Biotechnol,* 7, pp. 53.

Basson, D. K., Berres, S. and Bürger, R. (2009) 'On models of polydisperse sedimentation with particle-size-specific hindered-settling factors', *Applied Mathematical Modelling,* 33(4), pp. 1815-1835.

Batchelor, G. K. (1982) 'Sedimentation in a dilute polydisperse system of interacting spheres. Part 1. General theory', *Journal of Fluid Mechanics,* 119, pp. 379-408.

Bauwens, C., Peerani, R., Niebruegge, S., Woodhouse, K., Kumacheva, E., Husain, M. and Zandstra, P. (2008) 'Control of human embryonic stem cell colony and aggregate size heterogeneity influences differentiation trajectories', *Stem Cells,* 26(9), pp. 2300-2310.

Bianco, P. and Robey, P. G. (2001) 'Stem cells in tissue engineering', *Nature,* 414(6859), pp. 118-121.

Boehler, R. M., Graham, J. G. and Shea, L. D. (2011) 'Tissue engineering tools for modulation of the immune response', *Biotechniques,* 51(4), pp. 239-40, 242, 244.

Boeuf, H., Hauss, C., DeGraeve, F., Baran, N. and Kedinger, C. (1997) 'Leukemia inhibitory factor-dependent transcriptional activation in embryonic stem cells', *Journal of Cell Biology,* 138(6), pp. 1207-1217.

Bonnans, C., Chou, J. and Werb, Z. (2014) 'Remodelling the extracellular matrix in development and disease', *Nat Rev Mol Cell Biol,* 15(12), pp. 786-801.

Bradley, J., Bolton, E. and Pedersen, R. (2002) 'Stem cell medicine encounters the immune system', *Nature Reviews Immunology,* 2(11), pp. 859-871.

Bratt-Leal, A., Carpenedo, R. and McDevitt, T. (2009) 'Engineering the Embryoid Body Microenvironment to Direct Embryonic Stem Cell Differentiation', *Biotechnology Progress,* 25(1), pp. 43-51.

Brown, P. and Lawler, D. (2003) 'Sphere Drag and Settling Velocity Revisited', *Journal of Environmental Engineering,* 129(3), pp. 222-231.

Burden, F. and Winkler, D. (2008) 'Bayesian regularization of neural networks', *Methods Mol Biol,* 458, pp. 25-44.

Burdon, T., Smith, A. and Savatier, P. (2002) 'Signalling, cell cycle and pluripotency in embryonic stem cells', *Trends in Cell Biology,* 12(9), pp. 432-438.

Buschke, D., Vivekanandan, A., Squirrell, J., Rueden, C., Eliceiri, K. and Ogle, B. (2013) 'Large particle multiphoton flow cytometry to purify intact embryoid bodies exhibiting enhanced potential for cardiomyocyte differentiation', *Integrative Biology,* 5(7), pp. 993-1003.

Buschke, D. G., Resto, P., Schumacher, N., Cox, B., Tallavajhula, A., Vivekanandan, A., Eliceiri, K. W., Williams, J. C. and Ogle, B. M. (2012) 'Microfluidic sorting of microtissues', *Biomicrofluidics,* 6(1), pp. 014116-014116-11.

Buttery, L., Bourne, S., Xynos, J., Wood, H., Hughes, F., Hughes, S., Episkopou, V. and Polak, J. (2001) 'Differentiation of osteoblasts and in vitro bone formation from murine embryonic stem cells', *Tissue Engineering,* 7(1), pp. 89-99.

Cai, J., Chen, J., Liu, Y., Miura, T., Luo, Y., Loring, J., Freed, W., Rao, M. and Zeng, X. (2006) 'Assessing self-renewal and differentiation in human embryonic stem cell lines', *Stem Cells,* 24(3), pp. 516-530.

Calvi, L., Adams, G., Weibrecht, K., Weber, J., Olson, D., Knight, M., Martin, R., Schipani, E., Divieti, P., Bringhurst, F., Milner, L., Kronenberg, H. and Scadden, D. (2003) 'Osteoblastic cells regulate the haematopoietic stem cell niche', *Nature,* 425(6960), pp. 841-846.

Cameron, C., Hu, W. and Kaufman, D. (2006) 'Improved development of human embryonic stem cell-derived embryoid bodies by stirred vessel cultivation', *Biotechnology and Bioengineering,* 94(5), pp. 938-948.

Caplan, A. I. (2007) 'Adult mesenchymal stem cells for tissue engineering versus regenerative medicine', *J Cell Physiol,* 213(2), pp. 341-7.

Carpenedo, R., Sargent, C. and Mcdevitt, T. (2007) 'Rotary suspension culture enhances the efficiency, yield, and homogeneity of embryoid body differentiation', *Stem Cells,* 25(9), pp. 2224-2234.

Cha, J. M., Bae, H., Sadr, N., Manoucheri, S., Edalat, F., Kim, K., Kim, S. B., Kwon, I. K., Hwang, Y.-S. and Khademhosseini, A. (2015) 'Embryoid body size-mediated differential endodermal and mesodermal differentiation using polyethylene glycol (PEG) microwell array', *Macromolecular Research,* 23(3), pp. 245-255.

Chambers, I. and Smith, A. (2004) 'Self-renewal of teratocarcinoma and embryonic stem cells', *Oncogene,* 23(43), pp. 7150-7160.

Chau, L. T., Frith, J. E., Mills, R. J., Menzies, D. J., Titmarsh, D. M. and Cooper-White, J. J. (2013) 'Microfluidic devices for developing tissue scaffolds', in Li, X. & Zhou, Y. (eds.) *Microfluidic Devices for Biomedical Applications*: Woodhead Publishing, pp. 363-387.

Chen, K. G., Mallon, B. S., Johnson, K. R., Hamilton, R. S., McKay, R. D. G. and Robey, P. G. (2014) 'Developmental insights from early mammalian embryos and core signaling pathways that influence human pluripotent cell growth and differentiation', *Stem Cell Research,* 12(3), pp. 610-621.

Chen, S., Fitzgerald, W., Zimmerberg, J., Kleinman, H. and Margolis, L. (2007) 'Cell-cell and cell-extracellular matrix interactions regulate embryonic stem cell differentiation', *Stem Cells,* 25(3), pp. 553-561.

Chhabra, R. P., Agarwal, S. and Chaudhary, K. (2003) 'A note on wall effect on the terminal falling velocity of a sphere in quiescent Newtonian media in cylindrical tubes', *Powder Technology,* 129(1–3), pp. 53-58.

Choi, D., Lee, H. J., Jee, S., Jin, S., Koo, S. K., Paik, S. S., Jung, S. C., Hwang, S. Y., Lee, K. S. and Oh, B. (2005) 'In vitro differentiation of mouse embryonic stem cells: enrichment of endodermal cells in the embryoid body', *Stem Cells,* 23(6), pp. 817-27.

Choi, J. W., Park, E. J., Shin, H. S., Shin, I. S., Ra, J. C. and Koh, K. S. (2014) 'In vivo differentiation of undifferentiated human adipose tissue-derived mesenchymal stem cells in critical-sized calvarial bone defects', *Ann Plast Surg,* 72(2), pp. 225-33.

Choi, Y., Chung, B., Lee, D., Khademhosseini, A., Kim, J. and Lee, S. (2010) 'Controlled-size embryoid body formation in concave microwell arrays', *Biomaterials,* 31(15), pp. 4296-4303.

Chung, C. H., Golub, E. E., Forbes, E., Tokuoka, T. and Shapiro, I. M. (1992) 'Mechanism of action of beta-glycerophosphate on bone cell mineralization', *Calcif Tissue Int,* 51(4), pp. 305-11.

Chung, Y., Klimanska, I. and Becker, S. (2008) 'Human embryonic stem cells produced without destruction of embryos', *Regenerative Medicine,* 3(2), pp. 135-135.

Clause, K. C., Liu, L. J. and Tobita, K. (2010) 'Directed stem cell differentiation: the role of physical forces', *Cell communication & adhesion,* 17(2), pp. 48-54.

Clifton, J., McDonald, P., Plater, A. and Oldfield, F. (1999) 'An investigation into the efficiency of particle size separation using Stokes' Law', *Earth Surface Processes and Landforms,* 24(8), pp. 725-730.

Cohen, Y. and Metzner, A. B. (1981) 'Wall effects in laminar flow of fluids through packed beds', *AIChE Journal,* 27(5), pp. 705-715.

Cooper, G. M. (2000) *The Cell - A Molecular Approach 2nd Edition.* Sunderland (MA): Sinauer Associates.

Cormier, J. T., zur Nieden, N. I., Rancourt, D. E. and Kallos, M. S. (2006) 'Expansion of undifferentiated murine embryonic stem cells as aggregates in suspension culture bioreactors', *Tissue Eng,* 12(11), pp. 3233-45.

Costa, I. G., Roepcke, S., Hafemeister, C. and Schliep, A. (2008) 'Inferring differentiation pathways from gene expression', *Bioinformatics,* 24(13), pp. i156-i164.

Coucouvanis, E. and Martin, G. R. (1995) 'Signals for death and survival: a two-step mechanism for cavitation in the vertebrate embryo', *Cell,* 83(2), pp. 279-87.

Dado, D., Sagi, M., Levenberg, S. and Zemel, A. (2012) 'Mechanical control of stem cell differentiation', *Regen Med,* 7(1), pp. 101-16.

Dang, S., Gerecht-Nir, S., Chen, J., Itskovitz-Eldor, J. and Zandstra, P. (2004) 'Controlled, scalable embryonic stem cell differentiation culture', *Stem Cells,* 22(3), pp. 275-282.

Dang, S., Kyba, M., Perlingeiro, R., Daley, G. and Zandstra, P. (2002) 'Efficiency of embryoid body formation and hematopoietic development from embryonic stem cells in different culture systems', *Biotechnology and Bioengineering,* 78(4), pp. 442-453.

Dasgupta, A., Hughey, R., Lancin, P., Larue, L. and Moghe, P. (2005) 'E-cadherin synergistically induces hepatospecific phenotype and maturation of embryonic stem cells in conjunction with hepatotrophic factors', *Biotechnology and Bioengineering,* 92(3), pp. 257-266.

Day, M. (1990) 'The no-slip condition of fluid dynamics', *Erkenntnis,* 33(3), pp. 285-296.

De Filippis, L. and Binda, E. (2012) 'Concise Review: Self-Renewal in the Central Nervous System: Neural Stem Cells from Embryo to Adult', *Stem Cells Translational Medicine,* 1(4), pp. 298-308.

Deleyrolle, L., Ericksson, G., Morrison, B., Lopez, J., Burrage, K., Burrage, P., Vescovi, A., Rietze, R. and Reynolds, B. (2011) 'Determination of Somatic and Cancer Stem Cell Self-Renewing Symmetric Division Rate Using Sphere Assays', *Plos One,* 6(1).

Diamond, H., Ornellas, M., Orfao, A., Gomes, B., Campos, M., Fernandez, T., da Silva, R., Alves, G., Lage, C., da Silva, D., Moellmann-Coelho, A., da Cruz, G., Bouzas, L. and Abdelhay, E. (2011) 'Acute myeloid leukemia of donor origin after allogeneic stem cell transplantation from a sibling who harbors germline XPD and XRCC3 homozygous polymorphisms', *Journal of Hematology & Oncology,* 4(39), pp. 1-8.

Dias, A. D., Unser, A. M., Xie, Y., Chrisey, D. B. and Corr, D. T. (2014) 'Generating size-controlled embryoid bodies using laser direct-write', *Biofabrication,* 6(2), pp. 025007.

Dingli, D., Traulsen, A. and Michor, F. (2007) '(A) symmetric stem cell replication and cancer', *Plos Computational Biology,* 3(3), pp. 482-487.

Doostmohammadi, A., Dabiri, S. and Ardekani, A. M. (2014) 'A numerical study of the dynamics of a particle settling at moderate Reynolds numbers in a linearly stratified fluid', *Journal of Fluid Mechanics,* 750, pp. 5-32.

Dvir-Ginzberg, M., Gamlieli-Bonshtein, I., Agbaria, R. and Cohen, S. (2003) 'Liver tissue engineering within alginate scaffolds: effects of cell-seeding density on hepatocyte viability, morphology, and function', *Tissue Eng,* 9(4), pp. 757-66.

Dvorak, P., Dvorakova, D., Koskova, S., Vodinska, M., Najvirtova, M., Krekac, D. and Hampl, A. (2005) 'Expression and potential role of fibroblast growth factor 2 and its receptors in human embryonic stem cells', *Stem cells,* 23(8), pp. 1200-1211.

Ebben, J., Zorniak, M., Clark, P. and Kuo, J. (2011) 'Introduction to Induced Pluripotent Stem Cells: Advancing the Potential for Personalized Medicine', *World Neurosurgery,* 76(3-4), pp. 270-275.

Edmondson, R., Broglie, J. J., Adcock, A. F. and Yang, L. (2014) 'Three-Dimensional Cell Culture Systems and Their Applications in Drug Discovery and Cell-Based Biosensors', *Assay and Drug Development Technologies,* 12(4), pp. 207-218.

Eiselleova, L., Matulka, K., Kriz, V., Kunova, M., Schmidtova, Z., Neradil, J., Tichy, B., Dvorakova, D., Pospisilova, S., Hampl, A. and Dvorak, P. (2009) 'A complex role for FGF-2 in self-renewal, survival, and adhesion of human embryonic stem cells', *Stem Cells,* 27(8), pp. 1847-57.

Eminli, S., Foudi, A., Stadtfeld, M., Maherali, N., Ahfeldt, T., Mostoslavsky, G., Hock, H. and Hochedlinger, K. (2009) 'Differentiation stage determines potential of hematopoietic cells for reprogramming into induced pluripotent stem cells', *Nature Genetics,* 41(9), pp. 968-U29.

Evan, G. and Vousden, K. (2001) 'Proliferation, cell cycle and apoptosis in cancer', *Nature,* 411(6835), pp. 342-348.

Fehling, H. J., Lacaud, G., Kubo, A., Kennedy, M., Robertson, S., Keller, G. and Kouskoff, V. (2003) 'Tracking mesoderm induction and its specification to the hemangioblast during embryonic stem cell differentiation', *Development,* 130(17), pp. 4217-27.

Fok, E. Y. and Zandstra, P. W. (2005) 'Shear-controlled single-step mouse embryonic stem cell expansion and embryoid body-based differentiation', *Stem Cells,* 23(9), pp. 1333-42.

Fu, Q., Saiz, E., Rahaman, M. and Tomsia, A. (2011) 'Bioactive glass scaffolds for bone tissue engineering: state of the art and future perspectives', *Materials Science & Engineering C-Materials For Biological Applications,* 31(7), pp. 1245-1256.

Fu, Y., Nie, H., Ho, M., Wang, C. and Wang, C. (2008) 'Optimized bone regeneration based on sustained release from three-dimensional fibrous PLGA/HAp composite scaffolds loaded with BMP-2', *Biotechnology and Bioengineering,* 99(4), pp. 996-1006.

Ge, D., Song, K., Guan, S., Dai, M., Ma, X., Liu, T. and Cui, Z. (2012) 'Effect of the neurosphere size on the viability and metabolism of neural stem/progenitor cells', *African Journal of Biotechnology,* 11(17), pp. 3976-3985.

Genbacev, O., Krtolica, A., Zdravkovic, P., Zdravkovic, T., Brunette, E., Powell, S., Nath, A., Caceres, E., McMaster, M., McDonagh, S., Li, Y., Mandalam, R., Lebkowski, J. and Fisher, S. (2005) 'Serum-free derivation of human embryonic stem cell lines on human placental fibroblast feeders', *Fertility and Sterility,* 83(5), pp. 1517-1529.

Gepstein, L. (2002) 'Derivation and Potential Applications of Human Embryonic Stem Cells', *Circulation Research,* 91(10), pp. 866-876.

Giancola, R., Bonfini, T. and Iacone, A. (2012) 'Cell therapy: cGMP facilities and manufacturing', *Muscles, Ligaments and Tendons Journal,* 2(3), pp. 243-247.

Glossop, J. R. and Cartmell, S. H. (2009) 'Effect of fluid flow-induced shear stress on human mesenchymal stem cells: differential gene expression of IL1B and MAP3K8 in MAPK signaling', *Gene Expr Patterns,* 9(5), pp. 381-8.

Gorczynski, R. M., Miller, R. G. and Phillips, R. A. (1970) 'Homogeneity of antibody-producing cells as analysed by their buoyant density in gradients of Ficoll', *Immunology,* 19(5), pp. 817-829.

Gothard, D., Roberts, S. J., Shakesheff, K. M. and Buttery, L. D. (2009) 'Controlled embryoid body formation via surface modification and avidin–biotin cross-linking', *Cytotechnology,* 61(3), pp. 135-144.

Greber, B., Wu, G., Bernemann, C., Joo, J., Han, D., Ko, K., Tapia, N., Sabour, D., Sterneckert, J., Tesar, P. and Scholer, H. (2010) 'Conserved and Divergent Roles of FGF Signaling in Mouse Epiblast Stem Cells and Human Embryonic Stem Cells', *Cell Stem Cell,* 6(3), pp. 215-226.

Griffin, M. F., Butler, P. E., Seifalian, A. M. and Kalaskar, D. M. (2015) 'Control of stem cell fate by engineering their micro and nanoenvironment', *World Journal of Stem Cells,* 7(1), pp. 37-50.

Grompe, M. (2005) 'Embryonic stem cells without embryos?', *Nature Biotechnology,* 23(12), pp. 1496-1497.

Gu, Q., Hao, J., Zhao, X. Y., Li, W., Liu, L., Wang, L., Liu, Z. H. and Zhou, Q. (2012) 'Rapid conversion of human ESCs into mouse ESC-like pluripotent state by optimizing culture conditions', *Protein Cell,* 3(1), pp. 71-9.

Gutierrez-Aranda, I., Ramos-Mejia, V., Bueno, C., Munoz-Lopez, M., Real, P. J., Mácia, A., Sanchez, L., Ligero, G., Garcia-Parez, J. L. and Menendez, P. (2010) 'Human Induced Pluripotent Stem Cells Develop Teratoma More Efficiently and Faster Than Human Embryonic Stem Cells Regardless the Site of Injection', *Stem Cells (Dayton, Ohio),* 28(9), pp. 1568-1570.

Han, N.-W., Bhakta, J. and Carbonell, R. G. (1985) 'Longitudinal and Lateral Dispersion in Packed Beds: Effect of Column Length and Particle Size Distribution', *AIChE,* 31, pp. 277-288.

Hashemi, S., Soudi, S., Shabani, I., Naderi, M. and Soleimani, M. (2011) 'The promotion of stemness and pluripotency following feeder-free culture of embryonic stem cells on collagen-grafted 3-dimensional nanofibrous scaffold', *Biomaterials,* 32(30), pp. 7363-7374.

Hentze, H., Soong, P. L., Wang, S. T., Phillips, B. W., Putti, T. C. and Dunn, N. R. (2009) 'Teratoma formation by human embryonic stem cells: Evaluation of essential parameters for future safety studies', *Stem Cell Research,* 2(3), pp. 198-210.

Hernández-García, D., Castro-Obregón, S., Gómez-López, S., Valencia, C. and Covarrubias, L. (2008) 'Cell death activation during cavitation of embryoid bodies is mediated by hydrogen peroxide', *Experimental Cell Research,* 314(10), pp. 2090-2099.

Herzenberg, L. A., Sweet, R. G. and Herzenberg, L. A. (1976) 'Fluorescence-activated cell sorting', *Sci Am,* 234(3), pp. 108-117.

Hunter, D. M., Iveson, S. M. and Galvin, K. P. (2014) 'The role of viscosity in the density fractionation of particles in a laboratory-scale Reflux Classifier', *Fuel,* 129, pp. 188-196.

Hwang, N. S., Varghese, S. and Elisseeff, J. (2008) 'Controlled differentiation of stem cells', *Adv Drug Deliv Rev,* 60(2), pp. 199-214.

Hwang, Y., Chung, B., Ortmann, D., Hattori, N., Moeller, H. and Khademhosseini, A. (2009) 'Microwell-mediated control of embryoid body size regulates embryonic stem cell fate via differential expression of WNT5a and WNT11', *Proceedings of the National Academy of Sciences of the United States of America,* 106(40), pp. 16978-16983.

Hwang, Y., Suk, S., Lin, S., Tierney, M., Du, B., Seo, T., Mitchell, A., Sacco, A. and Varghese, S. (2013) 'Directed in vitro myogenesis of human embryonic stem cells and their in vivo engraftment', *PLoS One,* 8(8), pp. e72023.

Hyslop, L., Stojkovic, M., Armstrong, L., Walter, T., Stojkovic, P., Przyborski, S., Herbert, M., Murdoch, A., Strachan, T. and Lako, M. (2005) 'Downregulation of NANOG induces differentiation of human embryonic stem cells to extraembryonic lineages', *Stem Cells,* 23(8), pp. 1035-1043.

Itskovitz-Eldor, J., Schuldiner, M., Karsenti, D., Eden, A., Yanuka, O., Amit, M., Soreq, H. and Benvenisty, N. (2000) 'Differentiation of human embryonic stem cells into embryoid bodies comprising the three embryonic germ layers', *Molecular Medicine,* 6(2), pp. 88-95.

Jacobs, C., Yellowley, C., Davis, B., Zhou, Z., Cimbala, J. and Donahue, H. (1998) 'Differential effect of steady versus oscillating flow on bone cells', *Journal of Biomechanics,* 31(11), pp. 969-976.

Jahanshahi, M., Najafpour, G., Ebrahimpour, M., Hajizadeh, S. and Shahavi, M. H. (2009) 'Evaluation of hydrodynamic parameters of fluidized bed adsorption on purification of nano-bioproducts', *Physica status solidi,* 6(10), pp. 2199-2206.

Jayakumar, R., Chennazhi, K., Srinivasan, S., Nair, S., Furuike, T. and Tamura, H. (2011) 'Chitin Scaffolds in Tissue Engineering', *International Journal of Molecular Sciences,* 12(3), pp. 1876-1887.

Jukes, J. M., van Blitterswijk, C. A. and de Boer, J. (2010) 'Skeletal tissue engineering using embryonic stem cells', *J Tissue Eng Regen Med,* 4(3), pp. 165-80.

Jungreuthmayer, C., Jaasma, M., Al-Munajjed, A., Zanghellini, J., Kelly, D. and O'Brien, F. (2009) 'Deformation simulation of cells seeded on a collagen-GAG scaffold in a flow perfusion bioreactor using a sequential 3D CFD-elastostatics model', *Medical Engineering & Physics,* 31(4), pp. 420-427.

Kai, D., Prabhakaran, M., Jin, G. and Ramakrishna, S. (2011) 'Guided orientation of cardiomyocytes on electrospun aligned nanofibers for cardiac tissue engineering', *Journal of Biomedical Materials Research Part B-Applied Biomaterials,* 98B(2), pp. 379-386.

Kami, D., Watakabe, K., Yamazaki-Inoue, M., Minami, K., Kitani, T., Itakura, Y., Toyoda, M., Sakurai, T., Umezawa, A. and Gojo, S. (2013) 'Large-scale cell production of stem cells for clinical application using the automated cell processing machine', *BMC Biotechnology,* 13, pp. 102-102.

Kang, L., Hancock, M. J., Brigham, M. D. and Khademhosseini, A. (2010) 'Cell confinement in patterned nanoliter droplets in a microwell array by wiping', *J Biomed Mater Res A,* 93(2), pp. 547-57.

Karageorgiou, V. and Kaplan, D. (2005) 'Porosity of 3D biornaterial scaffolds and osteogenesis', *Biomaterials,* 26(27), pp. 5474-5491.

Karau, A., Benken, C., Thommes, J. and Kula, M. R. (1997) 'The influence of particle size distribution and operating conditions on the adsorption performance in fluidized beds', *Biotechnol Bioeng,* 55(1), pp. 54-64.

Karp, J. M., Yeh, J., Eng, G., Fukuda, J., Blumling, J., Suh, K.-Y., Cheng, J., Mahdavi, A., Borenstein, J., Langer, R. and Khademhosseini, A. (2007) 'Controlling size, shape and homogeneity of embryoid bodies using poly(ethylene glycol) microwells', *Lab on a Chip,* 7(6), pp. 786-794.

Ker, D. F., Weiss, L. E., Junkers, S. N., Chen, M., Yin, Z., Sandbothe, M. F., Huh, S. I., Eom, S., Bise, R., Osuna-Highley, E., Kanade, T. and Campbell, P. G. (2011) 'An engineered approach to stem cell culture: automating the decision process for real-time adaptive subculture of stem cells', *PLoS One,* 6(11), pp. e27672.

Khoo, M. L., McQuade, L. R., Smith, M. S., Lees, J. G., Sidhu, K. S. and Tuch, B. E. (2005) 'Growth and differentiation of embryoid bodies derived from human embryonic stem cells: effect of glucose and basic fibroblast growth factor', *Biol Reprod,* 73(6), pp. 1147-56.

Kim, D., Kim, C., Moon, J., Chung, Y., Chang, M., Han, B., Ko, S., Yang, E., Cha, K., Lanza, R. and Kim, K. (2009) 'Generation of Human Induced Pluripotent Stem Cells by Direct Delivery of Reprogramming Proteins', *Cell Stem Cell,* 4(6), pp. 472-476.

Kim, K., Doi, A., Wen, B., Ng, K., Zhao, R., Cahan, P., Kim, J., Aryee, M., Ji, H., Ehrlich, L., Yabuuchi, A., Takeuchi, A., Cunniff, K., Hongguang, H., Mckinney-Freeman, S., Naveiras, O., Yoon, T., Irizarry, R., Jung, N., Seita, J., Hanna, J., Murakami, P., Jaenisch, R., Weissleder, R., Orkin, S., Weissman, I., Feinberg, A. and Daley, G. (2010) 'Epigenetic memory in induced pluripotent stem cells', *Nature,* 467(7313), pp. 285-U60.

King, J. and Miller, W. (2007) 'Bioreactor development for stem cell expansion and controlled differentiation', *Current Opinion in Chemical Biology,* 11(4), pp. 394-398.

Kinney, M., Saeed, R. and McDevitt, T. (2012) 'Systematic analysis of embryonic stem cell differentiation in hydrodynamic environments with controlled embryoid body size', *Integrative Biology,* 4(6), pp. 641-650.

Kinney, M. A., Hookway, T. A., Wang, Y. and McDevitt, T. C. (2014) 'Engineering three-dimensional stem cell morphogenesis for the development of tissue models and scalable regenerative therapeutics', *Annals of biomedical engineering,* 42(2), pp. 352-367.

Klimanskaya, I., Rosenthal, N. and Lanza, R. (2008) 'Derive and conquer: sourcing and differentiating stem cells for therapeutic applications', *Nat Rev Drug Discov,* 7(2), pp. 131-142.

Koike, M., Sakaki, S., Amano, Y. and Kurosawa, H. (2007) 'Characterization of embryoid bodies of mouse embryonic stem cells formed under various culture conditions and estimation of differentiation status of such bodies', *J Biosci Bioeng,* 104(4), pp. 294-9.

Koivisto, H., Hyvarinen, M., Stromberg, A., Inzunza, J., Matilainen, E., Mikkola, M., Hovatta, O. and Teerijoki, H. (2004) 'Cultures of human embryonic stem cells: serum replacement medium or serum-containing media and the effect of basic fibroblast growth factor', *Reproductive Biomedicine Online,* 9(3), pp. 330-337.

Konert, M. and Vandenberghe, J. E. F. (1997) 'Comparison of laser grain size analysis with pipette and sieve analysis: a solution for the underestimation of the clay fraction', *Sedimentology,* 44(3), pp. 523-535.

Kreke, M. R., Huckle, W. R. and Goldstein, A. S. (2005) 'Fluid flow stimulates expression of osteopontin and bone sialoprotein by bone marrow stromal cells in a temporally dependent manner', *Bone,* 36(6), pp. 1047-55.

Krishnamoorthy, P. (2010) 'Sedimentation model and analysis for differential settling of two - particle - size suspensions in the Stokes region', *International Journal of Sediment Research,* 25(2), pp. 119-133.

Kronenberg, H. (2003) 'Developmental regulation of the growth plate', *Nature,* 423(6937), pp. 332-336.

Kuehnle, I. and Goodell, M. (2002) 'The therapeutic potential of stem cells from adults', *British Medical Journal,* 325(7360), pp. 372-376.

Kumar, R. M., Cahan, P., Shalek, A. K., Satija, R., Jay DaleyKeyser, A., Li, H., Zhang, J., Pardee, K., Gennert, D., Trombetta, J. J., Ferrante, T. C., Regev, A., Daley, G. Q. and Collins, J. J. (2014) 'Deconstructing transcriptional heterogeneity in pluripotent stem cells', *Nature,* 516(7529), pp. 56-61.

Kurosawa, H. (2007) 'Methods for inducing embryoid body formation: In vitro differentiation system of embryonic stem cells', *Journal of Bioscience and Bioengineering,* 103(5), pp. 389-398.

Kurosawa, H., Kimura, M., Noda, T. and Amano, Y. (2006) 'Effect of oxygen on in vitro differentiation of mouse embryonic stem cells', *Journal of Bioscience and Bioengineering,* 101(1), pp. 26-30.

Langenbach, F., Naujoks, C., Smeets, R., Berr, K., Depprich, R., Kubler, N. and Handschel, J. (2013) 'Scaffold-free microtissues: differences from monolayer cultures and their potential in bone tissue engineering', *Clinical Oral Investigations,* 17(1), pp. 9-17.

Lapidus, L. and Elgin, J. C. (1957) 'Mechanics of vertical-moving fluidized systems', *AIChE Journal,* 3(1), pp. 63-68.

Lau, R., Hassan, M. S., Wong, W. and Chen, T. (2010) 'Revisit of the Wall Effect on the Settling of Cylindrical Particles in the Inertial Regime', *Industrial & Engineering Chemistry Research,* 49(18), pp. 8870-8876.

Lehmann, R., Zuellig, R. A., Kugelmeier, P., Baenninger, P. B., Moritz, W., Perren, A., Clavien, P. A., Weber, M. and Spinas, G. A. (2007) 'Superiority of small islets in human islet transplantation', *Diabetes,* 56(3), pp. 594-603.

Lillehoj, P., Tsutsui, H., Valamehr, B., Wu, H. and Ho, C. (2010) 'Continuous sorting of heterogeneous-sized embryoid bodies', *Lab on a Chip,* 10(13), pp. 1678-1682.

Lin, D.-Q., Tong, H.-F., van de Sandt, E. J. A. X., den Boer, P., Golubović, M. and Yao, S.-J. (2013) 'Evaluation and characterization of axial distribution in expanded bed. I. Bead size, bead density and local bed voidage', *Journal of Chromatography A,* 1304, pp. 78-84.

Lin, R. Z. and Chang, H. Y. (2008) 'Recent advances in three-dimensional multicellular spheroid culture for biomedical research', *Biotechnol J,* 3(9-10), pp. 1172-84.

Lin, Y., Wang, L. L., Zhang, P. B., Wang, X., Chen, X. S., Jing, X. B. and Su, Z. H. (2006) 'Surface modification of poly(L-lactic acid) to improve its cytocompatibility via assembly of polyelectrolytes and gelatin', *Acta Biomaterialia,* 2(2), pp. 155-164.

Lister, R., Pelizzola, M., Kida, Y., Hawkins, R., Nery, J., Hon, G., Antosiewicz-Bourget, J., O'Malley, R., Castanon, R., Klugman, S., Downes, M., Yu, R., Stewart, R., Ren, B., Thomson, J., Evans, R. and Ecker, J. (2011) 'Hotspots of aberrant epigenomic reprogramming in human induced pluripotent stem cells', *Nature,* 471(7336), pp. 68-U84.

Liu, T. X., Zhang, J. W., Tao, J., Zhang, R. B., Zhang, Q. H., Zhao, C. J., Tong, J. H., Lanotte, M., Waxman, S., Chen, S. J., Mao, M., Hu, G. X., Zhu, L. and Chen, Z. (2000) 'Gene expression networks underlying retinoic acid-induced differentiation of acute promyelocytic leukemia cells', *Blood,* 96(4), pp. 1496-504.

Liu, Z., Tang, Y., Lü, S., Zhou, J., Du, Z., Duan, C., Li, Z. and Wang, C. (2013) 'The tumourigenicity of iPS cells and their differentiated derivates', *Journal of Cellular and Molecular Medicine,* 17(6), pp. 782-791.

Losino, N., Luzzani, C., Solari, C., Boffi, J., Tisserand, M. L., Sevlever, G., Baranao, L. and Guberman, A. (2011) 'Maintenance of murine embryonic stem cells' self-renewal and pluripotency with increase in proliferation rate by a bovine granulosa cell line-conditioned medium', *Stem Cells Dev,* 20(8), pp. 1439-49.

Lowe, S., Cepero, E. and Evan, G. (2004) 'Intrinsic tumour suppression', *Nature,* 432(7015), pp. 307-315.

Machado, H. L., Kittrell, F. S., Edwards, D., White, A. N., Atkinson, R. L., Rosen, J. M., Medina, D. and Lewis, M. T. (2013) 'Separation by Cell Size Enriches for Mammary Stem Cell Repopulation Activity', *Stem Cells Translational Medicine,* 2(3), pp. 199-203.

Magyar, J., Nemir, M., Ehler, E., Suter, N., Perriard, J., Eppenberger, H., Hunkeler, D., Cherrington, A., Prokop, A. and Rajotte, R. (2001) 'Mass production of embryoid bodies in microbeads', *Bioartificial Organs Iii: Tissue Sourcing, Immunoisolation, and Clinical Trials,* 944, pp. 135-143.

Malatesta, P., Hartfuss, E. and Gotz, M. (2000) 'Isolation of radial glial cells by fluorescent-activated cell sorting reveals a neuronal lineage', *Development,* 127(24), pp. 5253-5263.

Maltman, D. J. and Przyborski, S. A. (2010) 'Developments in three-dimensional cell culture technology aimed at improving the accuracy of in vitro analyses', *Biochem Soc Trans,* 38(4), pp. 1072-5.

Mansour Ghaffari, M., Faujan Bin, H. A., Mahiran, B. and Mohd Basyaruddin Abdul, R. (2010) 'Artificial neural network modeling studies to predict the yield of enzymatic synthesis of betulinic acid ester', *Electronic Journal of Biotechnology; Vol 13, No 3 (2010)*.

Marolt, D., Knezevic, M. and Novakovic, G. (2010) 'Bone tissue engineering with human stem cells', *Stem Cell Research & Therapy,* 1, pp. 1-10.

Martin, G. (1981) 'Isolation of a pluripotent cell-line from early mouse embryos cultured in medium conditioned by teratocarcinoma stem-cells', *Proceedings of the National Academy of Sciences of the United States of America-Biological Sciences,* 78(12), pp. 7634-7638.

Masliyah, J. H. (1979) 'Hindered settling in a multi-species particle system', *Chemical Engineering Science,* 34(9), pp. 1166-1168.

McBride, S. H., Falls, T. and Knothe Tate, M. L. (2008) 'Modulation of stem cell shape and fate B: mechanical modulation of cell shape and gene expression', *Tissue Eng Part A,* 14(9), pp. 1573-80.

McKinney-Freeman, S. and Daley, G. (2007) 'Derivation of Hematopoietic Stem Cells from Murine Embryonic Stem Cells', *Journal of Visualized Experiments : JoVE,* (2), pp. 162.

Mehta, D. and Hawley, M. C. (1969) 'Wall Effect in Packed Columns', *Industrial & Engineering Chemistry Process Design and Development,* 8(2), pp. 280-282.

Messana, J., Hwang, N., Coburn, J., Elisseeff, J. and Zhang, Z. (2008) 'Size of the embryoid body influences chondrogenesis of mouse embryonic stem cells', *Journal of Tissue Engineering and Regenerative Medicine,* 2(8), pp. 499-506.

Mimeault, M. and Batra, S. (2008) 'Recent progress on tissue-resident adult stem cell biology and their therapeutic implications', *Stem Cell Reviews,* 4(1), pp. 27-49.

Miura, T., Ando, A., Hirano, K., Ogura, C., Kanazawa, T., Ikeguchi, M., Seki, A., Nishihara, S. and Hamaguchi, S. (2014) 'Proliferation assay of mouse embryonic stem (ES) cells exposed to atmospheric-pressure plasmas at room temperature', *Journal of Physics D: Applied Physics,* 47(44), pp. 445402.

Miyamoto, D. and Nakazawa, K. (2016) 'Differentiation of mouse iPS cells is dependent on embryoid body size in microwell chip culture', *J Biosci Bioeng*.

Mizuno, M. and Kuboki, Y. (2001) 'Osteoblast-related gene expression of bone marrow cells during the osteoblastic differentiation induced by type I collagen', *J Biochem,* 129(1), pp. 133-8.

Mogi, A., Ichikawa, H., Matsumoto, C., Hieda, T., Tomotsune, D., Sakaki, S., Yamada, S. and Sasaki, K. (2009) 'The method of mouse embryoid body establishment affects structure and developmental gene expression', *Tissue and Cell,* 41(1), pp. 79-84.

Mogi, A., Takei, S., Shimizu, H., Miura, H., Tomotsune, D. and Sasaki, K. (2013) 'Effects of fluid dynamic forces created by rotary orbital suspension culture on cardiomyogenic differentiation of human embryonic stem cells', *J Med Biol Eng,* 34(2), pp. 101-108.

Mohamet, L., Lea, M. and Ward, C. (2010) 'Abrogation of E-Cadherin-Mediated Cellular Aggregation Allows Proliferation of Pluripotent Mouse Embryonic Stem Cells in Shake Flask Bioreactors', *Plos One,* 5(9).

Mohr, J. C., Zhang, J., Azarin, S. M., Soerens, A. G., de Pablo, J. J., Thomson, J. A., Lyons, G. E., Palecek, S. P. and Kamp, T. J. (2010) 'The Microwell Control of Embryoid Body Size in order to Regulate Cardiac Differentiation of Human Embryonic Stem Cells', *Biomaterials,* 31(7), pp. 1885.

Moon, S.-H., Ju, J., Park, S.-J., Bae, D., Chung, H.-M. and Lee, S.-H. (2014) 'Optimizing human embryonic stem cells differentiation efficiency by screening size-tunable homogenous embryoid bodies', *Biomaterials,* 35(23), pp. 5987-5997.

Mora, C. F., Kwan, A. K. H. and Chan, H. C. (1998) 'Particle size distribution analysis of coarse aggregate using digital image processing', *Cement and Concrete Research,* 28(6), pp. 921-932.

Mori, H., Ninomiya, K., Kino-oka, M., Shofuda, T., Islam, M. O., Yamasaki, M., Okano, H., Taya, M. and Kanemura, Y. (2006) 'Effect of neurosphere size on the growth rate of human neural stem/progenitor cells', *J Neurosci Res,* 84(8), pp. 1682-91.

Morrison, S. and Kimble, J. (2006) 'Asymmetric and symmetric stem-cell divisions in development and cancer', *Nature,* 441(7097), pp. 1068-1074.

Mostafa, S., Papoutsakis, E. and Miller, W. (2001) 'Oxygen tension modulates the expression of cytokine receptors, transcription factors, and lineage-specific markers in cultured human megakaryocytes', *Experimental Hematology,* 29(7), pp. 873-883.

Mouw, J. K., Ou, G. and Weaver, V. M. (2014) 'Extracellular matrix assembly: a multiscale deconstruction', *Nat Rev Mol Cell Biol,* 15(12), pp. 771-785.

Murray, P. and Edgar, D. (2001) 'The regulation of embryonic stem cell differentiation by leukaemia inhibitory factor (LIF)', *Differentiation,* 68(4-5), pp. 227-234.

Muschler, G. F., Nakamoto, C. and Griffith, L. G. (2004) 'Engineering Principles of Clinical Cell-Based Tissue Engineering', *The Journal of Bone & Joint Surgery,* 86(7), pp. 1541-1558.

Nakagami, H., Nakagawa, N., Takeya, Y., Kashiwagi, K., Ishida, C., Hayashi, S., Aoki, M., Matsumoto, K., Nakamura, T., Ogihara, T. and Morishita, R. (2006) 'Model of vasculogenesis from embryonic stem cells for vascular research and regenerative medicine', *Hypertension,* 48(1), pp. 112-9.

Nakamura, M. and Okano, H. (2013) 'Cell transplantation therapies for spinal cord injury focusing on induced pluripotent stem cells', *Cell Res,* 23(1), pp. 70-80.

Nam, K. H., Yong, W., Harvat, T., Adewola, A., Wang, S., Oberholzer, J. and Eddington, D. T. (2010) 'Size-based separation and collection of mouse pancreatic islets for functional analysis', *Biomed Microdevices,* 12(5), pp. 865-74.

Ng, E., Davis, R., Azzola, L., Stanley, E. and Elefanty, A. (2005) 'Forced aggregation of defined numbers of human embryonic stem cells into embryoid bodies fosters robust, reproducible hematopoietic differentiation', *Blood,* 106(5), pp. 1601-1603.

Ng, Y. and Chase, H. (2007) 'Separation and enrichment of neural stem cells using segregation in an expanded bed', *Biotechnology Letters,* 29(11), pp. 1745-1751.

Nonaka, J., Yoshikawa, M., Ouji, Y., Matsuda, R., Nishimura, F., Yamada, S., Nakase, H., Moriya, K., Nishiofuku, M., Ishizaka, S. and Sakaki, T. (2008) 'CoCl(2) inhibits neural differentiation of retinoic acid-treated embryoid bodies', *J Biosci Bioeng,* 106(2), pp. 141-7.

Nsiah, B. A., Ahsan, T., Griffiths, S., Cooke, M., Nerem, R. M. and McDevitt, T. C. (2014) 'Fluid shear stress pre-conditioning promotes endothelial morphogenesis of embryonic stem cells within embryoid bodies', *Tissue Eng Part A,* 20(5-6), pp. 954-65.

Ntambi, J. M. and Young-Cheul, K. (2000) 'Adipocyte Differentiation and Gene Expression', *The Journal of Nutrition,* 130(12), pp. 3122S-3126S.

Ohnuki, Y. and Kurosawa, H. (2013) 'Effects of hanging drop culture conditions on embryoid body formation and neuronal cell differentiation using mouse embyonic stem cells: Optimization of culture conditions for the formation of well-controlled embryoid bodies', *Journal of Bioscience and Bioengineering,* 115(5), pp. 571-574.

Okano, H., Nakamura, M., Yoshida, K., Okada, Y., Tsuji, O., Nori, S., Ikeda, E., Yamanaka, S. and Miura, K. (2013) 'Steps Toward Safe Cell Therapy Using Induced Pluripotent Stem Cells', *Circulation Research*, 112(3), pp. 523-533. DOI: 10.1161/CIRCRESAHA.111.256149.

Osorno, R. and Chambers, I. (2011) 'Transcription factor heterogeneity and epiblast pluripotency', *Philosophical Transactions of the Royal Society of London B: Biological Sciences,* 366(1575), pp. 2230-2237.

Park, C.-H., Minn, Y.-K., Lee, J.-Y., Choi, D. H., Chang, M.-Y., Shim, J.-W., Ko, J.-Y., Koh, H.-C., Kang, M. J., Kang, J. S., Rhie, D.-J., Lee, Y.-S., Son, H., Moon, S. Y., Kim, K.-S. and Lee, S.-H. (2005) 'In vitro and in vivo analyses of human embryonic stem cell-derived dopamine neurons', *Journal of Neurochemistry,* 92(5), pp. 1265-1276.

Parsons, H. T., Christiansen, K., Knierim, B., Carroll, A., Ito, J., Batth, T. S., Smith-Moritz, A. M., Morrison, S., McInerney, P., Hadi, M. Z., Auer, M., Mukhopadhyay, A., Petzold, C. J., Scheller, H. V., Loqué, D. and Heazlewood, J. L. (2012) 'Isolation and Proteomic Characterization of the Arabidopsis Golgi Defines Functional and Novel Components Involved in Plant Cell Wall Biosynthesis', *Plant Physiology,* 159(1), pp. 12-26.

Pendleton, C., Li, Q., Chesler, D. A., Yuan, K., Guerrero-Cazares, H. and Quinones-Hinojosa, A. (2013) 'Mesenchymal stem cells derived from adipose tissue vs bone marrow: in vitro comparison of their tropism towards gliomas', *PLoS One,* 8(3), pp. e58198.

Pettinato, G., Wen, X. and Zhang, N. (2014) 'Formation of Well-defined Embryoid Bodies from Dissociated Human Induced Pluripotent Stem Cells using Microfabricated Cell-repellent Microwell Arrays', *Sci. Rep.,* 4, pp. 1-11.

Pino, A. M., Rosen, C. J. and Rodríguez, J. P. (2012) 'In Osteoporosis, differentiation of mesenchymal stem cells (MSCs) improves bone marrow adipogenesis', *Biological Research,* 45, pp. 279-287.

Poh, Y.-C., Chen, J., Hong, Y., Yi, H., Zhang, S., Chen, J., Wu, D. C., Wang, L., Jia, Q., Singh, R., Yao, W., Tan, Y., Tajik, A., Tanaka, T. S. and Wang, N. (2014) 'Generation of organized germ layers from a single mouse embryonic stem cell', *Nat Commun,* 5.

Pokrywczynska, M., Adamowicz, J., Sharma, A. K. and Drewa, T. (2014) 'Human urinary bladder regeneration through tissue engineering - an analysis of 131 clinical cases', *Exp Biol Med (Maywood),* 239(3), pp. 264-71.

Polo, J., Liu, S., Figueroa, M., Kulalert, W., Eminli, S., Tan, K., Apostolou, E., Stadtfeld, M., Li, Y., Shioda, T., Natesan, S., Wagers, A., Melnick, A., Evans, T. and Hochedlinger, K. (2010) 'Cell type of origin influences the molecular and functional properties of mouse induced pluripotent stem cells', *Nature Biotechnology,* 28(8), pp. 848-U130.

Prathalingam, N., Ferguson, L., Young, L., Lietz, G., Oldershaw, R., Healy, L., Craig, A., Lister, H., Binaykia, R., Sheth, R., Murdoch, A. and Herbert, M. (2012) 'Production and validation of a good manufacturing practice grade human fibroblast line for supporting human embryonic stem cell derivation and culture', *Stem Cell Research & Therapy,* 3(2), pp. 1-13.

Przyborski, S. A. (2005) 'Differentiation of human embryonic stem cells after transplantation in immune-deficient mice', *Stem Cells,* 23(9), pp. 1242-1250.

Ramirez, J. M., Gerbal-Chaloin, S., Milhavet, O., Qiang, B., Becker, F., Assou, S., Lemaitre, J. M., Hamamah, S. and De Vos, J. (2011) 'Brief report: benchmarking human pluripotent stem cell markers during differentiation into the three germ layers unveils a striking heterogeneity: all markers are not equal', *Stem Cells,* 29(9), pp. 1469-74.

Randle, W., Cha, J., Hwang, Y., Chan, K., Kazarian, S., Polak, J. and Mantalaris, A. (2007) 'Integrated 3-dimensional expansion and osteogenic differentiation of murine embryonic stem cells', *Tissue Engineering,* 13(12), pp. 2957-2970.

Ravi, M., Paramesh, V., Kaviya, S. R., Anuradha, E. and Solomon, F. D. (2015) '3D cell culture systems: advantages and applications', *J Cell Physiol,* 230(1), pp. 16-26.

Redenti, S., Neeley, W., Rompani, S., Saigal, S., Yang, J., Klassen, H., Langer, R. and Young, M. (2009) 'Engineering retinal progenitor cell and scrollable poly(glycerol-sebacate) composites for expansion and subretinal transplantation', *Biomaterials,* 30(20), pp. 3405-3414.

Rezania, A., Bruin, J. E., Arora, P., Rubin, A., Batushansky, I., Asadi, A., O'Dwyer, S., Quiskamp, N., Mojibian, M., Albrecht, T., Yang, Y. H. C., Johnson, J. D. and Kieffer, T. J. (2014) 'Reversal of diabetes with insulin-producing cells derived in vitro from human pluripotent stem cells', *Nat Biotech,* 32(11), pp. 1121-1133.

Rhodes, M. J. (2008) *Introduction to Particle Technology.* 2nd edn.

Richards, M., Fong, C., Chan, W., Wong, P. and Bongso, A. (2002) 'Human feeders support prolonged undifferentiated growth of human inner cell masses and embryonic stem cells', *Nature Biotechnology,* 20(9), pp. 933-936.

Riss, T. L., Moravec, R. A., Niles, A. L., Benink, H. A., Worzella, T. J. and Minor, L. (2004) 'Cell Viability Assays', in Sittampalam, G.S., Coussens, N.P., Nelson, H., Arkin, M., Auld, D., Austin, C., Bejcek, B., Glicksman, M., Inglese, J., Iversen, P.W., Li, Z., McGee, J., McManus, O., Minor, L., Napper, A., Peltier, J.M., Riss, T., Trask, O.J., Jr. & Weidner, J. (eds.) *Assay Guidance Manual*. Bethesda (MD): Eli Lilly & Company and the National Center for Advancing Translational Sciences.

Robbins, J., Gulick, J., Sanchez, A., Howles, P. and Doetschman, T. (1990) 'Mouse embryonic stem cells express the cardiac myosin heavy chain genes during development in vitro', *J Biol Chem,* 265(20), pp. 11905-9.

Robertson, N., Brook, F., Gardner, R., Cobbold, S., Waldmann, H. and Fairchild, P. (2007) 'Embryonic stem cell-derived tissues are immunogenic but their inherent privilege promotes the induction of tolerance', *Proceedings of the National Academy of Sciences of the United States of America,* 104(52), pp. 20920-20925.

Rosado-de-Castro, P. H., Pimentel-Coelho, P. M., Barbosa da Fonseca, L. M., de Freitas, G. R. and Mendez-Otero, R. (2013) 'The Rise of Cell Therapy Trials for Stroke: Review of Published and Registered Studies', *Stem Cells and Development,* 22(15), pp. 2095-2111.

Ruiz, S., Panopoulos, A. D., Herrerías, A., Bissig, K.-D., Lutz, M., Berggren, W. T., Verma, I. M. and Belmonte, J. C. I. (2011) 'A high proliferation rate is required for cell reprogramming and maintenance of human embryonic stem cell identity', *Current biology : CB,* 21(1), pp. 45-52.

Rumman, M., Dhawan, J. and Kassem, M. (2015) 'Concise Review: Quiescence in Adult Stem Cells: Biological Significance and Relevance to Tissue Regeneration', *STEM CELLS,* 33(10), pp. 2903-2912.

Rungarunlert, S., Klincumhom, N., Tharasanit, T., Techakumphu, M., Pirity, M. K. and Dinnyes, A. (2013) 'Slow Turning Lateral Vessel Bioreactor Improves Embryoid Body Formation and Cardiogenic Differentiation of Mouse Embryonic Stem Cells', *Cellular Reprogramming,* 15(5), pp. 443-458.

Sakai, Y., Yoshiura, Y. and Nakazawa, K. (2011) 'Embryoid body culture of mouse embryonic stem cells using microwell and micropatterned chips', *Journal of Bioscience and Bioengineering,* 111(1), pp. 85-91.

Salama, A. I. A. (2000) 'Mechanical Techniques: Particle Size Separation', in Wilson, I.D. (ed.) *Encyclopedia of Separation Science*. Oxford: Academic Press, pp. 3277-3289.

Schmitz, B., Radbruch, A., Kummel, T., Wickenhauser, C., Korb, H., Hansmann, M. L., Thiele, J. and Fischer, R. (1994) 'Magnetic activated cell sorting (MACS)--a new immunomagnetic method for megakaryocytic cell isolation: comparison of different separation techniques', *Eur J Haematol,* 52(5), pp. 267-75.

Schnerch, A., Cerdan, C. and Bhatia, M. (2010) 'Distinguishing Between Mouse and Human Pluripotent Stem Cell Regulation: The Best Laid Plans of Mice and Men', *STEM CELLS,* 28(3), pp. 419-430.

Schoen, F. J. and Levy, R. J. (1999) 'Tissue heart valves: Current challenges and future research perspectives', *Journal of Biomedical Materials Research,* 47(4), pp. 439-465.

Schroeder, M., Niebruegge, S., Werner, A., Willbold, E., Burg, M., Ruediger, M., Field, L., Lehmann, J. and Zweigerdt, R. (2005) 'Differentiation and lineage selection of mouse embryonic stem cells in a stirred bench scale bioreactor with automated process control', *Biotechnology and Bioengineering,* 92(7), pp. 920-933.

Schwartz, C. E. and Smith, J. M. (1953) 'Flow Distribution in Packed Beds', *Industrial & Engineering Chemistry,* 45(6), pp. 1209-1218.

Schwartz, S. D., Regillo, C. D., Lam, B. L., Eliott, D., Rosenfeld, P. J., Gregori, N. Z., Hubschman, J.-P., Davis, J. L., Heilwell, G., Spirn, M., Maguire, J., Gay, R., Bateman, J., Ostrick, R. M., Morris, D., Vincent, M., Anglade, E., Del Priore, L. V. and Lanza, R. (2015) 'Human embryonic stem cell-derived retinal pigment epithelium in patients with age-related macular degeneration and Stargardt's macular dystrophy: follow-up of two open-label phase 1/2 studies', *The Lancet,* 385(9967), pp. 509-516.

Serra, M., Brito, C., Correia, C. and Alves, P. M. (2012) 'Process Engineering of human pluripotent stem cells for clinical application', *Trends in Biotechnology*, 30, pp. 350-359.

Sharma, S., Raju, R., Sui, S. and Hu, W. (2011) 'Stem cell culture engineering - process scale up and beyond', *Biotechnology Journal,* 6(11), pp. 1317-1329.

Shimokawa, M. and Sato, T. (2015) 'Back to 2D Culture for Ground State of Intestinal Stem Cells', *Cell Stem Cell,* 17(1), pp. 5-7.

Sibulkin, M. 1962. Transition from Turbulent to Laminar Pipe Flow. Physics of Fluids.

Sidney, L. E., Kirkham, G. R. and Buttery, L. D. (2014) 'Comparison of osteogenic differentiation of embryonic stem cells and primary osteoblasts revealed by responses to IL-1beta, TNF-alpha, and IFN-gamma', *Stem Cells Dev,* 23(6), pp. 605-17.

Sila-Asna, M., Bunyaratvej, A., Maeda, S., Kitaguchi, H. and Bunyaratavej, N. (2007) 'Osteoblast differentiation and bone formation gene expression in strontium-inducing bone marrow mesenchymal stem cell', *Kobe J Med Sci,* 53(1-2), pp. 25-35.

Singer, Zakary S., Yong, J., Tischler, J., Hackett, Jamie A., Altinok, A., Surani, M A., Cai, L. and Elowitz, Michael B. (2014) 'Dynamic Heterogeneity and DNA Methylation in Embryonic Stem Cells', *Molecular Cell,* 55(2), pp. 319-331.

Smith, A. (2001) 'Embryo-derived stem cells: Of mice and men', *Annual Review of Cell and Developmental Biology,* 17, pp. 435-462.

Smukler, S., Runciman, S., Xu, S. and van der Kooy, D. (2006) 'Embryonic stem cells assume a primitive neural stem cell fate in the absence of extrinsic influences', *Journal of Cell Biology,* 172(1), pp. 79-90.

Soares, F. A. C., Chandra, A., Thomas, R. J., Pedersen, R. A., Vallier, L. and Williams, D. J. (2014) 'Investigating the feasibility of scale up and automation of human induced pluripotent stem cells cultured in aggregates in feeder free conditions', *Journal of Biotechnology,* 173(100), pp. 53-58.

Soeth, E., Grigoleit, U., Moellmann, B., Roder, C., Schniewind, B., Kremer, B., Kalthoff, H. and Vogel, I. (2005) 'Detection of tumor cell dissemination in pancreatic ductal carcinoma patients by CK 20 RT-PCR indicates poor survival', *J Cancer Res Clin Oncol,* 131(10), pp. 669-76.

Soncin, F., Mohamet, L., Eckardt, D., Ritson, S., Eastham, A., Bobola, N., Russell, A., Davies, S., Kemler, R., Merry, C. and Ward, C. (2009) 'Abrogation of E-Cadherin-Mediated Cell-Cell Contact in Mouse Embryonic Stem Cells Results in Reversible LIF-Independent Self-Renewal', *Stem Cells,* 27(9), pp. 2069-2080.

Spiess, A.-N. and Neumeyer, N. (2010) 'An evaluation of R2 as an inadequate measure for nonlinear models in pharmacological and biochemical research: a Monte Carlo approach', *BMC Pharmacology*, 10(6), pp. 1-11.

Stappenbeck, T. and Miyoshi, H. (2009) 'The Role of Stromal Stem Cells in Tissue Regeneration and Wound Repair', *Science,* 324(5935), pp. 1666-1669.

Stenderup, K., Justesen, J., Clausen, C. and Kassem, M. (2003) 'Aging is associated with decreased maximal life span and accelerated senescence of bone marrow stromal cells', *Bone,* 33(6), pp. 919-926.

Stojkovic, M., Lako, M., Strachan, T. and Murdoch, A. (2004) 'Derivation, growth and applications of human embryonic stem cells', *Reproduction,* 128(3), pp. 259-267.

Stolberg, S. and McCloskey, K. (2009) 'Can Shear Stress Direct Stem Cell Fate?', *Biotechnology Progress,* 25(1), pp. 10-19.

Strom, S., Inzunza, J., Grinnemo, K., Hohmnberg, K., Matilainen, E., Stromberg, A., Blennow, E. and Hovatta, O. (2007) 'Mechanical isolation of the inner cell mass is effective in derivation of new human embryonic stem cell lines', *Human Reproduction,* 22(12), pp. 3051-3058.

Taber, L. A., Zhang, J. and Perucchio, R. (2006) 'Computational Model for the Transition From Peristaltic to Pulsatile Flow in the Embryonic Heart Tube', *Journal of Biomechanical Engineering,* 129(3), pp. 441-449.

Taheri, E. S., Jahanshahi, M., Hamed Mosavian, M. T. and Shahavi, M. H. (2012) 'Investigation of hydrodynamic parameters in a novel expanded bed configuration: Local axial dispersion characterization and an empirical correlation study', *Brazilian Journal of Chemical Engineering*, 29, pp. 725-739.

Tamm, C., Pijuan Galitó, S. and Annerén, C. (2013) 'A Comparative Study of Protocols for Mouse Embryonic Stem Cell Culturing', *PLoS ONE,* 8(12), pp. e81156.

Taylor, C., Bolton, E. and Bradley, J. (2011) 'Immunological considerations for embryonic and induced pluripotent stem cell banking', *Philosophical Transactions of the Royal Society B-Biological Sciences,* 366(1575), pp. 2312-2322.

Thomson, J., Itskovitz-Eldor, J., Shapiro, S., Waknitz, M., Swiergiel, J., Marshall, V. and Jones, J. (1998) 'Embryonic stem cell lines derived from human blastocysts', *Science,* 282(5391), pp. 1145-1147.

Toh, W. S., Lee, E. H. and Cao, T. (2011) 'Potential of human embryonic stem cells in cartilage tissue engineering and regenerative medicine', *Stem Cell Rev,* 7(3), pp. 544-59.

Toh, Y. and Voldman, J. (2011) 'Fluid shear stress primes mouse embryonic stem cells for differentiation in a self-renewing environment via heparan sulfate proteoglycans transduction', *Faseb Journal,* 25(4), pp. 1208-1217.

Tomov, M. L., Olmsted, Z. T. and Paluh, J. L. (2015) 'The Human Embryoid Body Cystic Core Exhibits Architectural Complexity Revealed by use of High Throughput Polymer Microarrays', *Macromolecular Bioscience,* 15(7), pp. 892-900.

Tong, X. D. and Sun, Y. (2002) 'Particle size and density distributions of two dense matrices in an expanded bed system', *Journal of Chromatography A*, 977(2), pp. 173-182.

Toyooka, Y., Shimosato, D., Murakami, K., Takahashi, K. and Niwa, H. (2008) 'Identification and characterization of subpopulations in undifferentiated ES cell culture', *Development,* 135(5), pp. 909-918.

Trounson, A. and McDonald, C. (2015) 'Stem Cell Therapies in Clinical Trials: Progress and Challenges', *Cell Stem Cell,* 17(1), pp. 11-22.

Trounson, A., Thakar, R., Lomax, G. and Gibbons, D. (2011) 'Clinical trials for stem cell therapies', *Bmc Medicine,* 9(52), pp. 1-7.

Unger, C., Skottman, H., Blomberg, P., Dilber, M. and Hovatta, O. (2008) 'Good manufacturing practice and clinical-grade human embryonic stem cell lines', *Human Molecular Genetics,* 17, pp. R48-R53.

Valamehr, B., Jonas, S. J., Polleux, J., Qiao, R., Guo, S., Gschweng, E. H., Stiles, B., Kam, K., Luo, T.-J. M., Witte, O. N., Liu, X., Dunn, B. and Wu, H. (2008) 'Hydrophobic surfaces

for enhanced differentiation of embryonic stem cell-derived embryoid bodies', *Proceedings of the National Academy of Sciences,* 105(38), pp. 14459-14464.

Valenti, M. T., Carbonare, L. D., Donatelli, L., Bertoldo, F., Zanatta, M. and Lo Cascio, V. (2008) 'Gene expression analysis in osteoblastic differentiation from peripheral blood mesenchymal stem cells', *Bone,* 43(6), pp. 1084-1092.

Van Winkle, A., Gates, I. and Kallos, M. (2012) 'Mass Transfer Limitations in Embryoid Bodies during Human Embryonic Stem Cell Differentiation', *Mass Transfer Limitations in Embryoid Bodies during Human Embryonic Stem Cell Differentiation,* Vol. 196(1), pp. 34-47.

Vangsness, C. T., Jr., Sternberg, H. and Harris, L. (2015) 'Umbilical Cord Tissue Offers the Greatest Number of Harvestable Mesenchymal Stem Cells for Research and Clinical Application: A Literature Review of Different Harvest Sites', *Arthroscopy,* 31(9), pp. 1836-43.

Vats, A., Tolley, N. S., Bishop, A. E. and Polak, J. M. (2005) 'Embryonic stem cells and tissue engineering: delivering stem cells to the clinic', *Journal of the Royal Society of Medicine,* 98(8), pp. 346-350.

Vdović, N., Obhođaš, J. and Pikelj, K. (2010) 'Revisiting the particle-size distribution of soils: comparison of different methods and sample pre-treatments', *European Journal of Soil Science,* 61(6), pp. 854-864.

Venugopal, J., Prabhakaran, M., Zhang, Y., Low, S., Choon, A. and Ramakrishna, S. (2010) 'Biomimetic hydroxyapatite-containing composite nanofibrous substrates for bone tissue engineering', *Philosophical Transactions of the Royal Society a-Mathematical Physical and Engineering Sciences,* 368(1917), pp. 2065-2081.

Wang, L., Yang, B., Wang, R. and Du, X. (2008) 'Extraction of pepsin-soluble collagen from grass carp (Ctenopharyngodon idella) skin using an artificial neural network', *Food Chemistry,* 111(3), pp. 683-686.

Wang, Y., Chou, B.-K., Dowey, S., He, C., Gerecht, S. and Cheng, L. (2013) 'Scalable expansion of human induced pluripotent stem cells in the defined xeno-free E8 medium under adherent and suspension culture conditions', *Stem Cell Research,* 11(3), pp. 1103-1116.

Watt, F. M., Frye, M. and Benitah, S. A. (2008) 'MYC in mammalian epidermis: how can an oncogene stimulate differentiation?', *Nat Rev Cancer,* 8(3), pp. 234-242.

Watt, F. M. and Huck, W. T. S. (2013) 'Role of the extracellular matrix in regulating stem cell fate', *Nat Rev Mol Cell Biol,* 14(8), pp. 467-473.

Willerth, S. M., Arendas, K. J., Gottlieb, D. I. and Sakiyama-Elbert, S. E. (2006) 'Optimization of Fibrin Scaffolds for Differentiation of Murine Embryonic Stem Cells into Neural Lineage Cells', *Biomaterials,* 27(36), pp. 5990-6003.

WILLIAMS, R., HILTON, D., PEASE, S., WILLSON, T., STEWART, C., GEARING, D., WAGNER, E., METCALF, D., NICOLA, N. and GOUGH, N. (1988) 'MYELOID-LEUKEMIA INHIBITORY FACTOR MAINTAINS THE DEVELOPMENTAL POTENTIAL OF EMBRYONIC STEM-CELLS', *Nature,* 336(6200), pp. 684-687.

Willoughby, N., Hjorth, R. and Titchener-Hooker, N. (2000) 'Experimental measurement of particle size distribution and voidage in an expanded bed adsorption system', *Biotechnology and Bioengineering,* 69(6), pp. 648-653.

Wolfe, R. P. and Ahsan, T. (2013) 'Shear stress during early embryonic stem cell differentiation promotes hematopoietic and endothelial phenotypes', *Biotechnol Bioeng,* 110(4), pp. 1231-42.

Wolfe, R. P., Leleux, J., Nerem, R. M. and Ahsan, T. (2012) 'Effects of shear stress on germ lineage specification of embryonic stem cells', *Integr Biol (Camb),* 4(10), pp. 1263-73.

Xu, C., Inokuma, M., Denham, J., Golds, K., Kundu, P., Gold, J. and Carpenter, M. (2001) 'Feeder-free growth of undifferentiated human embryonic stem cells', *Nature Biotechnology,* 19(10), pp. 971-974.

Xu, F., Sridharan, B., Wang, S., Gurkan, U., Syverud, B. and Demirci, U. (2011) 'Embryonic stem cell bioprinting for uniform and controlled size embryoid body formation', *Biomicrofluidics,* 5(2), pp. 1-8.

Xu, H., Han, D., Dong, J., Shen, G., Chai, G., Yu, Z., Lang, W. and Ai, S. (2010) 'Rapid prototyped PGA/PLA scaffolds in the reconstruction of mandibular condyle bone defects', *International Journal of Medical Robotics and Computer Assisted Surgery,* 6(1), pp. 66-72.

Yamanaka, S. (2008) 'Pluripotency and nuclear reprogramming', *Philosophical Transactions of the Royal Society B-Biological Sciences,* 363(1500), pp. 2079-2087.

Yamanaka, S. (2009a) 'A Fresh Look at iPS Cells', *Cell,* 137(1), pp. 13-17.

Yamanaka, S. (2009b) 'Elite and stochastic models for induced pluripotent stem cell generation', *Nature,* 460(7251), pp. 49-52.

Yamashita, J., Itoh, H., Hirashima, M., Ogawa, M., Nishikawa, S., Yurugi, T., Naito, M. and Nakao, K. (2000) 'Flk1-positive cells derived from embryonic stem cells serve as vascular progenitors', *Nature,* 408(6808), pp. 92-6.

Yeatts, A. and Fisher, J. (2011) 'Bone tissue engineering bioreactors: Dynamic culture and the influence of shear stress', *Bone,* 48(2), pp. 171-181.

Ying, Q., Nichols, J., Chambers, I. and Smith, A. (2003) 'BMP induction of Id proteins suppresses differentiation and sustains embryonic stem cell self-renewal in collaboration with STAT3', *Cell,* 115(3), pp. 281-292.

Youn, B. S., Sen, A., Behie, L. A., Girgis-Gabardo, A. and Hassell, J. A. (2006) 'Scale-up of breast cancer stem cell aggregate cultures to suspension bioreactors', *Biotechnol Prog,* 22(3), pp. 801-10.

Youn, B. S., Sen, A., Kallos, M. S., Behie, L. A., Girgis-Gabardo, A., Kurpios, N., Barcelon, M. and Hassell, J. A. (2005) 'Large-scale expansion of mammary epithelial stem cell aggregates in suspension bioreactors', *Biotechnol Prog,* 21(3), pp. 984-93.

Yourek, G., McCormick, S., Mao, J. and Reilly, G. (2010) 'Shear stress induces osteogenic differentiation of human mesenchymal stem cells', *Regenerative Medicine,* 5(5), pp. 713-724.

Yun, J., Yao, S. and Lin, D. (2005) 'Variation of the local effective axial dispersion coefficient with bed height in expanded beds', *Chemical Engineering Journal,* 109(1-3), pp. 123-131.

Yun, J., Yao, S., Lin, D., Lu, M. and Zhao, W. (2004) 'Modeling axial distributions of adsorbent particle size and local voidage in expanded bed', *Chemical Engineering Science,* 59(2), pp. 449-457.

Zhang, R. and Ma, P. (2004) 'Biomimetic polymer/apatite composite scaffolds for mineralized tissue engineering', *Macromolecular Bioscience,* 4(2), pp. 100-111.

Zhou, J., Hu, L., Yu, Z., Zheng, J., Yang, D., Bouvet, M. and Hoffman, R. M. 'Marker Expression in Circulating Cancer Cells of Pancreatic Cancer Patients', *Journal of Surgical Research,* 171(2), pp. 631-636.

Zhou, J., Zhang, Y., Lin, Q., Liu, Z., Wang, H., Duan, C., Wang, Y., Hao, T., Wu, K. and Wang, C. (2010) 'Embryoid bodies formation and differentiation from mouse embryonic stem cells in collagen/Matrigel scaffolds', *J Genet Genomics,* 37(7), pp. 451-60.

Zimmermann, W. H., Schneiderbanger, K., Schubert, P., Didie, M., Munzel, F., Heubach, J. F., Kostin, S., Neuhuber, W. L. and Eschenhagen, T. (2002) 'Tissue engineering of a differentiated cardiac muscle construct', *Circ Res,* 90(2), pp. 223-30.

zur Nieden, N. I., Kempka, G. and Ahr, H. J. (2003) 'In vitro differentiation of embryonic stem cells into mineralized osteoblasts', *Differentiation,* 71(1), pp. 18-27.

Zweigerdt, R. (2009) 'Large Scale Production of Stem Cells and Their Derivatives', in Martin, U. (ed.) *Engineering of Stem Cells*. Berlin, Heidelberg: Springer Berlin Heidelberg, pp. 201-235.